

**Characterisation of cytosolic prion protein-  
mediated putative cytotoxicity in neuronal cell  
lines**

Dissertation  
zur Erlangung des Doktorgrades  
der Naturwissenschaften

vorgelegt beim Fachbereich Biowissenschaften  
der Johann Wolfgang Goethe-Universität Frankfurt am Main

von  
Jana Mehlhase  
aus Mittweida

Langen (Hessen) 2006

vom Fachbereich Biowissenschaften der Johann Wolfgang Goethe-Universität als  
Dissertation angenommen.

Dekan: Prof. Dr. Rüdiger Wittig  
Gutachter: Prof. Dr. Anna Starzinski-Powitz  
Prof. Dr. Johannes Löwer

Datum der Disputation: .....

---

## Table of contents

<b>1</b>	<b>Summary</b> .....	<b>I</b>
1.1	German Summary.....	I
1.2	English Summary.....	IV
<b>2</b>	<b>Introduction</b> .....	<b>1</b>
2.1	Prion diseases and infectivity.....	1
2.2	Cellular prion protein.....	2
2.2.1	Characteristics and structure of PrP <sup>C</sup> .....	2
2.2.2	Biosynthesis and endosomal trafficking of PrP <sup>C</sup> .....	3
2.2.3	Putative functions of PrP <sup>C</sup> .....	4
2.3	Neurotoxicity of pathological prion protein.....	6
2.3.1	PrP <sup>Sc</sup> and neurotoxicity.....	6
2.3.2	ER-stress and PrP misfolding.....	7
2.4	PrP <sup>C</sup> proteolysis and the proteasomal system.....	8
2.5	Cytosolic PrP.....	9
2.5.1	Cytotoxicity of cytosolic PrP.....	11
2.6	Ecdysone-inducible expression system.....	12
2.7	Objectives.....	15
<b>3</b>	<b>Materials and Methods</b> .....	<b>16</b>
3.1	Materials and chemicals.....	16
3.1.1	Materials and equipments.....	16
3.1.2	Chemicals.....	16
3.1.3	Enzymes.....	18
3.1.4	Cells and media.....	18
3.1.5	Kits.....	19
3.1.6	Antibodies.....	19
3.2	Molecular biology.....	20
3.2.1	Plasmids.....	20
3.2.2	Construction of vectors encoding transgene PrPs.....	21
3.2.3	Polymerase chain reaction.....	22
3.2.4	Oligonucleotides.....	23

---

3.2.5 Agarose gel electrophoresis .....	23
3.2.6 Restriction and ligation .....	24
3.2.7 DNA purification .....	24
3.2.8 Photometric determination of DNA concentration.....	25
3.2.9 Working with bacteria .....	25
3.3 Cell biology and biochemistry .....	27
3.3.1 Cultivation of eukaryotic cells .....	27
3.3.2 Determination of the cell number.....	28
3.3.3 Flow cytometry analysis .....	28
3.3.4 Viability assays.....	29
3.3.5 Caspase-3 activity assay.....	29
3.3.6 Proteinase K digestion .....	30
3.3.7 SDS-PAGE.....	30
3.3.8 Immunoblot analysis.....	31
3.3.9 Proteasome activity assay.....	31
3.3.10 Immunofluorescence .....	33
3.3.11 Immunoprecipitation .....	34
3.3.12 Cellular fractionation.....	34
3.4 Statistics and fitting .....	34
<b>4 Results .....</b>	<b>35</b>
4.1 Generation and expression of Cy-PrP and PM-PrP .....	35
4.1.1 Generation of Cy-PrP and PM-PrP.....	35
4.1.2 Ecdysone-inducible expression system.....	37
4.2 Analysis of cytotoxicity in Cy-PrP expressing cells .....	39
4.2.1 Cell viability in Cy-PrP expressing N2a cells .....	39
4.2.2 Cell viability in Cy-PrP expressing 293T cells .....	42
4.2.3 Caspase-3 activity in Cy-PrP expressing N2a cells.....	43
4.3 Proteolysis of Cy-PrP and PM-PrP in N2a cells .....	44
4.3.1 Kinetics of Cy-PrP and PM-PrP proteolysis.....	44
4.3.2 Role of proteasome in Cy-PrP and PM-PrP proteolysis .....	47
4.3.3 Viability in Cy-PrP expressing N2a cells after proteasome inhibition ...	51
4.4 Cellular localisation of Cy-PrP and PM-PrP in N2a cells.....	53
4.4.1 Intracellular localisation of Cy-PrP.....	53
4.4.2 Cy-PrP co-localisation with Hsc70 in EEA1 positive vesicles .....	57

---

4.4.3 Binding of Cy-PrP by Hsc70 .....	60
4.5 Stable Cy-PrP expressing neuronal cell lines .....	62
4.5.1 Cy-PrP and PM-PrP expressing N2a cells .....	62
4.5.2 Phenotype of N2a-Cy-PrP cell lines .....	64
4.5.3 Localisation of Cy-PrP in N2a-Cy-PrP cell lines .....	65
4.5.4 Cy-PrP and PM-PrP expressing PrP <sup>0/0</sup> neuronal precursors .....	67
<b>5 Discussion .....</b>	<b>69</b>
5.1 Cy-PrP toxicity and proteasome in cell culture .....	69
5.1.1 Cy-PrP is <i>per se</i> not toxic to neuronal cells .....	69
5.1.2 Stability and proteolysis of Cy-PrP .....	71
5.1.3 Retro-translocated Cy-PrP .....	73
5.1.4 Cy-PrP/membrane interaction as toxic event .....	75
5.2 Cy-PrP localisation in early endosomal vesicles .....	75
5.3 Hsc70/Hsp70 - prevention against Cy-PrP toxicity .....	78
5.4 Cy-PrP and N2a cell morphology .....	82
5.5 Putative consequences for Cy-PrP expression <i>in vivo</i> .....	83
<b>6 References .....</b>	<b>84</b>
<b>7 Abbreviations .....</b>	<b>102</b>

# 1 Summary

## 1.1 German Summary

Prionenerkrankungen sind neurodegenerative Erkrankungen, neuropathologisch charakterisiert durch spongiforme Vakuolenbildungen im Hirngewebe, den Verlust neuronaler Zellen sowie die verstärkte Proliferation von Mikroglia und Astroglia. Die molekularen Mechanismen für eine derartige Prionen-vermittelte Neurodegeneration sind jedoch nicht vollständig aufgeklärt. In jüngster Vergangenheit wurden Beobachtungen gemacht, die annehmen lassen, dass eine zytosolische fehlgefaltete Form des zellulären Prionoproteins (PrP<sup>C</sup>) der Auslöser für solch einen neuronalen Zelltod sein könnte. Dabei wird angenommen, dass eine Beeinträchtigung des proteasomalen Proteolysesystems eine Ursache für diese zytosolische Akkumulation von PrP darstellt. Die Akkumulation von zytosolischem PrP ist entweder die Folge eines Rücktransports von unreifem nicht-nativ gefaltetem PrP aus dem endoplasmatischen Retikulum (ER), welches unter diesen Bedingungen nicht abgebaut wird (ER-assoziiertes Abbau, ERAD) oder ist zurückzuführen auf einen unzureichenden post-translationalen ER-Import bei gesteigerter Genexpression. In der Tat wurde *in vivo* und *in vitro* ein zytotoxisches Potential für ein zytosolisch exprimiertes PrP (Cy-PrP) gezeigt. Mit Hilfe kultivierter Zelllinien wurden diesbezüglich jedoch widersprüchliche Ergebnisse publiziert, die nicht für eine generelle Toxizität des Cy-PrPs sprechen. Dennoch könnte eine Cy-PrP-vermittelte neuronale Toxizität eine zentrale Rolle bei der Pathogenese von Prionenerkrankungen spielen. Um diesem Mechanismus detaillierter auf den Grund zu gehen, wurden in dieser Studie neuronale N2a Zellen etabliert, die Cy-PrP sowohl transient induzierbar als auch stabil exprimieren.

Mit Hilfe dieses Zellmodells konnten folgende Beobachtungen gemacht werden: Erstens, die transiente Expression von Cy-PrP über einen Zeitraum von 24 h und 48 h war nicht ausreichend, um im signifikanten Maßstab Zelltod in neuronalen Zellen zu induzieren. Dazu wurde zum einen die Vitalität der Zellen mittels MTT-Test gemessen. Zum anderen wurde die Freisetzung von Lactat-Dehydrogenase (LDH) aus den Zellen bestimmt zur Abschätzung der Cy-PrP vermittelten

Zytotoxizität. Um diese Daten zu untermauern wurde zusätzlich getestet, ob eine Cy-PrP Expression zu einer spezifischen Aktivierung der Caspase-3 führt, einem zentralen Parameter innerhalb der Apoptose-Signalwege. Auch hier konnte keine Cy-PrP spezifische Caspase-3-Aktivierung nachgewiesen werden. Um zelltyp-abhängige Effekte auszuschließen wurde das Cy-PrP in nicht-neuronalen Zellen exprimiert, zeigte jedoch auch hier keinen zytotoxischen Effekt in den MTT-Vitalitätstests.

Auf Grund der postulierten biochemischen Ähnlichkeiten von Cy-PrP und PrP<sup>Sc</sup> wurde das Cy-PrP im zweiten Teil der Arbeit bezüglich seiner Proteinase K-Resistenz, seiner Halbwertszeit und intrazellulären Proteolyse näher charakterisiert. Ersteres wurde ermittelt durch den Verdau der Zelllysate mit unterschiedlichen Protease K-Konzentrationen gefolgt von Immunoblotanalysen zur Detektion der resistenten Cy-PrP-Mengen. Im Gegensatz zum PrP<sup>Sc</sup>, welches kontinuierlich von den als positive Kontrolle eingesetzten N2a58/22L-Zellen gebildet wird, wurde das Cy-PrP durch die Proteinase-K-Behandlung vollständig verdaut. Zur Bestimmung der Halbwertszeiten von Cy-PrP und dem vollständigen Prionprotein (PM-PrP) wurden Degradationsexperimente durchgeführt. Mit Hilfe der dazu durchgeführten Immunoblotanalysen konnte ein intrazellulärer Abbau des Cy-PrPs beobachtet werden. Dabei war die Abbaukinetik des Cy-PrPs vergleichbar mit der des PM-PrPs. Nähere Untersuchungen mit Hilfe des proteasomalen Inhibitors Epoxomicin zeigten, dass die Cy-PrP-Proteolyse Proteasom-vermittelt ist. Im Vergleich dazu erfolgte der Abbau des reifen, glycosylierten PM-PrPs unabhängig von der Inhibitorzugabe und war demzufolge nicht Proteasom-vermittelt.

Drittens, obwohl die Cy-PrP-Proteolyse durch das Proteasom erfolgt, hatte die Überexpression von Cy-PrP keinen Einfluß auf die intrazelluläre Proteasomaktivität und das proteasomale Expressionslevel. Um zu untersuchen, ob eine Beeinträchtigung der Proteasomaktivität eine Cy-PrP-vermittelte Zytotoxizität auslösen kann, wurden MTT-Tests in Anwesenheit des spezifischen Proteasominhibitors Epoxomicin durchgeführt. Trotz Inhibition des Proteasoms konnte nach 24 stündiger Cy-PrP-Expression keine Cy-PrP-vermittelte Zytotoxizität detektiert werden.

Viertens, intrazelluläre Lokalisationsstudien mit Hilfe von Fraktionierungsexperimenten und Immunfluoreszenzanalysen ergaben eine inhomogene

intrazelluläre Verteilung des Cy-PrPs, charakterisiert durch starke Aggregat-ähnliche Detektionsmuster in den Immunfluoreszenzanalysen. Dieses Lokalisationsmuster wurde sowohl in den transient exprimierenden Zellen als auch in den stabilen N2a-Cy-PrP Zelllinien beobachtet. Kolokalisationsstudien mit verschiedenen Zellkompartiment-spezifischen Markern ergaben keine ER- und Golgi-Lokalisation für das Cy-PrP. Dagegen wurde das PM-PrP wie erwartet Membran-ständig und im Golgi detektiert. Interessanterweise konnte hier gezeigt werden, dass die großen intrazellulären Cy-PrP-Akkumulationsherde mit endosomalen EEA-1 positiven Vesikeln und mit Hsc70, der konstitutiven Form des Hsp70, kolokalisierten. Dabei war zu beobachten, dass das zytosolische Hsc70 in den Mock-Kontrollen und PM-PrP-exprimierenden Zellen intrazellulär homogen verteilt war. Die Expression von Cy-PrP verursachte jedoch eine zelluläre Umverteilung von Hsc70, beobachtbar als Aggregat-ähnliches Detektionsmuster in den Immunfluoreszenzanalysen. Dabei hatte die Expression von Cy-PrP oder PM-PrP keinen Einfluß auf das Expressionslevel von Hsc70, analysiert in Immunoblotexperimenten.

Fünftens, in dieser Arbeit gelang es zum ersten Mal stabile Cy-PrP-exprimierende Zelllinien zu etablieren. Dabei wurden zwei verschiedene Parentalzelllinien verwendet – die neuronalen N2a Zellen und die PrP<sup>0/0</sup> neuronalen Vorläufer-Zellen. Diese Zelllinien zeigten keine Anzeichen von Apoptose wie verringerte Proliferation oder Chromatinkondensation. In den PrP<sup>0/0</sup> neuronalen Vorläufer-Zellen kolokalisierte das Cy-PrP ebenfalls mit endosomalen EEA-1 positiven Vesikeln und mit Hsc70.

Diese Ergebnisse lassen den Schluß zu, dass allein das Auftreten von zytosolischem PrP nicht primär den neuronalen Zelltod initiieren muß. Zusätzlich könnte die effiziente Entfernung des Cy-PrPs aus dem Zytosol durch einen gezielten Transport in endosomale Vesikel eine erfolgreiche Methode sein, um eine toxische zytosolische PrP-Akkumulation zu unterbinden, was letztendlich von Zelltyp zu Zelltyp in seiner Leistungsfähigkeit variieren kann. Die beobachtete Kolokalisation von Cy-PrP und Hsc70 in solchen endosomalen Vesikeln könnte ein erster Hinweis darauf sein, dass Hsc70 eine wichtige Regulatorfunktion bei der kontrollierten Entstehung von amorphen Cy-PrP Aggregaten und deren Transport in endosomale Vesikel übernimmt. Diese Hsc70-abhängige Translokation von Cy-



PrP könnte einen wesentlichen Schutzmechanismus gegen eine toxische Akkumulation von Cy-PrP in N2a-Zellen widerspiegeln.

## 1.2 English Summary

Prion diseases are a complex group of fatal neurodegenerative disorders with a broad host spectrum, which are characterised by strong neuronal cell loss, spongiform vacuolation and astrocytic proliferation. The molecular mechanisms of prion-mediated neurodegeneration are not yet fully understood. Recently, it has been proposed that neuronal cell death might be triggered by cytosolic accumulation of misfolded cellular prion protein (PrP<sup>C</sup>) due to impairment of proteasomal degradation. Cytosolic PrP<sup>C</sup> could result from either retro-translocation via the endoplasmic reticulum-associated degradation system (ERAD) or abortive translocation of PrP<sup>C</sup> into the ER. Indeed, expression of cytosolic PrP (Cy-PrP) was shown to be neurotoxic both *in vivo* and *in vitro*. However, contradicting results on cytosolic PrP-mediated neurotoxicity in cultured cells have been reported. Cytosolic PrP-mediated cytotoxicity may play a central role in the pathogenesis of prion diseases. In order to investigate the molecular mechanisms of this process, a detailed analysis of N2a cells conditionally expressing cytosolic PrP (Cy-PrP) was performed in this study. The following results were obtained: First, Cy-PrP expression is not *per se* sufficient to trigger cytotoxicity in N2a cells independently of proteasome inhibition. Second, Cy-PrP is degraded with kinetics resembling the degradation of cell membrane-anchored full-length PM-PrP. In this process, the 20/26S proteasome was responsible for Cy-PrP degradation while the proteolysis of matured full length PM-PrP is not affected by the proteasomal system. Third, Cy-PrP accumulates in fine foci when expressed at high levels and co-localises with the cytosolic chaperone Hsc70 in EEA-1 positive endocytic vesicles. From these data it was proposed that the chaperone Hsc70 acts as a regulator for the controlled formation of amorphous Cy-PrP aggregates and their transport to endosomal vesicles. This Hsc70-dependent mechanism may confer protection to N2a cells against toxic accumulation of Cy-PrP in the cytosol.

## 2 Introduction

### 2.1 Prion diseases and infectivity

In the past decade, transmissible spongiform encephalopathies (TSE) or prion diseases have achieved enhanced attention in the media due to the appearance of bovine spongiform encephalopathy (BSE) or “mad cow disease” in the UK. Due to the potential for human infection, BSE has strongly influenced medical, agricultural, economic and political issues in Europe and (Chesebro, 2003). Presently, Scrapie (Sc), BSE and CWD are the most prominent prion diseases in the animal kingdom (Chesebro, 2003). Creutzfeldt-Jacob disease (CJD), kuru, Gerstmann-Sträussler-Scheinker disease (GSS), fatal familial insomnia (FFI) and new variant of Creutzfeldt-Jacob disease (vCJD) are the prion diseases in human. Irrespective of their sporadic, infectious or familial origin, the prion diseases are transmissible disorders in which infectivity is associated with the replication and accumulation of PrP<sup>Sc</sup>, a disease-related insoluble form of the host derived cellular prion protein (PrP<sup>C</sup>). According to the “protein-only” hypothesis, PrP<sup>Sc</sup> is the infectious agent that may convert PrP<sup>C</sup> to PrP<sup>Sc</sup> in a self-propagating reaction (Prusiner, 1998). Additionally, different experimental data have demonstrated that transmission of infectivity is closely connected to PrP<sup>C</sup> (Brandner *et al.*, 1996b; Bueler *et al.*, 1993; Legname *et al.*, 2004; Prusiner *et al.*, 1993). Recently, it has been shown that PrP<sup>C</sup> has to be membrane anchored to mediate transmission of PrP<sup>Sc</sup>-infectivity (Chesebro *et al.*, 2005).

The clinical symptoms of TSE diseases vary in humans. They have in common a progressive development of severe motoric disturbance and dementia leading to death within few months to several years after diagnosis, which can be years to decades after the initial infection in transmissible cases.

Neuropathology of prion disease is characterised by extensive neuronal death, accompanied by spongiform vacuolation as well as astro- and microgliosis, usually combined with widespread deposits of extracellular amyloid aggregates. These aggregates often contain the causative agent PrP<sup>Sc</sup>. Abnormal PrP accumulation occurs in the majority of, but not all, prion diseases.

## 2.2 Cellular prion protein

### 2.2.1 Characteristics and structure of PrP<sup>C</sup>

Murine PrP<sup>C</sup> is a glycoprotein encoded by the highly conserved prion protein gene, *Prnp*, containing three exons with the open reading frame (*ORF*) in exon 3 (Fig. 5). Transcription of the *ORF* sequence and its translation generates PrP with a size of 253 amino acids (Fig. 1). The N-terminal signal peptide (NSP) of the precursor form of the prion protein directs PrP through the endoplasmatic reticulum (ER) and the Golgi apparatus to the cell surface. PrP<sup>C</sup> is N-glycosylated at two asparagin residues located in the C-terminal part of PrP (aa 181 and 197) (Bolton *et al.*, 1985). Attachment of a glycosylphosphatidylinositol (GPI) anchor occurs at position 231 of PrP (Stahl *et al.*, 1987).

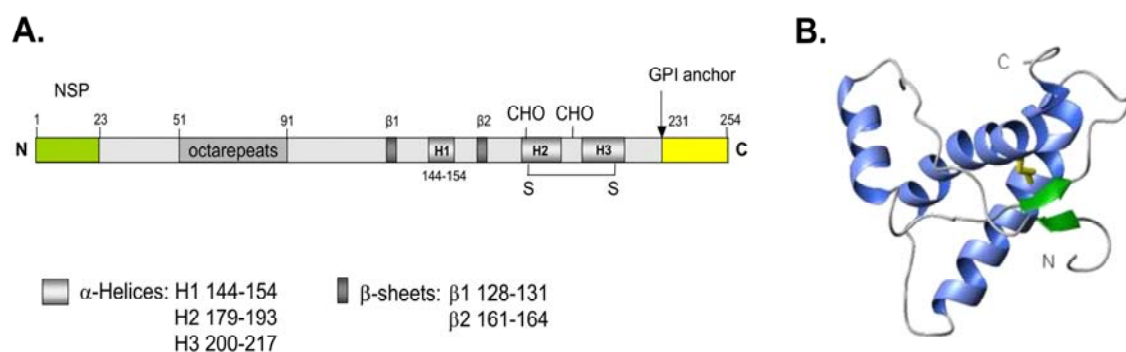


**Fig. 1 Structure of the prion protein.** (A) The cellular prion protein consists of a flexible N-terminal and a globular C-terminal domain. The C-terminal structure contains mainly  $\alpha$ -helical arrangements and two small  $\beta$ -sheet secondary elements. The N-terminus possesses the copper-binding octarepeats; the protein has a signal peptide (NSP) for membrane targeting and is post-translationally modified by addition of two glycosylations as well as a glycosylphosphatidylinositol (GPI) membrane anchor. (B) The nuclear magnetic resonance (NMR) derived structure of mouse PrP (121-231) contains a two stranded anti-parallel beta-sheet and three alpha-helices (Riek *et al.*, 1996a).

In addition, a single disulfide bridge is formed between the cysteine residues at position 179 and 214 (Safar *et al.*, 1990). PrP<sup>C</sup> is attached to the cell membrane through the GPI anchor (Stahl *et al.*, 1987).

The three-dimensional structure of PrP<sup>C</sup>, determined by nuclear magnetic resonance (NMR) spectroscopy (Fig. 1B) and circular dichroism analysis of recombinant murine PrP (Hornemann *et al.*, 1997; Riek *et al.*, 1996b; Riek *et al.*, 1997), consists of a disordered N-terminal region (aa 1-120) and a C-terminal region (121-231) composed of three  $\alpha$ -helices and two  $\beta$ -strands flanking the first  $\alpha$ -helix (Fig. 1A). Although the primary structure of PrP<sup>C</sup> and PrP<sup>Sc</sup> are the same, the two isoforms are very different at the level of secondary structure. PrP<sup>Sc</sup> has a much higher proportion of  $\beta$ -sheets than PrP<sup>C</sup> (45% compared to 3%) (Prusiner, 1998). Typically, PrP<sup>C</sup> occurs as non-, mono- and diglycosylated form correlating with a molecular weight of 27-35 kDa in immunoblot analyses and is, in contrast to the pathological PrP<sup>Sc</sup>, sensitive to proteinase K (PK) treatment. Although the *Prnp* gene is highly conserved as well as the three-dimensional protein structure of PrPs from different species are quite similar, there exist some differences in the primary structure of PrPs in different species. The latter allows distinguishing PrPs from different species by specific anti-PrP antibodies. In this study a chimerical mouse-hamster-mouse PrP, called MH2M PrP (Scott *et al.*, 1993) was overexpressed in neuronal cells. The transgene MH2M PrP contains an epitope, which is not present in murine PrP. This epitope is specifically recognised by the 3F4 antibody and allows distinguishing between host-derived murine PrP and transgene PrP.

### 2.2.2 Biosynthesis and endosomal trafficking of PrP<sup>C</sup>

The biosynthetic pathway followed by PrP<sup>C</sup> is similar to that of other membrane and secreted proteins. Synthesised PrP<sup>C</sup> contains a specific N-terminal signal peptide (NSP) and a C-terminal hydrophobic GPI anchor sequence (Fig. 1A), which are both responsible for co- or post-translational PrP<sup>C</sup> translocation into the rough endoplasmic reticulum (ER), wherefrom PrP<sup>C</sup> transits the Golgi on its way to the cell surface (Harris, 2003). During PrP maturation in the ER, PrP<sup>C</sup> is subjected to several post-translational modifications, including cleavage of the N-terminal signal peptide, addition of N-linked oligosaccharide chains (see Fig. 1), formation of a single disulphide bond, and attachment of the GPI anchor following cleavage of the GPI sequence (Haraguchi *et al.*, 1989; Stahl *et al.*, 1987; Turk *et al.*, 1988). The N-linked oligosaccharide chains added within the ER are subsequently

modified in the Golgi to yield complex-type chains that contain sialic acid and are resistant to endoglycosidase H, but sensitive to Peptide N-glycosidase F (PNGaseF). The majority of PrP<sup>C</sup> is found in detergent-resistant raft domains on the cell surface (Gorodinsky and Harris, 1995; Naslavsky *et al.*, 1997; Vey *et al.*, 1996). After delivery of PrP<sup>C</sup> to the cell surface not all PrP<sup>C</sup> molecules remain there. Some PrP<sup>C</sup> molecules constitutively cycle between the plasma membrane and the endocytic compartment (Shyng *et al.*, 1993). Kinetics analysis demonstrates that PrP<sup>C</sup> molecules cycle through the cell with a transit time of ~60 min. In the process, internalised PrP<sup>C</sup> co-localises with different endosomal markers (Magalhaes *et al.*, 2002). The endocytic recycling pathway is of interest concerning the prion generation, since the initial steps in the conversion of PrP<sup>C</sup> into PrP<sup>Sc</sup> may take place on the plasma membrane or following internalisation of PrP<sup>C</sup> (Borchelt *et al.*, 1992; Caughey and Raymond, 1991).

### 2.2.3 Putative functions of PrP<sup>C</sup>

While the exact function of the cellular prion protein (PrP<sup>C</sup>) is still unclear, there are several references due to increasing knowledge on the localisation and interaction of PrP<sup>C</sup> with other molecules. The reported putative functions include e.g. antioxidant properties (Brown *et al.*, 1997c; Brown *et al.*, 1999; Sakudo *et al.*, 2005a; Senator *et al.*, 2004; Wong *et al.*, 2001), regulatory activity in copper metabolism (Brown *et al.*, 1997a; Korte *et al.*, 2003; Varela-Nallar *et al.*, 2006; Vassallo and Herms, 2003), neuronal differentiation (Chen *et al.*, 2003; Mouillet-Richard *et al.*, 1999; Mouillet-Richard *et al.*, 2000; Sales *et al.*, 2002; Steele *et al.*, 2006), neuroprotective signalling and synaptic function (Collinge *et al.*, 1994; Criado *et al.*, 2005; Maglio *et al.*, 2006; Re *et al.*, 2006; Whittington *et al.*, 1995). The latter is interesting in terms of the *in vivo* situation. PrP<sup>C</sup> was found in presynaptic nerve terminals, synapses in the brain and neuromuscular junctions (Brown, 2001; Fournier *et al.*, 1995; Fournier *et al.*, 2000; Haeberle *et al.*, 2000; Herms *et al.*, 1999; Sales *et al.*, 1998). Furthermore, PrP<sup>C</sup> may be a constituent of the synaptic vesicle membrane, since the PrP<sup>C</sup> interacting protein synapsin I is associated with small synaptic vesicles (Spielhaupter and Schatzl, 2001) and PrP<sup>C</sup> co-localises with the presynaptic vesicle protein synaptophysin (Fournier *et al.*, 1995). PrP<sup>C</sup> affects the neurotransmitter release via synaptic vesicles as shown for

acetylcholine in neuromuscular junction (Re *et al.*, 2006). This would suggest a role in the recycling of the vesicles or a more direct role in the synaptic activity. The latter has been substantiated by some electrophysiological studies conducted in mice devoid of PrP<sup>C</sup>, which exhibit weakened GABA<sub>A</sub>-mediated fast inhibition (Collinge *et al.*, 1994) and impaired long-term potentiation (Collinge *et al.*, 1994; Criado *et al.*, 2005; Maglio *et al.*, 2006; Whittington *et al.*, 1995). Recombinant PrP induces rapid polarisation and development of synapses in embryonic rat hippocampal neurons (Kanaani *et al.*, 2005). *In vivo* accumulation of PrP deposits correlates with abnormal synaptic protein expression in the cerebellum of CJD brains (Ferrer, 2002), and scrapie-infected mice showed a loss of synapses associated with abnormal PrP precedes (Jeffrey *et al.*, 2000), intrinsic dysfunction of cortical and hippocampal neurons (Jefferys *et al.*, 1994) and altered properties of the membrane and synapses (Johnston *et al.*, 1997). In summary, it seems that PrP<sup>C</sup> is not required for most vital synaptic functions, but appears to be important for the fine-tuning of neuronal function. The other putative functions of PrP<sup>C</sup> mentioned above are closely associated with its synaptic function. PrP<sup>C</sup> binds copper via histidines in the octarepeat region and could regulate the copper concentration in the synaptic region of neurons and decrease oxidative stress in synapses (Herms *et al.*, 1999; Kretzschmar *et al.*, 2000; Morot-Gaudry-Talarmain *et al.*, 2003). The latter anti-oxidative activity of PrP<sup>C</sup> has been shown i.a. as copper/zinc-dependent superoxid dismutase activity (Brown *et al.*, 1997b; Brown *et al.*, 1999; Brown and Besinger, 1998; Rachidi *et al.*, 2003; Sakudo *et al.*, 2005b). Signalling function of PrP<sup>C</sup> has been demonstrated by the activation of the non-receptor tyrosine kinase fyn (Kanaani *et al.*, 2005; Mouillet-Richard *et al.*, 2000; Santuccione *et al.*, 2005), which is enriched in brain synaptosomes and has been implicated in long term potentiation (Grant *et al.*, 1992) - a further cellular pathway through which PrP<sup>C</sup> influences the synaptic function.

## 2.3 Neurotoxicity of pathological prion protein

### 2.3.1 PrP<sup>Sc</sup> and neurotoxicity

Neuronal cell loss is a hallmark of prion diseases. Several studies in humans and in mice models of diverse types of prion diseases indicate that neuronal dysfunction and cell death occur through apoptosis, i.e. observed as nuclear DNA condensation and fragmentation as well as caspase-3 activation (Chiesa *et al.*, 2000; Dorandeu *et al.*, 1998; Ferrer, 1999; Giese *et al.*, 1995; Gray *et al.*, 1999; Lucassen *et al.*, 1995). A key area of controversy in the field is the toxicity of the disease-associated isoform PrP<sup>Sc</sup> itself. Although PrP<sup>Sc</sup> is associated with the pathology and infectivity of prion diseases, the link between PrP<sup>Sc</sup> and neurotoxicity is unclear. PrP<sup>C</sup> conversion to PrP<sup>Sc</sup> could cause neurotoxicity through the loss of the normal function of PrP<sup>C</sup>. Compelling evidence for cytotoxicity of PrP<sup>Sc</sup> are: i) PrP<sup>Sc</sup> accumulation in the brain is a hallmark of TSEs, ii) PrP derived peptides e.g. PrP106-126 and PrP82-146 with PrP<sup>Sc</sup>-like characteristics including high  $\beta$ -sheet content, amyloid fibrillar structure and detergent insolubility are toxic *in vitro* and *in vivo* (Bahadi *et al.*, 2003; Bergstrom *et al.*, 2005; Carimalo *et al.*, 2005; Ferreira *et al.*, 2006; Forloni *et al.*, 1993; Salmona *et al.*, 2003). iii) there is a good temporal correlation between the accumulation of PrP<sup>Sc</sup> and the appearance of pathology and clinical symptoms. However, a lot of results using transgenic animal models argue against such a simple relationship between PrP<sup>Sc</sup> accumulation and neurodegeneration: i) Neuronal degeneration was observed in the absence of detectable PrP<sup>Sc</sup> or neuronal damage was not detected despite of high levels of PrP<sup>Sc</sup> (Chesebro *et al.*, 2005; Chiesa and Harris, 2001; Ersdal *et al.*, 2005; Hill and Collinge, 2003). ii) PrP knock out animals do not develop neuropathological and phenotypic alterations similar to TSE-affected animals (Bueler *et al.*, 1993; Manson *et al.*, 1994; Weissmann and Flechsig, 2003). Indeed, adaptive mechanisms during neurodevelopment might compensate the loss of PrP<sup>C</sup> function, masking any phenotype, whereas the loss of PrP<sup>C</sup> function in the adult CNS might be deleterious. However, it has been demonstrated that PrP<sup>C</sup> depletion in the post-mitotic neurons of adult mice also results in healthy animals with no detectable

neuronal cell loss (Mallucci *et al.*, 2002), which also suggests that the loss PrP<sup>C</sup> function may not be the trigger for neurodegeneration. And iii) host PrP<sup>C</sup> expression is necessary for cytotoxicity, since PrP<sup>Sc</sup> itself is not directly toxic to PrP<sup>0/0</sup> neurons (Brandner *et al.*, 1996a; Bueler *et al.*, 1992). Thereby, PrP<sup>Sc</sup> cytotoxicity is only observed in neurons expressing plasma membrane anchored PrP<sup>C</sup> on their cell surface (Chesebro *et al.*, 2005). Additionally, it has been shown that depletion of PrP<sup>C</sup> in conditional PrP knockout mice after prion infection not only stops the development of neuronal damage but also reverses the pathology (Mallucci *et al.*, 2003). Hence, PrP<sup>C</sup> is an indispensable substrate to elicit disease in the brain, and deposition of prions alone does not support neurodegeneration. These findings have kindled a series of further questions on the mechanisms of brain damage in TSEs. So far, it has been postulated that the neurotoxic initiator might be an abnormal form of the host PrP<sup>C</sup>.

### **2.3.2 ER-stress and PrP misfolding**

More recently, it has been published that PrP<sup>Sc</sup> induces apoptosis in N2a cells by activation of the ER-stress response characterised through ER-calcium release, up-regulation of ER chaperones and activation of caspase-12 followed by caspase-3 activation (Hetz *et al.*, 2003). In support of these observations made *in vitro*, caspase-12 activation and induction of ER-stress inducible chaperones were also detected in brains from scrapie-infected mice and humans affected by CJD (Hetz *et al.*, 2003; Hetz *et al.*, 2005; Yoo *et al.*, 2002). PrP can interact with several ER chaperones including Bip, calnexin and protein disulfide isomerase (PDI) (Capellari *et al.*, 2000; Hetz *et al.*, 2005; Jin *et al.*, 2000). However, no direct accumulation of PrP<sup>Sc</sup> in the ER has been described in the TSEs, yet. Rather it has been postulated that changes in the calcium homeostasis might be the trigger for PrP<sup>Sc</sup>-mediated ER-stress and apoptosis (Ferreiro *et al.*, 2006; Hetz *et al.*, 2003; Kristensson *et al.*, 1993; Sandberg *et al.*, 2004; Wong *et al.*, 1996; Yadavalli *et al.*, 2004). Severe ER calcium alterations are also reflected in the accumulation of misfolded proteins in the ER, because calcium is essential for the proper folding of proteins in the ER (Bushmarina *et al.*, 2006; Verkhratsky, 2002; Zhang and Kaufman, 2006). Different overexpressed mutant PrPs associated with human prion diseases were found to be accumulated in the ER in several cell lines



(Campana *et al.*, 2006; Drisaldi *et al.*, 2003; Gu *et al.*, 2003; Negro *et al.*, 2001). Furthermore, ER-stress has also been associated with the pathogenesis of other neurodegenerative disorders, including Alzheimer disease (AD), Parkinson's disease (PD) and Huntington disease (HD) (Campana *et al.*, 2006; Ferreira *et al.*, 2006; Katayama *et al.*, 2004; Lindholm *et al.*, 2006; Ryu *et al.*, 2002; Sherman and Goldberg, 2001; Smith *et al.*, 2005) - all characterised by accumulation of abnormal proteins mostly found as aggregates in the brain.

## 2.4 PrP<sup>C</sup> proteolysis and the proteasomal system

The proteasome is a multi-subunit protease complex located in the cytoplasm and nucleus. Mostly, substrates are modified by Ubiquitin-ligases-mediated poly-ubiquitination followed by ATP-dependent degradation through the 26S proteasome (20S core proteasome and 19S regulator). Particularly, under stress conditions such as oxidative stress and/or intracellular accumulation of malfunctioned and misfolded proteins the proteasome is the major defence system in the cell to prevent "waste overload" (Mehlhase and Grune, 2002). As a membrane-anchored protein, mature PrP<sup>C</sup> is not a natural substrate for the proteasomal 20S/26S system. A small percentage (1-5 %) of the internalised molecules are proteolytically cleaved near residue 110 in the endosomes, and the N- and C-terminal cleavage products are then secreted (Harris *et al.*, 1993; Shyng *et al.*, 1993). Some of the membrane-anchored protein is released into the extracellular medium by cleavage within the GPI anchor followed by proteolytic attack at amino acid 110/111/112 ( $\alpha$ -cleavage) by zinc-metalloproteases of the desintegrin and metalloprotease (ADAM) family in the brain (Cisse *et al.*, 2005; Hooper, 2005; Jimenez-Huete *et al.*, 1998; Vincent *et al.*, 2001).

Analysis of proteasome-dependent PrP<sup>C</sup> proteolysis revealed that the half life or maturation kinetics of wild type-PrP (wt-PrP) or two different mutant PrPs (PG14 and D177N) were unaffected by treatment with specific proteasome inhibitors PSI1 and lactacystin in CHO cells (Drisaldi *et al.*, 2003). In contrast, mutant PrP associated with GSS can be rapidly degraded (half life 10 min) in a cell culture model (Zanusso *et al.*, 1999). Following proteasome inhibition with lactacystin, the protein accumulates and forms aggregates in the ER, Golgi apparatus, and

nucleus. In the absence of proteasome inhibition, the mutant PrP does not form aggregates, suggesting that impairment of the proteasome system may also be involved in pathogenesis of the human disease (Zanusso *et al.*, 1999).

## 2.5 Cytosolic PrP

Secretory or membrane proteins are correctly folded and post-translationally modified in the ER lumen by ER chaperones and supporting calcium ions. However, a small portion of misfolded or incorrectly modified proteins retains in the ER and is subjected to a quality control process by which they are retro-translocated into the cytoplasm and degraded by the proteasome, a process named ER-associated degradation (ERAD) (Bonifacino and Weissman, 1998; Tsai *et al.*, 2002). ER chaperones, like Bip, are implicated in the process of recognition for the proteasomal degradation. This mechanism is intended to ensure that abnormally folded proteins, or those that are not properly modified or assembled into multi-subunit complexes, do not reach the plasma membrane where they might cause cellular damage.

In the case of PrP<sup>C</sup> around 10 % of translated PrP<sup>C</sup> appears to be retro-translocated from ER into the cytosol (Yedidia *et al.*, 2001). Such cytosolic PrP (Cy-PrP) might be characterised by cleaved NSP and GPI anchor sequences. When the proteasomal system is impaired by specific inhibitors such as epoxomicin or MG132, retro-translocated wild type PrP<sup>C</sup> (wt-PrP) or mutant PrP accumulates throughout the cytoplasm (Borchelt *et al.*, 1990; Ma and Lindquist, 2001; Ma and Lindquist, 2002a; Wang *et al.*, 2005; Yedidia *et al.*, 2001). In transfected CHO and PC12 cells expressing PrP from the cytomegalovirus (CMV) promoter, proteasome inhibitors induced accumulation of a non-glycosylated PrP form in the cytosolic environment. However, this PrP contained the N-terminal signal peptide, indicating that it originated from abortive translocation rather than retrograde transport from ER lumen.

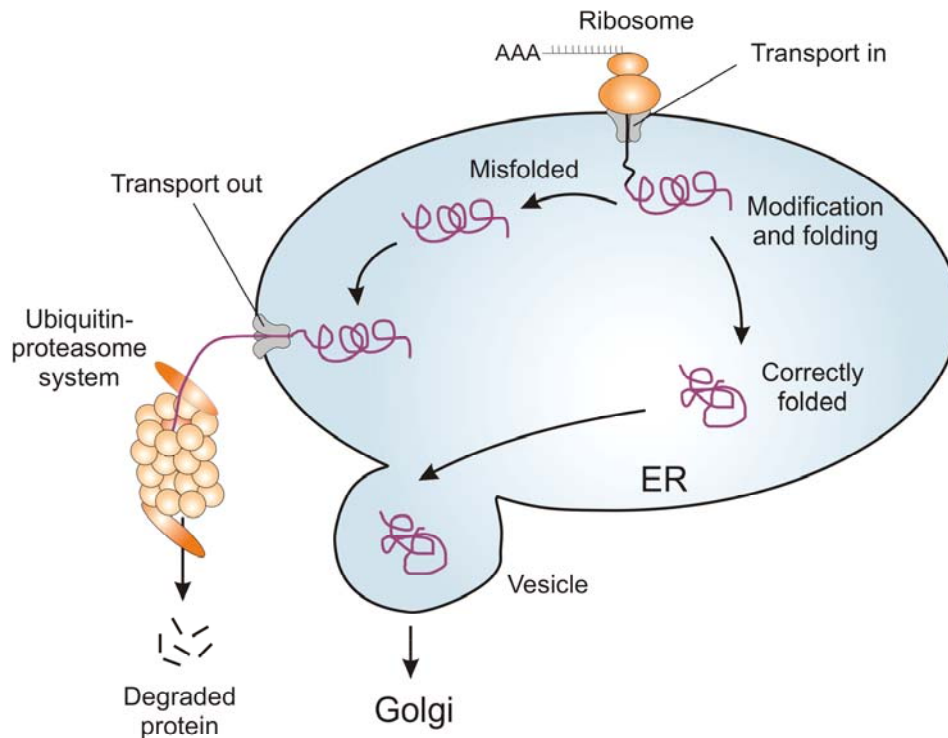


**Fig. 2** Schematic view of maturation of membrane proteins and ER-associated degradation pathway of misfolded forms. Proteins are co-translationally imported into the ER lumen followed by cleavage of the NSPs and different post-translational modifications such as N-linked glycosylation. Correctly folded and modified proteins are transported to the Golgi for final maturation. A small portion of the protein is misfolded or wrongly modified. This is a signal for the ER quality control system to promote their retro-translocation to the cytosol followed by proteasome-mediated degradation.

Otherwise, it has been shown that proteasome inhibition failed to cause PrP accumulation in the cytoplasm in cells expressing endogenous level of PrP and in primary neurons from transgenic (tg) mice expressing PrP<sup>C</sup> from the endogenous promoter (Drisaldi *et al.*, 2003). Thus, it has been proposed that the occurrence of PrP in the cytosol is dependent on its expression level and CMV-driven PrP overexpression saturates the translocation machinery. Indeed, proteasome inhibitors seem also to induce strong transcription of CMV-driven cDNAs (Biasini *et al.*, 2004; Drisaldi *et al.*, 2003). Nevertheless, under physiological conditions the possibility remains that low amounts of cytosolic PrP are produced by abortive translocation or retro-translocation, and accumulate to a toxic level if not removed by the proteasomal system. The level of tolerable Cy-PrP might be also dependent

on its structure and binding to cytosolic protective proteins such as heat shock proteins (HSPs).

### **2.5.1 Cytotoxicity of cytosolic PrP**

The presence of cytosolic PrP suggests that dysfunction of the proteasomal machinery during aging could result in the accumulation of cytotoxic PrP molecules in the cytoplasm. Recent work has highlighted this novel possible role of a dysfunctional proteasome system in the initiation of prion disease. This might explain the onset of some cases of sporadic prion diseases. Lindquist and colleagues showed that inhibition of the proteasome leads to accumulation of cytosolic PrP, which is spontaneously converted into a PK-resistant PrP<sup>Sc</sup>-like species in a neuronal cell model (Ma and Lindquist, 1999; Ma *et al.*, 2002a). Removal of the proteasome inhibitor from the medium did not stop the generation of the PrP<sup>Sc</sup>-like species suggesting a self-perpetuating process once it has been triggered – a characteristic feature of PrP<sup>Sc</sup>-replication (see also 2.1). Accordingly, it was examined in different cell models whether cytosolic PrP species trigger cell death and apoptosis (Fioriti *et al.*, 2005; Ma *et al.*, 2002b; Rane *et al.*, 2004; Roucou *et al.*, 2003). However, it remains controversial whether cytosolic PrP is cytotoxic at a very low level and in a cell type dependent manner. On one hand accumulation of cytosolic PrP in presence of proteasome inhibition is toxic to N2a cells but not to COS 1 and mouse NIH3T3 fibroblasts suggesting that cytosolic PrP is only toxic to neuronal cell types (Ma *et al.*, 2002b). On the other hand, it is assumed that traces of PrP in the cytosol are extremely toxic to neurons and responsible for initiation of neurodegeneration in prion disease since low level expression of Cy-PrP *in vivo* induces massive neuronal cell loss in the granular layer of the cerebellum (Ma *et al.*, 2002b). The latter is supported by the fact that the generation of stably cytosolic PrP-expressing neuronal cell lines failed so far. In contrast to these observations, retro-translocated overexpressed wt-PrP, mutant PrP and Cy-PrP itself are not toxic to human primary neurons, nor is Cy-PrP toxic in two human neuroblastoma cell lines, BE(2)-M17 and SK-N-SH, treated with the proteasomal inhibitor epoxomicin (Roucou *et al.*, 2003). Moreover, Cy-PrP expression appears to protect human neurons against BAX-mediated cell death as previously observed with wt-PrP. N2a cells expressing CMV-driven wt-PrP or

mutant PrPs show no altered morphology or viability after exposure to proteasome inhibitors (Fioriti *et al.*, 2005). Rather, PrP overexpression appears to have a protective effect under such conditions. Furthermore, neurons in the forebrain tolerate higher expression levels of Cy-PrP as granular cerebellar neurons *in vivo* (Wang *et al.*, 2006). Cytotoxic potential of Cy-PrP might be also dependent on the interaction with other cytosolic proteins. As published currently, Cy-PrP-induced apoptosis after proteasome inhibition in human SH-SY5Y neuroblastoma cells involves coaggregation of Cy-PrP with anti-apoptotic Bcl2 (Rambold *et al.*, 2006). Further prominent candidates are members of the heat shock protein (Hsp) family that could control or influence folding reaction to a PrP<sup>Sc</sup>-like structure. Generally, chaperones are potent suppressors of neurodegeneration *in vivo* (Nollen and Morimoto, 2002; Tanaka *et al.*, 2002; Tidwell *et al.*, 2004). After proteasome inhibition retro-translocated Cy-PrP forms aggregates, often in association with Hsc70 in an aggresome-like state (Ma *et al.*, 2001). The expression level of Hsps varies in normal and scrapie-infected cells and brain tissue (Belay and Brown, 2006; Foster *et al.*, 1995; Guzhova *et al.*, 2001; Manzerra and Brown, 1996; Prusiner, 1998; Tanaka *et al.*, 2002; Tatzelt *et al.*, 1995; Voisin *et al.*, 1996) as well as in the different neuronal cell subtypes in the brain in CJD (Kovacs *et al.*, 2001), which might influence the cytotoxicity of Cy-PrP *in vitro* and *in vivo*.

Currently, no complete model exists to explain all these controversial data and it is not certain whether cytosolic occurring PrP is toxic *per se* for neurons or whether the whole process of impaired ERAD is necessary to induce cytotoxicity (kinetics of ER translocation, ER-stress-mediated apoptosis and involved chaperones). Nevertheless, different neuronal cell types might tolerate different distinct amounts of cytosolic PrP by a currently unknown mechanism.

## **2.6 Ecdysone-inducible expression system**

To clarify the cytotoxic potential of Cy-PrP to neuronal cells, an inducible rather than a constitutive expression system was sought to conduct the *in vitro* neurotoxicity experiments. The most widely used Tet-On/Tet-OFF inducible expression system (Baron *et al.*, 1997; Gossen and Bujard, 1992), in which gene expression depends on tetracycline, was not adapted in this study due to major

concerns about reported interactions of PrP with tetracycline (Forloni *et al.*, 2002; Tagliavini *et al.*, 2000). Thus, the ecdysone-inducible dual vector system (Invitrogen) was used, in which gene expression can be regulated through the addition of the ecdysone ponasterone A (PonA), a natural glucocorticoid originating from insects (No *et al.*, 1996; Saez *et al.*, 2000). The vector pVgRXR expresses both VgEcR and RXR, which bind together to form the modified heterodimeric nuclear glucocorticoid receptor VgRXR as transactivator (Fig. 3). The gene of interest is cloned into the multiple cloning site of the pIND vector containing the glucocorticoid receptor recognition element (E/GRE), which is bound by the transactivator VgRXR.

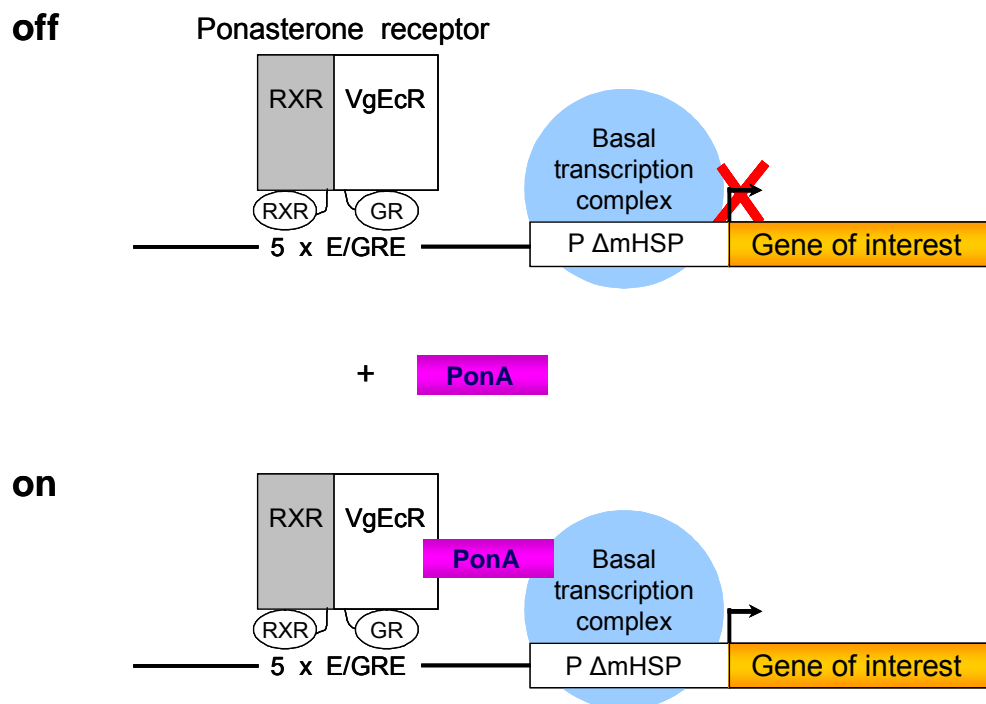


**Fig. 3 Regulation of transcription using the ecdysone-inducible system.** The synthetic receptor VgEcR is a fusion of the ligand-binding and dimerisation domain of the *Drosophila* ecdysone receptor (EcR), the DNA-binding domain of the glucocorticoid receptor (GR), and the transcriptional activation domain of herpes simplex virus (HSV) VP16. VgEcR and human retinoid X receptor  $\alpha$  (RXR) bind as a heterodimer to five copies of the E/GRE recognition sequence (5 $\times$  E/GRE), which are located upstream of the minimal heat shock promoter (P  $\Delta$ mHSP). The E/GRE recognition sequence consists of inverted half-site recognition elements for the RXR and the GR DNA-binding domains. In the absence of PonA (the inducer), the promoter is tightly repressed by co-repressors. When PonA binds to VgEcR, the co-repressors are released, co-activators are recruited, and the complex becomes transcriptionally active.

A comparison of tetracycline-based and ecdysone-based inducible systems reveals that the ecdysone regulatory system exhibits lower basal activity and higher inducibility *in vitro* and *in vivo* (Galimi *et al.*, 2005; Meyer-Ficca *et al.*, 2004; No *et al.*, 1996; Senner *et al.*, 2001). The latter is extremely target-dependent and has to be verified for each target protein. Since ecdysone administration has no apparent effect on mammalian cells, its use for regulating genes should be excellent for transient inducible expression of eventually toxic genes or extremely regulative genes in cell cultures, transgenic mice and for gene therapy.

## 2.7 Objectives

The truncated cytosolic form (Cy-PrP) of PrP<sup>C</sup> is *in vivo* toxic to neurons in the cerebellum of transgenic Cy-PrP-expressing mice and is leading to clinical symptoms like in prion disease. *In vitro* Cy-PrP toxicity is controversial discussed and the mechanisms for selective observed toxicity are unknown. To analyse the cytotoxic potential of Cy-PrP and the underlying mechanisms, *in vitro* neuronal cell models were established to analyse effects of transiently and stably expressed Cy-PrP on N2a cells. Thereby, a set of different experiments were performed to address the following questions:

1. Examination of the cytotoxic potential of inducibly expressed Cy-PrP using different viability and apoptosis assays
2. Role of the proteasome in Cy-PrP-mediated cytotoxicity
3. Analysis of Cy-PrP stability and proteolysis to determine Cy-PrP properties in comparison to PrP<sup>Sc</sup>
4. Subcellular distribution of Cy-PrP by co-localisation with different cell compartment markers and chaperones
5. Generation of stably Cy-PrP expressing cells as cellular models for further investigations of the Cy-PrP metabolism and its effects on cell signalling and survival



## 3 Materials and Methods

### 3.1 Materials and chemicals

#### 3.1.1 Materials and equipments

Absorption and fluorescence in viability assays, proteasome and caspase-3 activity were measured in the „GENios plus“ platereader (Tecan). For fluorescence experiments, samples were analysed in black 96 well plates (Nunc, #137101). Flasks from Greiner and dishes from Nunc were used for cell cultivation. DNA concentration was determined by measuring DNA absorption in the “GeneQuant pro” photometer (Amersham Pharmacia).

Materials for semi-dry immunoblotting:

0.2 µm Protran BA-83 nitrocellulose	Schleicher and Schuell, #10401396
0.2 µm Optitran BA-S 83 nitrocellulose	Schleicher and Schuell, #10439396
Blotpaper Protean XI size	BioRad, #170-3968
Blotpaper xi size	BioRad, #170-3969

#### 3.1.2 Chemicals

All chemical used for molecular and biochemical methods are listed alphabetically as follows:

<b>Name</b>	<b>Company</b>	<b>Cat.-No.</b>
acetic acid	Roth	T179.1
agarose	Invitrogen	15510-027
ampicillin	Roth	K029.2
7-amino-4-methylcoumarin (AMC)	BACHEM	Q-1025
aprotinin	Roth	A162.2
ATP-Mg	Sigma	A-9187
deoxycholal	Sigma	D-6750

---

bis-benzimid (Hoechst)	Sigma	B2261
boric acid	Sigma	B-6768
bovine serum albumin (BSA)	Sigma	A7906
dNTP	New England Biolabs	N0446S
dimethylsulfoxide (DMSO)	Sigma	D-2650
dithiothreitol (DTT)	Sigma	D-9163
ethanol	Roth	5054.1
ethidium bromide	Sigma	E-8751
epoxomicin	Calbiochem	324800
Ficoll type 400	Amersham pharmacia	17-0300-10
genitacin	Invitrogen	10131-027
glycine (99 %)	Sigma	G-5516
glycerol (99 %)	Sigma	G-8898
isopropanol	Roth	9866.1
leupeptin	Sigma	L8511
methanol	Roth	4627.5
3-(4,5-dimethylthiazol-2-yl)-2,5-diphenyltetrazolium bromide (MTT)	Roth	4022.1
NaCl	Sigma	S7653
NP40 10%	Sigma	74388
phenol-chloroform	Roth	A156.1
ponasterone A	Sigma	P-3490
puromycin	Sigma	P9620
SDS (Lauryl sulfate)	Sigma	L-4390
suc-LLVY-AMC	Calbiochem	539142
sucrose	Fluka	84099
Tris-HCl	Roth	9090.1
Tween 20	BioRad	170-6531
zeocin	Invitrogen	R250-01

### 3.1.3 Enzymes

All restriction enzymes and corresponding buffers were purchased from New England Biolabs and used according to the manufacturer's instructions.

<b>Name</b>	<b>Company</b>	<b>Cat.-No.</b>
Ampli-Taq	Roche Applied Biosystems	N8080152
PNGaseF	Sigma	G5166
Proteinase K	Roche Applied Biosystem	1 429 868
T4 DNA Ligase	New England Biolabs	M0202S

### 3.1.4 Cells and media

All media (fluid and plates) as well as trypsin (0.25 % trypsin in PBS, 1 mM EDTA) and PBS solutions were prepared by colleagues of the media and reagent facility at the Paul-Ehrlich-Institut according to the generally used receipts (Sambrook and Russel, 2001). SOC medium for bacterial transformations was purchased from Invitrogen (#15544034).

For cultivation of eukaryotic cells DMEM/Glutamax medium (Gibco, #21885-108) and Optimem medium (Gibco, #31985-047) were used. Media were supplemented with fetal bovine serum (Gibco, #10270-106, Lot 40G9943K). Horse serum (Gibco, #26050-070) was used as blocking reagent for immunoblotting.

The following cell lines were used:

N2a	murine neuroblastoma cell line (ATCC: CCL-131)
HEK293T	human embryonal kidney cell line expressing the large T antigen (ATCC: CRL-11268)
PrP <sup>0/0</sup>	PrP <sup>C</sup> knock out (Zurich I) cerebellar neuronal precursor cell line (gift by D. Rossi, Mailand)

### 3.1.5 Kits

All kits were used according to the manufacturer's directions.

**Table 1 Alphabetical order of the used kits**

Name	Company	Cat.No	Application
BCA Kit	Pierce	23227	Protein concentration
CytoTox-one Kit	Promega	G7890	Cytotoxicity assay (LDH)
EndoFree Plasmid Maxi Kit	Qiagen	12362	Plasmid DNA preparation
QIAfilter Plasmid Midi Kit	Qiagen	12243	Plasmid DNA preparation
Qiaprep Spin Miniprep Kit	Qiagen	27106	Plasmid DNA preparation
QIAquick gel extraction Kit	Qiagen	28704	DNA gel extraction
QIAquick PCR purification Kit	Qiagen	28106	DNA fragment purification
Re-Blot Plus Kit	Chemicon	2500-S	Western striping reagent

### 3.1.6 Antibodies

Antibodies for immunoblotting (IB), immunoprecipitation (IP), immunofluorescence (IF) and FACS analyses were used as shown in Table 2

**Table 2 Summary of all used antibodies and their application**

Primary antibody	Origin	Dilution IB/IP	Dilution IF/FACS	Company/ Cat.No.
$\beta$ -actin	mouse IgG1	1:40.000		Sigma/ A5441
Calnexin	Rabbit	1:2.000		Stressgen/ SPA-860
EEA1	rabbit		1:300	Calbiochem/ 324610
GAPDH	mouse IgG	1:20.000		Abcam/ ab9484
Giantin	Rabbit		1:500	Convance/ PRB-114C
Hsc70	rat IgG1		1:300	QED/ 11042-200

Hsc70	Goat	1:5.000		Santa Cruz/ Sc-1059
PDI	mouse IgG1		1:300	QED/ 11080-50
3F4 PrP(hu)	mouse IgG2a	1:2-5.000	1:250	Chemicon/ MAB1562
SAF32 PrP	mouse IgG2b	1:100		Cayman/ 189720
6H4 PrP	mouse IgG1	1:500		Prionics/ 01-010
R340 PrP	Rabbit	1:500		gift from Aguzzi
20S $\alpha$ 5	Rabbit	1:1.000		Affinity/ ABR- PA11962C-100
Isotype IgG2a	mouse IgG2a		1:250	Becton Dickenson, #553454
Isotype IgG1	mouse IgG1		1:300	Becton Dickenson, #553447
<b>secondary antibody</b>	<b>Origin</b>	<b>Dilution IB</b>	<b>Dilution IF</b>	<b>Company/ Cat.No.</b>
$\alpha$ -mouse-HRP	Goat	1: 15.000		Zytomed/ 81-6720
$\alpha$ -rabbit-HRP	Donkey	1:20.000		Amersham Pharmacia/ NA9340
$\alpha$ -goat-HRP	Donkey	1:10.000		Dianova/ 705-035-147
$\alpha$ -mouse-A594	Goat		1:1.000	Molecular Probes/ A- 21135
$\alpha$ -mouse-A488	Goat		1:500	Molecular Probes/ A- 21121
$\alpha$ -rabbit-A488	Goat		1:500	Molecular Probes/ A- 11070
$\alpha$ -rat-A488	Goat		1:500	Molecular Probes/ A- 11006
$\alpha$ -mouse-RPE	Goat		1:1.000 (FACS)	Dako/ 115-116-171

## 3.2 Molecular biology

### 3.2.1 Plasmids

The plasmids pIND and pcDNA3.1 were used for generation of Cy-PrP and PM-PrP encoding vectors. Plasmid pVgRXR is part of the ecdysone-inducible expression system and encodes the transactivator protein VgRXR. The linearised

plasmid pGEM-Teasy was used for intermediate cloning steps of PCR-fragments harbouring single adenosine (A) overhangs via T/A-cloning.

<b>Name</b>	<b>Resistance gene bacteria/mammalian</b>	<b>Company</b>
pGEM-Teasy	Ampicillin	Promega
pUC18	Ampicillin	gift from M. Hamdorff
pVgRXR	zeocin/zeocin	Invitrogen
pIND	ampicillin/geneticin	Invitrogen
pcDNA3.1 (+)	ampicillin/geneticin	Invitrogen

To ensure correctly inserted transgenic sequences, plasmid DNA was sent to MWG for sequencing.

### 3.2.2 Construction of vectors encoding transgene PrPs

Full length PrP (PM-PrP) and cytosolic PrP (Cy-PrP) were cloned into the ecdysone-inducible vector pIND (Invitrogen) for transient experiments and into pcDNA3.1 (Promega) for generation of stable cell lines. From genomic DNA of MH2M transgenic mice, the open reading frame encoding the mouse-hamster-mouse chimeric PrP was amplified by PCR and cloned into a pPrPcDNA vector generating the pPrPcDNAMH2M plasmid (supplied by G. Barenco, unpublished), which served as template for the following cloning steps. DNA-fragments encoding Cy-PrP and PM-PrP were amplified by PCR using the primers Cy-PrP-for/-rev and F1-for/F2-rev containing the restriction sites *BamHI* and *EcoRI* (see table 3). Amplified PrP fragments were ligated into linearised pGEM-Teasy plasmid (Promega) according to the manufactures protocol. From pGEM-Teasy, Cy-PrP and PM-PrP fragments were removed through *BamHI-EcoRI* restriction followed by ligation into *BamHI/EcoRI* digested target vectors pIND and pcDNA3.1. Sequencing (MWG Biotech) of pIND and pcDNA3.1 using the primers pIND-for/-rev and T7-for/BGH-rev(pCR3.1) (see table 3) verified correct cloning of Cy-PrP and PM-PrP into pIND and pcDNA3.1 vectors.

### 3.2.3 Polymerase chain reaction

In the polymerase chain reaction (PCR), DNA-dependent DNA-polymerases amplify specific DNA sequences of different origins, such as plasmid, genomic or complementary DNA bordered by two primer sequences (Mullis and Faloona, 1987; Saiki et al., 1985). In this study Taq-polymerase (Roche Applied Biosystems) isolated from *Thermophilus aquaticus* was used, which shows a temperature optimum of 72 °C. One complete PCR cycle contains a DNA denaturation step at 94 °C followed by primer annealing to the single stranded DNA template. The annealing temperature (TD) is adjusted according to length and composition of the DNA template. The TD can be calculated roughly corresponding to the Wallace rule (Suggs et al., 1981) as follows:  $TD = 4 \times (G+C) + 2 \times (A+T)$  or tested by temperature gradient PCR as done in this study. DNA elongation is performed at 70-75 °C corresponding to the Taq-polymerase activity optimum. The length of the template determines the elongation time, since Taq-polymerase has an amplification activity of approximately 1 kb DNA/min. Multi-repeating of the cycle leads to amplification of the DNA-fragment in an exponential manner. For amplification of PrP sequences the following PCR mix (50 µl) was used:

1x PCR buffer (20 mM Tris/HCl, pH 7.5; 100 mM KCl; 1.5 mM MgCl<sub>2</sub>; 1 mM DTT; 0.1 mM EDTA, 0.5 % Tween 20; 0.5 % Nonidet P40; 0.01 % gelatine)  
0.5 pmol/µl of each primer  
300 µM dNTPs  
2.5 units Ampli-Taq  
10-20 ng template (plasmid DNA)

PCR was performed at following conditions:

94 °C 2.5 min

94 °C 30 sec

gradient 45-65 °C 45 sec

72 °C 45 sec

72 °C 4 min; subsequent cool down to 4 °C



29 cycles

All PCR reactions were performed in a “PTC200” Peltier thermal cycler (MJ Research). Analysis of PCR fragments were performed in 1 % agarose gel followed by purification of the PCR sample using PCR purification kit (Qiagen).

Colony-PCR was used to identify bacterial clones containing the transgene DNA fragments. *E.coli* colonies were picked and transformed in PCR tubes followed by PCR as described above except the annealing temperature was 54 °C. Using the designed primers M13-for/-rev, pIND-for/rev and T7-for/ BGH-rev(pCR3.1) (see table 3) allowed testing of the right orientation of integrated fragments in the vectors pGEM-Teasy, pIND and pcDNA3.1.

### 3.2.4 Oligonucleotides

**Table 3 Sequences of used oligonucleotides**

Name	5'-sequence-3'
F1-for	ATCGGGATCCGCCACCATGGCGAACCTTGGCTACTGG
F2-rev	TGCGGAATTCACCTCACTCATCCCACGATCAGGAAGATGAGG
Cy-PrP-for	ATCGGGATCCGCCACCATGAAAAAGCGGCCAAAGC
Cy-PrP-rev	TGCGGAATTCACCTCACTCAGCTGGATCTTCTCCCGTCCG
M13-for	GTAAAACGACGGCCAG
M13-rev	CAGGAAACAGCTATGAC
pIND-for	AGAAAGAAGAACTCACACACAGC
pIND-rev	AACTAGAAGGCACAGTCGAGG
T7-for	TAATACGACTCACTATAGGG
BGH-rev(pCR3.1)	TAGAAGGCACAGTCGAGG

### 3.2.5 Agarose gel electrophoresis

For analytical and preparative purposes, DNA molecules were separated by agarose gel electrophoresis. Negatively charged DNA molecules migrate with different velocity dependent on their size through such a gel upon application of electric current. For DNA molecules with a size of 0.5-14 kb 1-2 % agarose gels were produced by dissolving agarose in Tris-acetate-EDTA (TAE) buffer by



heating in a microwave oven. Cooled agarose solution was supplemented with 0.5 µg/ml ethidium bromide for DNA labelling. DNA solution was mixed with 1/6 loading buffer and separated on gel at 120 V. 100 bp-, 1 kb- and 2-log-DNA ladders (New England Biolabs) served as DNA size standard. For preparative agarose gel electrophoresis, DNA fragments were cut out and purified using QIAquick gel extraction kit (Qiagen).

TAE buffer

40 mM Tris-acetate

1 mM EDTA

adjusted to pH 7.5

6 x loading buffer :

0.25 % bromphenolblue

0.25 % xylene-cyanol FF

15 % Ficoll (typ400, Pharmacia)

### **3.2.6 Restriction and ligation**

DNA molecules were digested with type II restriction endonucleases to provide DNA molecules for ligation or to analyse vectors for the correct transgene integration. All DNA restrictions were performed using commercially available restriction endonucleases from New England Biolabs (NEB, Schwalbach, Germany) according to the manufacturer's instructions. Ligation of two double stranded nucleic acid molecules was achieved by usage of T4 DNA ligase, which catalyses the formation of phosphodiester-bonds between the fragments, under consumption of ATP. 50-100 ng DNA with molar ratio of backbone to insert 1:3 were incubated with 100 U T4 DNA ligase (NEB) in ligase buffer (50 mM Tris-HCl pH 7.5, 10 mM MgCl<sub>2</sub>, 10 mM DTT, 1 mM ATP, 25 µg /ml BSA) with end volume of 20 µl at 4 °C overnight.

### **3.2.7 DNA purification**

#### **3.2.7.1 PCR purification kit**

DNA from restriction reactions or PCR samples were purified using the "QIAquick PCR purification kit" (Qiagen) according to the manufacturer's instructions.

Thereby, DNA molecules bind to silica-gel membrane. After washing, DNA was eluted with bidestillated water.

### **3.2.7.2 Phenol extraction and DNA precipitation**

Phenol extraction allows removal of proteins from DNA/RNA solution (Sambrook *et al.*, 2001). The DNA solution was filled up with water to 200 µl and mixed step by step 1:1 with phenol (pH 8.0), phenol-chlorophorm-isoamylalcohol (25:24:1, v/v) and chlorophorm. In between, each sample was centrifuged for 1 min at 16 100 x g and the aqueous phase was transferred into a new tube. DNA from the aqueous phase recovered after the last chlorophorm extraction was precipitated with 2.5 fold volume ethanol in presence of 0.3 M Na-acetate (pH 5.2) for 1 h at -80 °C or with 0.7 volume isopropanol at room temperature for 5 minutes. Precipitated DNA was centrifuged at 16100 x g at 4 °C for 30 min, washed twice with 70 % ethanol, dried and suspended in 50 µl of bidestillated water.

### **3.2.8 Photometric determination of DNA concentration**

DNA concentration was determined using ultraviolet absorption spectroscopy. Absorption at 260 nm ( $A_{260}$ ) and 280 nm ( $A_{280}$ ) was measured and DNA concentration was calculated as follows:

$$c [\mu\text{g/ml}] = A_{260} \times 50 \times \text{DF}$$

DF = dilution factor

50 = specific absorption coefficient for dsDNA

Absorption of 1.0 corresponds to 50 µg/ml double stranded DNA (Sambrook *et al.*, 2001). The ratio  $A_{260}/A_{280}$  served as value DNA purity. Pure DNA samples showed ratios of 1.8-2.0.

### **3.2.9 Working with bacteria**

#### **3.2.9.1 Cultivation of bacteria**

*E. coli* DH5α were grown as suspension culture in LB-medium (10 g/l peptone, 5 g/l yeast extract, 10 g/l NaCl pH 7.0 with NaOH) at 200 rpm or on LB agar plates (2 % agar in LB-medium) at 37°C overnight. Selection of transformed bacteria was

achieved by adding different antibiotics corresponding to the plasmid resistance genes (50 µg/ml ampicillin, 25 µg/ml zeocin). Identification of positive bacteria clones of pGEM-Teasy transformants were analysed by blue/white screening after cultivation on LB-agar plates containing 50 µg/ml X-Gal and 10 µg/ml IPTG. For long-term storage, 1 ml bacterial suspension was mixed with 1 ml DMSO solution (7 % v/v) and transferred to -80°C.

### **3.2.9.2 Generation of competent bacteria**

Chemically competent bacteria of the *E. coli* strain DH5α were produced as described by Hanahan (Hanahan *et al.*, 1991). Briefly, 200 ml LB-medium were inoculated with 2 ml of *E. coli* DH5α overnight culture and incubated at 200 rpm and 37°C until bacteria achieved the optical density of 0.2-0.3 at 600 nm (OD<sub>600</sub>). Following 10 min incubation on ice, bacteria were centrifuged at 5.000 x g for 10 min at 4°C and the pellet was suspended in 50 ml of cold 100 mM CaCl<sub>2</sub>. Centrifugation was repeated following 30 min incubation on ice and the pellet was suspended in 10 ml of cold 50 mM CaCl<sub>2</sub> supplemented with 20 % glycerine. 100 µl aliquots were frozen immediately in liquid nitrogen and stored at -80 °C.

### **3.2.9.3 Transformation of bacteria**

Chemically competent bacteria *E. coli* DH5α were thawed on ice. 50 µl bacteria suspension were mixed with 2-10 µl of ligation reaction or 1 ng pUC18 (as control) and incubated for 30 min on ice. Then, bacteria suspension was incubated at 42 °C for 60 sec and cooled down on ice for 2 min. After addition of 800 µl SOC medium bacteria were incubated at 37°C for 1-2 h. 100 – 400 µl transformed bacteria were plated on agar plates and cultivated at 37°C overnight.

### **3.2.9.4 Plasmid DNA preparation**

Plasmid-DNA isolation and purification was performed using plasmid preparation kits (Qiagen) according to the manufacturer's directions. Briefly, following bacterial lyses, the plasmid-DNA bound to an anion exchange column. The column was washed and plasmid DNA was eluted by bidestillated water. Plasmid-DNA concentration was determined photometrically (3.2.8). To identify correctly ligated

plasmid-DNA, 3 ml of bacterial transformants were prepared using Qiagen Mini-kit for low-scale plasmid-DNA isolation followed by DNA-restriction analysis and DNA-sequencing. Mini preparations were done with 3 ml of an overnight bacterial culture using the Mini-kit (Qiagen) to identify the correct ligated and amplified plasmid DNAs in optimised restriction analyses. To transfect plasmid-DNA into eukaryotic cells, 200 ml of bacterial transformants were prepared using Endo-free Maxi kit (Qiagen) for large-scale plasmid-DNA isolation with high purity. These purified plasmids were used in transfection experiments with eukaryotic cells.

### **3.3 Cell biology and biochemistry**

#### **3.3.1 Cultivation of eukaryotic cells**

All cell lines were cultured in Dulbecco's Modified Eagles Medium (DMEM; Gibco BRL, Eggenstein, Germany) supplemented with glutamax and 10 % fetal calf serum (Gibco BRL, Eggenstein, Germany) at 37 °C and 5 % CO<sub>2</sub>. For transient transfection 2 x 10<sup>6</sup> cells were seeded in T75 flasks and incubated for 24 h followed by transfection using Lipofectamin 2000 (Invitrogen) according to the manufacturer's directions. Plasmids encoding PM-PrP or Cy-PrP (4 µg) and the ecdysone receptor (4 µg) were transfected into N2A cells and 293T cells. After 24 h PrP expression was induced using 0.5-2 µM PonA (Invitrogen) for different periods of time as indicated. To generate stable Cy-PrP expressing cell lines, N2a cells were transfected with Cy-PrP or PM-PrP encoding plasmid pcDNA3.1 (Promega, 8 µg) followed by selection of antibiotic-resistant cell clones using 1 mg/ml G418 48 h post-transfection. After 3 weeks of antibiotic selection, Cy-PrP- and PM-PrP-expressing cell clones were further cultivated in 0.5 mg/ml G418 containing medium.

In the case of neuronal PrP<sup>0/0</sup> precursors, 1.4 x 10<sup>6</sup> cells were seeded in 10 cm dishes for 24 h and transfected with 24 µg Cy-PrP encoding plasmid pIRES2-puro in serum-free Optimem (Promega) using FUGENE transfection reagent (DNA:reagent 1:3). After 6 h incubation at 37 °C, FBS was added to a final concentration of 10 % and transfection procedure was elongated overnight at 37 °C followed by medium substitution against DMEM containing 10 % FBS.

Selection of antibiotic-resistant cell clones started 48 h post-transfection using medium supplemented with 2 µg/ml puromycin and 10 ng/ml basic fibroblast growth factor (BFGF, Sigma). Selected stable Cy-PrP-expressing cell clones were further cultivated in 1 µg/ml puromycin containing medium.

### 3.3.2 Determination of the cell number

Cells were incubated 1:1 (v/v) with 0.4 % trypan blue solution (Sigma, #T8154) for 5 min at room temperature and counted in a Neubauer chamber (Fischer, #9161078). Trypan blue is able to stain cells with compromised membrane integrity. Thus, living and dead cells can be distinguished by uptake of the blue dye into dead cells. Only living cells were used for cell number determination. Cell numbers were calculated as followed:

$$\text{cell no.} / 4 (s) \times 2 (DF) = X \times 10^4 \text{ cells/ ml}$$

s = no. of squares

DF = dilution factor

Same cell numbers were seeded for the experiments as indicated.

### 3.3.3 Flow cytometry analysis

To analyse green fluorescence protein (GFP) and PM-PrP expression in N2a and 293T cells, flow cytometry (FACS) was performed as follows: cells were washed with PBS, harvested with PBS containing 1 mM EDTA and centrifuged at 200 x g at 4 °C.  $10^5$  cells were equilibrated in 1 ml FACS buffer (1 % BSA, 5 mM EDTA, 0.01 %  $\text{NaN}_3$  in PBS) on ice. After centrifugation at 200 x g and 4 °C, cells were suspended in 500 µl FACS buffer and GFP fluorescence was measured with the “FACScan” machine (Becton Dickinson). For PM-PrP, cells were suspended in 100 µl FACS buffer containing 3F4 antibody 1: 1.000 dilution and incubated on ice for 30 min followed by washing with 4 ml FACS buffer. Then, cells were incubated with mouse-anti-goat-IgG-IR-PE-(Fab2) 1:200 in 100 µl FACS-Puffer 30 min on ice, washed twice with FACS buffer and suspended in 500 µl FACS buffer for FACS measurement. All measurements were analysed using the “Cell Quest” software from Becton Dickinson.

### 3.3.4 Viability assays

For cell viability analysis, 20.000 cells/well were plated in 96-well plates one day after transfection and grown for additional 24 h or 48 h in cell culture medium supplemented with 2  $\mu$ M PonA for transgene induction. Firstly, cell viability was quantified by the 3-(4,5-dimethylthiazol-2-yl)-2,5-diphenyltetrazolium bromide (MTT) method. Briefly, 10  $\mu$ l of MTT (2 mM) labelling reagent were added to each well, and the samples were incubated for 4 h at 37 °C. 100  $\mu$ l of solubilisation mixture (isopropanol/0.04 N HCl) were added to each well, and the samples were thoroughly mixed. Absorbance of blue formazan was measured with a plate reader at 560 nm. Optimisation of cell counts ensured an OD<sub>560</sub> of 0.2-1.0. Secondly, cell injury was monitored by measuring lactate dehydrogenase (LDH) release into the supernatant by using the CytoTox-one kit (Promega). LDH was assayed by an indirect fluorescence measurement of NADH formation during lactate oxidation to pyruvate using resazurin, with an excitation wavelength of 535 nm and an emission wavelength of 610 nm. For proteasome inhibition epoxomicin was diluted in DMSO (1 mM) and added at 50 nM to the culture medium for 16 h prior MTT or LDH measurement.

### 3.3.5 Caspase-3 activity assay

Cells transfected with mock plasmid, Cy-PrP or PM-PrP were lysed in 10 mM HEPES containing 2 mM EDTA, 0.1 % NP40, 1 mM DTT, 1 mM PMSF, 2  $\mu$ g/ml aprotinin and 2  $\mu$ g/ml leupeptin for 15 min at 4 °C followed by centrifugation at 10000 x g. Protein concentration was determined in supernatants by the micro-BCA assay (Pierce). 150  $\mu$ g protein of the supernatant were incubated with 50  $\mu$ M caspase-3 specific substrate DMQD-AMC for 60 min at 37 °C in reaction buffer (100 mM HEPES, 0.5 mM EDTA and 20 % glycerol) in presence or absence of 10 mM specific inhibitor AcDEQD-CHO. Caspase-3 mediated release of AMC as measured by fluorescence with an excitation wavelength of 380 nm and an emission wavelength of 465 nm (same principle as shown in Fig. 6 under 3.3.9) Non-specific caspase-3-like activity was calculated by subtraction of fluorescence of inhibitor treated samples. Values were normalised as percentage to mock-transfected cells.

### 3.3.6 Proteinase K digestion

Cells were lysed in lysis buffer (50 mM Tris pH 7.4, 150 mM NaCl, 0.1 % Triton X-100, 0.5 % DOC, 1 mM DTT, 2 mM EDTA and 1 µg /ml pepstatin and leupeptin) and incubated for 15 min on ice followed by centrifugation step at 10.000 x g for 3 min. Protein concentration was determined in supernatants by the micro-BCA assay (Pierce). Protein concentration was adjusted to 0.6 mg/ml by adding lysis buffer. 1 or 10 µg/ml proteinase K (PK, Roche diagnostics) was added to 200 µg protein and the volume was adjusted to 100 µl with PBS incubated at 37 °C for 30 min. Proteinase K activity was stopped by addition of 1 mM Pefablock (Serine protease inhibitor, Roche diagnostics) on ice. After 5 min samples were centrifuged at 16.000 x g for 45 min at 4 °C, supernatants were discarded and pellets were suspended in 20 µl sample buffer (see 3.3.7) followed by 5 min boiling at 95 °C. Detection of PK-resistant Cy-PrP was performed by immunoblot using 12 % SDS-PAGE and 3F4 antibody.

### 3.3.7 SDS-PAGE

Cells were washed with PBS, harvested with PBS containing 1 mM EDTA and centrifuged at 200 x g at 4°C. Cells were lysed in lysis buffer (50 mM Tris pH 7.4, 150 mM NaCl, 0.1 % Triton X-100, 0.5 % DOC and 1 mM DTT) and incubated for 30 min on ice. Lysates were homogenised by pulling up and down with „Omnifix-F 1ml“ syringes (Roth, #H999.1) using “0,4 x 22 mm, 27 G ¾” needle (Roth, #X133.1) before 10 min centrifugation step at 1.000 x g, Post-nuclear supernatants were collected and protein concentration was determined in supernatants by micro-BCA assay (Pierce). Equal amounts of protein were electrophoretically separated due to their molecular weight in 10 % or 12 % polyacrylamide gels (NuPAGE from Invitrogen or self-poured) according to Laemmli (Laemmli, 1970). Protein denaturation was achieved by 5 min incubation at 95 °C in presence of 5 % β-mercaptoethanol and 5 % SDS added to the sample buffer. Discontinuous SDS polyacrylamide gel electrophoresis (SDS-PAGE) was performed at 100-200 V with MES buffer (Invitrogen, #NP0002) using precast gels or the following running buffer using self cast gels:

SDS running buffer (1 l)

36 g glycine  
7.75 g Tris  
1.25 ml 20 % SDS  
add 250 ml aqua bidest

4 x sample buffer

200 mM Tris-HCl pH 6.8  
400 mM DTT  
20 % SDS  
40 % glycerol  
20 %  $\beta$ -mercaptoethanol  
0.4 % bromphenolblue

Seebly 2 plus and MultiMark (both from Invitrogen) were used as protein standards.

### 3.3.8 Immunoblot analysis

Electrophoretically separated proteins were transferred onto a 0.2  $\mu$ m nitrocellulose (Schleicher und Schuell) by semi-dry blotting at 15 V for 20-30 min using the "semi-dry cell chamber" from Bio-Rad. To block non-specific binding of the antibodies, the membrane was incubated with 10 % horse serum (Gibco) in PBS (pH 7.4) containing 0.1 % Tween 20. The blots were incubated with the primary antibodies (dilutions see Table 2, 3.1.6) 3F4 anti-PrP, anti-proteasome 20S subunit  $\alpha$ 5 (anti-20S $\alpha$ ), anti-Hsc70, anti-GAPDH, anti- $\beta$ -actin and anti-calnexin for 1h at room temperature. For the detection of primary antibodies, appropriate peroxidase conjugated secondary antibodies were used (3.1.6, Table 2) in conjunction with SuperSignal west pico chemiluminescence substrate (Pierce Chemical Co., Rockford, Illinois) according to the manufacturer's directions.

Semi-dry blot buffer:

3.03 g Tris  
14.4 g glycine  $\rightarrow$  adjusted to 1 l bidest

### 3.3.9 Proteasome activity assay

Cells were washed twice with PBS, harvested by scraping and lysed in 250 mM sucrose, 25 mM HEPES pH 7.8, 10 mM MgCl<sub>2</sub> and 1 mM EDTA by repeating freezing and thawing cycles. To remove non-lysed cells, nuclei and debris, the



lysates were centrifuged at  $16.100 \times g$  at  $4 \text{ }^\circ\text{C}$  for 30 min. Supernatants were used for activity assays.

The proteasome has three different catalytic activities promoted by inner ring  $\beta 1$ ,  $\beta 2$ - and  $\beta 5$ -unit. Thereby, chymotrypsin-like activity appears to play a major role and is characterised by cleavage behind LLVY sequence. Thus, AMC-conjugated LLVY substrate (LLVY-AMC) was used to determine specific ATP-dependent proteasome activity (Fig. 4). Proteasome-mediated cleavage behind the tyrosine releases free AMC resulting in fluorescence with an emission wavelength at 460 nm following excitation at 380 nm. The fluorescence can be observed as blue light bands in native proteasome activity gels or was measured at 460 nm in a fluorescence plate reader.

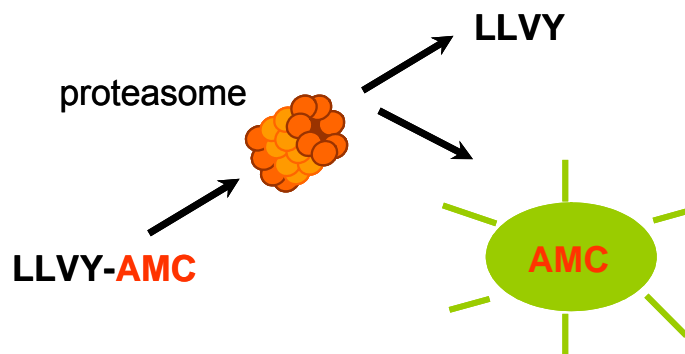


**Fig. 4 Principle for measurement of proteasome activity.** Proteasome peptide substrate LLVY is conjugated with fluorophor aminomethylcumarin (AMC). Bound AMC does not emit fluorescence. Proteasome-mediated cleavage behind the tyrosine releases free AMC, which emits light at 460 nm following excitation at 380 nm.

### 3.3.9.1 Native gel electrophoresis

200  $\mu\text{g}$  protein of supernatant were loaded on a non-denaturing 4.5 % Tris-Borat-EDTA gel (supplemented with 2.5 % sucrose) and electrophoretically separated at  $4 \text{ }^\circ\text{C}$  and 50 V for 20 h. The native gel was incubated in developing buffer (50 mM Tris pH 7.8, 25 mM KCl, 10 mM NaCl, 1.1 mM  $\text{MgCl}_2$ , 0.1 mM EDTA, 10% glycerol, 1mM DTT) for 15 min at RT. Visibility of proteasomal activity was achieved by incubation with 200  $\mu\text{M}$  LLVY-AMC substrate and 5 mM ATP (in developing buffer, pre-heated on  $37 \text{ }^\circ\text{C}$ ) for 15-30 min at RT followed by excitation

using UV light. Images were recorded with a digital camera (Olympus) to visualise the two fluorescent bands of active 26S and 30S proteasome complexes.

### **3.3.9.2 Plate reader assay (96 well)**

20 µg protein of the supernatant were incubated with 200 µM LLVY-AMC substrate and 5 mM ATP in incubation buffer (450 mM Tris pH 7.8 at 4 °C, 15 mM Mg-Acetate, 15 mM MgCl<sub>2</sub>, 90 mM KCl, 1 mM DTT) at 37 °C for 30 min. Prior fluorescence detection, 0-100 µM of free AMC-standard was added in the upper row of the 96 well plate. Non-specific proteasome activity was determined by addition of 50 nM epoxomicin (Epoxo). Values were normalised as percentage to mock cells.

### **3.3.10 Immunofluorescence**

Cells were cultured on cover slips in 24-well culture plates (40.000 cells/well) and induced with 0.5 µM PonA for 16 h. To visualise surface staining of PM-PrP, cells were washed in PBS and fixed in 4 % paraformaldehyde (PFA) for 20 min. 4 % PFA was prepared by heating 80 ml PBS to 60-70 °C and addition of 4 g PFA while stirring on a hot plate in the fume hood. Volume was adjusted to 100 ml with PBS, PFA was cooled down at room temperature and pH was adjusted to 7.4. For intracellular staining, cells were then incubated with 0.1 % Triton-X-100 in PBS containing Hoechst dye (bis-benzimid, 10 µg /ml) for 10 min at room temperature. After blocking with 1 % BSA in PBS for 30 min, cells were incubated with primary antibodies (dilutions see table 2, 2.1.6) against PrP (3F4 antibody), giantin, protein disulfide isomerase (PDI), early endosomal antigen 1 (EEA1), and Hsc70 in PBS at 37 °C for 1h. Alexa-594- and Alexa-488-labelled secondary antibodies (Molecular Probes) were used. After washing and embedding procedures (DakoCytomation, Dako, #S3023), the cells were examined by Zeiss LSM 510 scanning confocal microscope.

### **3.3.11 Immunoprecipitation**

100 ng protein of the cell lysates were incubated with a 1:500 dilution of the anti-PrP antibodies 6H4, R340 or SAF32 overnight at 4 °C. Antibody-protein complexes were immobilised by adding 20 µl magnetic protein G-sepharose beads (Amersham Pharmacia, # 71-7083-00 AG) for 1 h at 4 °C. After several washing steps with 500 µl PBS, the beads-bound antibody-protein complexes were dried 10 min in a spinvac (Eppendorf) and suspended in 1 x sample buffer without β-mercaptoethanol. After boiling for 5 min at 95 °C the immunoprecipitation samples were loaded on a gel for SDS-PAGE followed by immunoblot analysis with 3F4 anti-PrP antibody and anti-Hsc70 antibody (Table 2, 3.1.6).

### **3.3.12 Cellular fractionation**

Mock-, Cy-PrP- or PM-PrP-transfected N2a cells were washed with PBS, harvested with 1 mM EDTA in PBS and centrifuged at 200 x g at 4 °C. Cells were lysed by shaking in bidestillated water (bidest) containing 1 mM DTT at 4 °C for 1 h followed by centrifugation at 16.100 x g and 4 °C for 30 min. Supernatants served as soluble cytosolic fraction. Pellets were suspended in 50 µl NP40 containing buffer (50 mM Tris pH 7.4, 150 mM NaCl, 1 % NP40 and 1 mM DTT), incubated on ice for 15 min and centrifuged at 16.100 x g and 4 °C for 10 min. Supernatants comprised the insoluble membrane fraction.

## **3.4 Statistics and fitting**

Standard abbreviation and significance level were calculated using Origin6.0. To test the significant difference of two samples ( $n > 6$ ), populations was analysed with the t-test (two populations) using test type “independent” and a significance level of 0.05. Fitting of the kinetics of Cy-PrP and PM-PrP degradation were also done by Origin6.0.

## 4 Results

It has been shown for the first time in 2002 that small quantities of a new PrP isoform, called Cy-PrP, produced by retro-translocation from the ER into the cytosol induces cytotoxicity in neuronal N2a cells (Ma *et al.*, 2002b). In a transgenic mouse model Cy-PrP causes neuronal cell loss and gliosis in the granular layer of the cerebellum, which results in a phenotype characterised by ataxia, tail rigidity, frequent scratching and weight loss. These are typical symptoms associated with prion diseases. However, the mechanisms for neuronal cell death and the pathology caused by Cy-PrP are still unknown.

In this study the Cy-PrP protein was expressed in neuronal N2a cells, which served as model cell line, using an inducible expression system. The inducible Cy-PrP expression of Cy-PrP facilitates detailed characterisation of Cy-PrP-mediated cytotoxicity in a time dependent in this cell type.

### 4.1 Generation and expression of Cy-PrP and PM-PrP

#### 4.1.1 Generation of Cy-PrP and PM-PrP

N2a cells are murine neuroblastoma cells harbouring endogenous prion protein on their cell surface. Thus, transgene PrPs bearing an internal tag were cloned to distinguish them from the endogenous PrP. To avoid unspecific effects on protein conformation and function by common protein tags (Bian *et al.*, 2006; Ledent *et al.*, 1997; Supattapone *et al.*, 2000), a cDNA encoding a chimeric mouse-hamster-mouse PrP, MH2M (Scott *et al.*, 1993), was used to generate Cy-PrP and PM-PrP (Fig. 5).

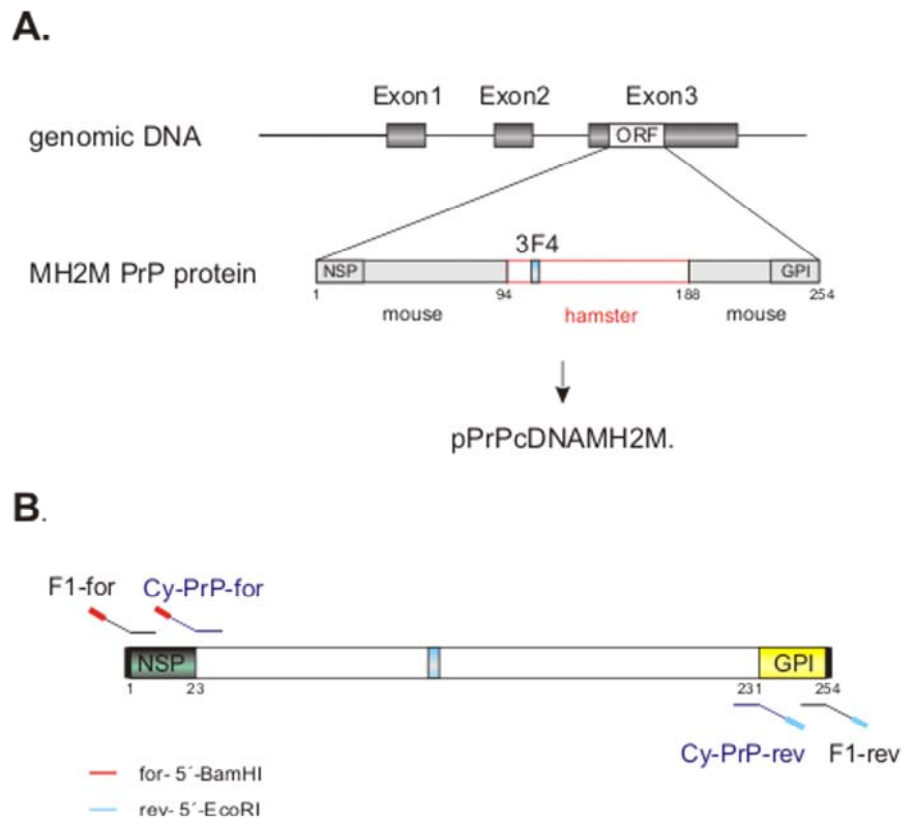


**Fig. 5 Generation of chimeric Cy-PrP and PM-PrP.** (A) Genomic DNA of transgenic MH2M mice encodes chimeric mouse-hamster-mouse PrP. The open reading frame (ORF) expresses MH2M-PrP protein (aa1-254) carrying the 3F4 anti-PrP antibody epitope (turquoise). cDNA of MH2M PrP from pPrPcDNAMH2M was used to generate Cy-PrP and PM-PrP. (B) PM-PrP and Cy-PrP DNA-fragments were amplified from pPrPcDNAMH2M by PCR using specific forward and reverse primer pairs providing BamHI and EcoRI restriction sites for subsequent cloning into destination vectors. The N-terminal signal peptide (NSP, green) and the C-terminal GPI anchor sequence (yellow) were excluded to generate Cy-PrP fragment.

The PM-PrP- and Cy-PrP-DNA-fragments were amplified from pPrPcDNAMH2M (M.G. Barenco, unpublished) by PCR using specific recombinant forward and reverse primer pairs with introduced BamHI and EcoRI restriction sites. These restriction sites were used for cloning into the destination vectors pIND and pcDNA3.1 to allow inducible and constitutive expression in eukaryotic cells. In addition to both PrP variants, the green fluorescence protein (GFP) was cloned into the pIND vector to test transfection efficiency and induction of gene expression after treatment with PonA. The generated constructs are listed in Table 4.

**Table 4** Generated plasmids encoding transgene PrP or GFP

Name of construct	Transgene
pIND-CyPrP	MH2M Cy-PrP
pIND-PMPPrP	MH2M PM-PrP
pcDNA-CyPrP	MH2M Cy-PrP
pcDNA-PMPPrP	MH2M PM-PrP
pIRES-puroCy-PrP	MH2M Cy-PrP
pIND-GFP	GFP

## 4.1.2 Ecdysone-inducible expression system

### 4.1.2.1 Functionality of the inducible expression system

To test the inducible expression system, N2a cells were transiently co-transfected with plasmids encoding the GFP and the transactivator VgRXR followed by PonA treatment. Induced GFP expression was monitored by fluorescence microscopy and quantified by FACS analysis (Fig. 6). Strong GFP expression was obtained after 1  $\mu$ M PonA treatment for 16 h, whereas non-treated cells showed almost no GFP expression (Fig. 6A).

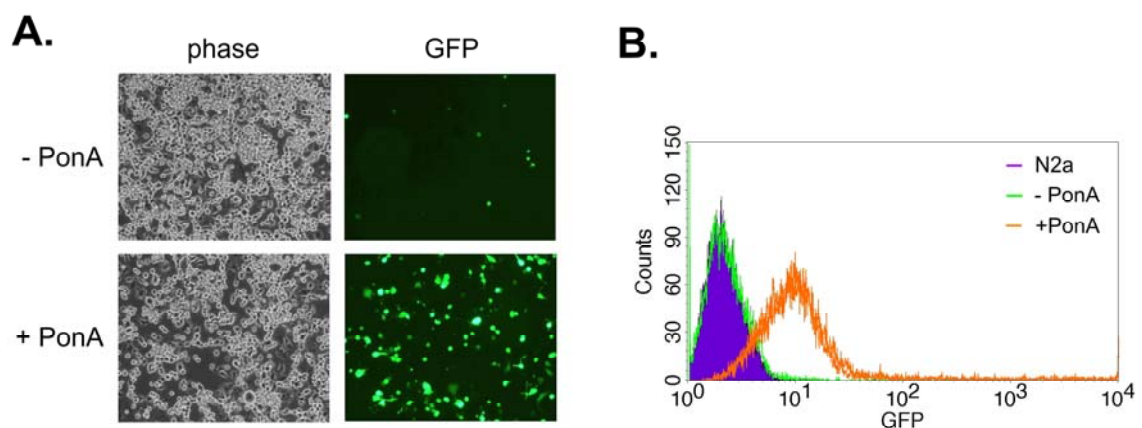


**Fig. 6 Proof of principle: ecdysone-inducible gene expression in N2a cells.** N2a cells were transiently co-transfected with transactivator VgRXR-encoding and GFP-encoding target plasmid. GFP expression was induced by adding PonA (1  $\mu$ M) for 16 h. (A) Immunofluorescence microscopy of GFP expression in presence or absence of PonA. (B) FACS analysis of GFP fluorescence after PonA treatment.

Relative quantification of GFP expression by FACS analysis showed 60-70 % transfection efficiency in PonA treated N2a cells (Fig. 6B), which was confirmed in at least three independent experiments. Increasing PonA concentrations from 0.5 to 2  $\mu$ M only weakly increased the GFP expression levels, whereby the GFP transfection efficiency was not affected (data not shown). These data demonstrated functionality of the ecdysone-inducible expression system in both N2a. The latter was confirmed in another cell line 293T (data not shown).

#### 4.1.2.2 Inducible expression of Cy-PrP and PM-PrP

Inducible expression of Cy-PrP and PM-PrP were tested in neuronal N2a cells and non-neuronal 293T cells in transient transfection experiments. After transfection, cells were cultivated in presence or absence of 1  $\mu$ M PonA for 16 h followed by preparation of cell extracts and the detection of Cy-PrP and PM-PrP by immunoblotting using the 3F4 antibody (Fig. 7).

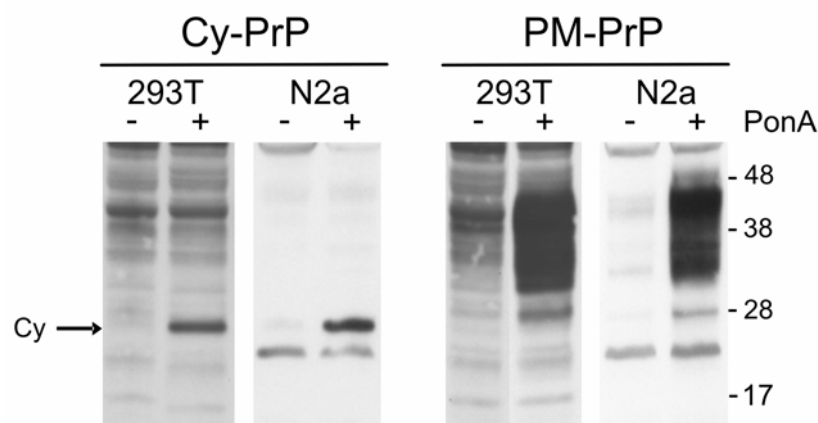


**Fig. 7 Cy-PrP and PM-PrP transiently expressed in N2a and 293T cells after induction with PonA.** Detection of Cy-PrP and PM-PrP in presence or absence of PonA (1 $\mu$ M) for 16 h using 3F4 antibody in immunoblot analysis. 3F4 antibody recognises only the transgenic 3F4-tagged PrP and not the endogenous murine PrP. The arrow indicates the single band of Cy-PrP around 27 kDa.

The expression of both, Cy-PrP and PM-PrP, was detectable in N2a and 293T cells (Fig. 7) upon PonA treatment. The PM-PrP protein (Fig. 7, right panel) showed the characteristic three band pattern caused by the different glycosylations, whereas Cy-PrP (Fig. 7, left panel) appeared as single band of

around 27 kDa due to missing glycosylations. This was confirmed by PNGaseF treatment, which did not alter the migration of the single band (data not shown). In contrast, untreated cells showed no expression of Cy-PrP and PM-PrP, respectively.

These data showed the induced expression of Cy-PrP and PM-PrP by the ecdysone-inducible expression system in N2a and 293T cells, which was used in all following transient transfection experiments.

As observed for GFP expression, increasing PonA concentration from 0.5 to 2  $\mu$ M showed no significant effect on Cy-PrP and PM-PrP expression levels in N2a cells, (data not shown). In the following experiments only 0.5  $\mu$ M PonA were used to analyse Cy-PrP and PM-PrP proteolysis and cellular distribution.

## **4.2 Analysis of cytotoxicity in Cy-PrP expressing cells**

### **4.2.1 Cell viability in Cy-PrP expressing N2a cells**

Small amounts of Cy-PrP should be extremely toxic to neuronal cells after 24 h of Cy-PrP expression (Ma *et al.*, 2002b). To examine this postulated cytotoxic potential of Cy-PrP in a neuronal cell line, viability assays were performed 24 h and 48 h after Cy-PrP induction in N2a cells (Fig. 8A and B). Cy-PrP expression was induced by treatment with 2  $\mu$ M of PonA to ensure that the inducer was given in excess for maximal transgene expression. Two methods based on different mechanisms were applied to detect Cy-PrP-specific effects on cell viability compared to cells expressing PM-PrP or to cells transfected with the empty vector (mock). The relative values were normalised to mock cells. Functionality of the assays is demonstrated by the Triton-X-100 sample. Data for relative cell viabilities determined by measurement of mitochondrial respiratory activity (MTT assay) are shown in Fig. 8A.



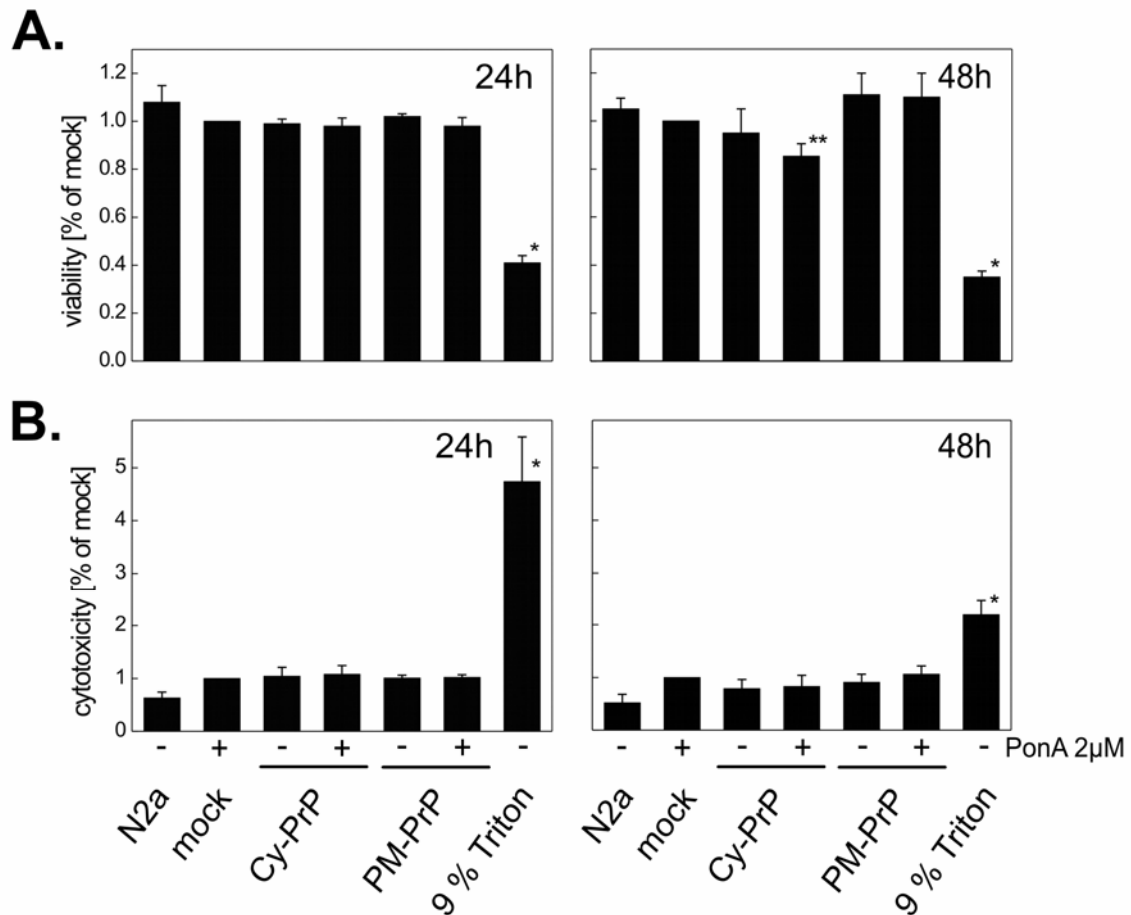


**Fig. 8 Viability and cytotoxicity in neuronal N2a cells after Cy-PrP and PM-PrP expression.** Cells were transiently transfected with Cy-PrP or PM-PrP and their expression was induced with 2  $\mu$ M PonA. Cell viability and cytotoxicity were measured by MTT assay (A) and LDH assay (B) 24 h or 48 h post-induction. Cells treated with 9 % triton served as positive control. The values (A-B) are shown as % of mock control (mean  $\pm$  SEM). Asterisks indicate values significantly different from mock controls ( $P^* \leq 0.05$ ). Two asterisks matter significance different to mock ( $P^* < 0.05$ ) but not to non-induced samples. The bars represent at least three independent experiments.

Cell viability of N2a cells was not affected by 24 h Cy-PrP expression (column + PonA) as compared to cells devoid of Cy-PrP (Column - PonA). No differences in cell viability were observed in comparison with PM-PrP-transfected (column 5) and PM-PrP-expressing cells (column 6) or with mock cells. After longer expression period (48h), cell viability is reduced around less than 20 % in N2a cells expressing Cy-PrP (right panel, column 4) as compared to mock cells. The detected reduction of cell viability was not significantly different to transfected cells devoid of Cy-PrP protein (right panel, column 3). PM-PrP transfection and 48 h expression did not effect the cellular survival (right panel, column 6). Triton-X-100

treated cells showed approximately 60-70 % reduction of cell viability at both time points ( $*P < 0.05$ ). Furthermore, cytotoxicity of Cy-PrP and PM-PrP expression in N2a cells were determined by measurement of cytosolic LDH release due to the loss of membrane integrity (LDH assay, Fig. 8B). Triton-X-100 treatment demonstrated cytotoxic effects ( $*P < 0.05$ ) after 24 h and 48 h. In contrast, neither cells expressing Cy-PrP (column 4) nor PM-PrP-expressing cells (column 6) answered with detectable releases of LDH. All transfected samples did not show increased cytotoxicity after 24 h and 48 h. Viability assays were not performed at longer time points due to decreasing Cy-PrP amounts observed 72 h post-transfection (data not shown). Indeed, the viability of Cy-PrP expressing cells was comparable to that observed for the PM-PrP expressing and mock transfected cells.

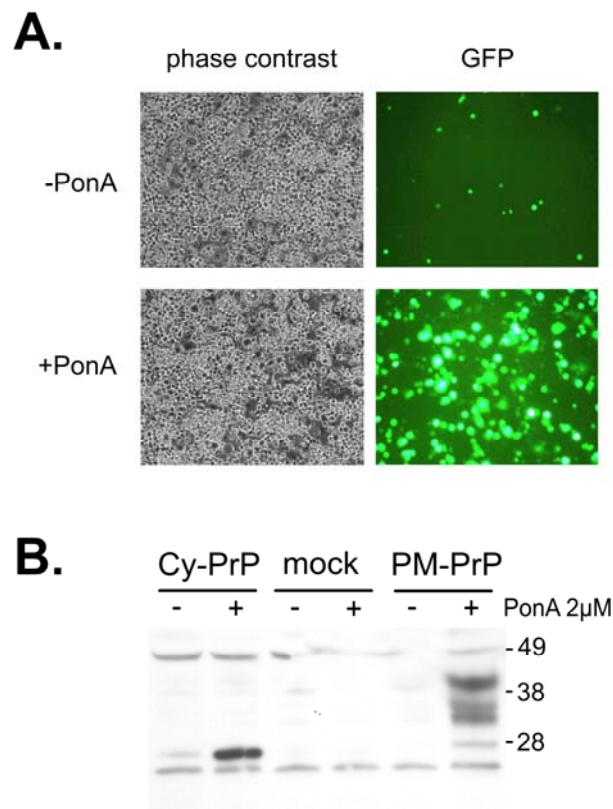


**Fig. 9 PonA induced gene expression in samples used for cell survival assays.** (A) PonA induced GFP expression after 24 h in the samples used for MTT and LDH assay. (B) One representative immunoblot of Cy-PrP and PM-PrP expression in the samples used for MTT and LDH assay at 24 h post-induction.

To monitor for transfection efficiency and PonA-mediated induction of gene expression, the GFP encoding plasmid was simultaneously transfected followed by visualisation of GFP expression by fluorescence microscope imaging (Fig. 9A). GFP was highly expressed 24 h post-induction with PonA, while most of the untreated cells did not express GFP. The weak background of GFP due to leakage of the inducible system in transiently transfected cells was negligible. The induction of Cy-PrP and PM-PrP expression in the cells used in both assays was monitored by immunoblot analysis using the 3F4- antibody (Fig. 9B). Cy-PrP and PM-PrP induction was clearly detected in the samples incubated with 2  $\mu$ M PonA.

#### 4.2.2 Cell viability in Cy-PrP expressing 293T cells

It was postulated that Cy-PrP might be toxic in a cell type dependent manner (Ma *et al.*, 2002b). In N2a cells, which express endogenous PrP<sup>C</sup>, no Cy-PrP-mediated cytotoxicity was measured (Fig. 8, see 4.2.1). If endogenous PrP<sup>C</sup> has an influence on toxicity of Cy-PrP, a cytotoxic effect should be measured in cells lacking endogenous PrP<sup>C</sup>. To address this question, cell survival of 293T cells expressing Cy-PrP and PM-PrP was tested using the MTT assay (Fig. 10).

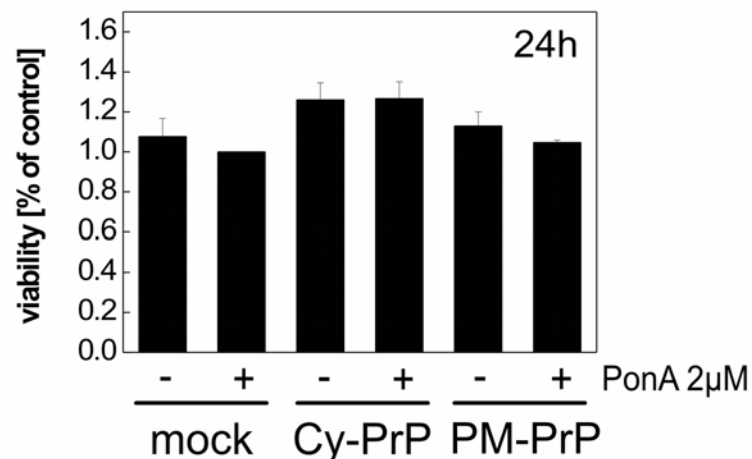


**Fig. 10 Viability after Cy-PrP and PM-PrP expression in 293T cells.** Cells were transiently transfected with Cy-PrP or PM-PrP and their expression was induced with 2  $\mu$ M PonA. Cell viability was measured by MTT assay 24 h post-induction. The viability values are shown as % of mock control (mean  $\pm$  SEM). The bars represent three independent experiments.

These are non-neuronal cells, which do express very low levels of endogenous PrP<sup>C</sup> (LeBlanc *et al.*, 2004). Transgene PrPs were similar expressed in both, N2a cells and 293T cells, after induction for 24 h with 2  $\mu$ M PonA (data not shown). Both Cy-PrP and PM-PrP expression did not affect cell viability of 293T cells (Fig. 10).

Taken together, Cy-PrP was neither toxic to neuronal N2a nor to non-neuronal 293T cells at the indicated time points. Hence, Cy-PrP toxicity seems to be not directly related to the endogenous PrP<sup>C</sup> level or the cell type in these *in vitro* models.

#### 4.2.3 Caspase-3 activity in Cy-PrP expressing N2a cells

In the previously published work (Ma *et al.* 2002b), Cy-PrP toxicity in N2a cells was analysed by a terminal-dUTP nick end labelling (TUNEL) assay, a method for determination of apoptosis. Within 24 h of Cy-PrP expression TUNEL positive cells increased from 6 to 14 %. This is not as high as expected for an extremely toxic protein. Establishment of the TUNEL-assay (fluorescent and colorimetric) for the N2a cell model used in this study failed due to lack of reproducibility. Thus, another apoptosis marker was chosen to detect cytotoxicity in N2a cells after 24 h of Cy-PrP expression. Since several apoptosis inducing pathways involve caspase-3 activation, a specific enzyme caspase-3 activity test was established and used to analyse apoptosis triggered by Cy-PrP or PM-PrP after 24 h expression (Fig. 11). Caspase-3 activity was analysed in cell lysates incubated with the AMC-conjugated caspase-3 specific substrate DMQD. Free cleaved AMC was detected by fluorescence measurement. Relative caspase-3 activity in Cy-PrP and PM-PrP expressing N2a cells was calculated from the fluorescence units and normalised to PonA-treated mock cells (Fig. 11). No specific increase of caspase-3 activity was detected in PonA-treated Cy-PrP expressing cells (column 4) as compared to non-treated (column 3) and mock cells (column 1 and 2) after 24 h. Similarly, PM-PrP expression (column 6) did not specifically affect caspase-3 activity in N2a cells.

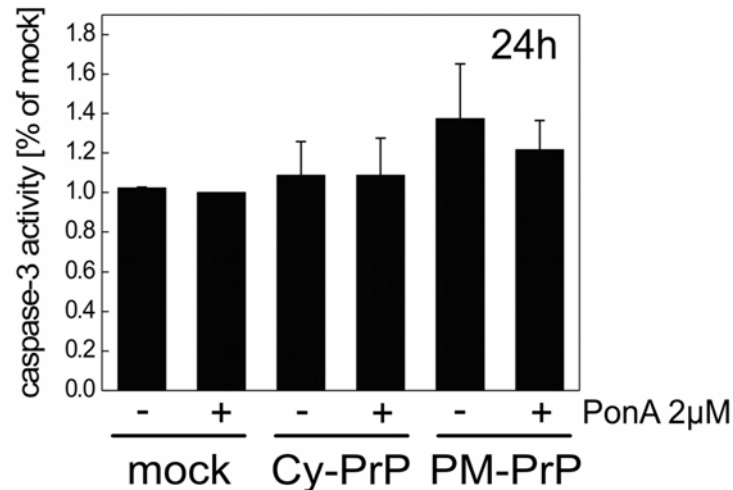


**Fig. 11 Caspase-3 activity in neuronal N2a cells after Cy-PrP and PM-PrP expression.** Cells were transiently transfected with Cy-PrP or PM-PrP and their expression was induced with 2  $\mu$ M PonA. Caspase-3 activity detected by fluorescence measurement of the cleaved AMC from the substrate peptide DMQD-AMC. The values are shown as % of mock control (mean  $\pm$  SEM). The data represent three independent experiments.

## 4.3 Proteolysis of Cy-PrP and PM-PrP in N2a cells

### 4.3.1 Kinetics of Cy-PrP and PM-PrP proteolysis

It has been shown that proteasome inhibition causes accumulation of Cy-PrP and that such Cy-PrP is detergent-insoluble and partially PK-resistant (Ma and Lindquist, 2002). Moreover, Cy-PrP appears to have the ability to promote further conversion of additional PrP to the same state. All these properties are also characteristic for PrP<sup>Sc</sup>, the TSE-infectious agent (Kocisko *et al.*, 1994; Prusiner, 1998). In order to see whether transiently expressed Cy-PrP has similar characteristics like PrP<sup>Sc</sup> when the proteasomal system is functional, cell extracts of N2a cells containing transiently expressed Cy-PrP (Fig. 12, 0  $\mu$ g/ml) were digested with 1 or 10  $\mu$ g/ml PK (Fig. 12, Cy-PrP 1 and 10  $\mu$ g/ml) and analysed by immunoblotting using 3F4 antibody. As a control served cell extracts from N2a cells harbouring PrP<sup>Sc</sup> (N2a58/22L).

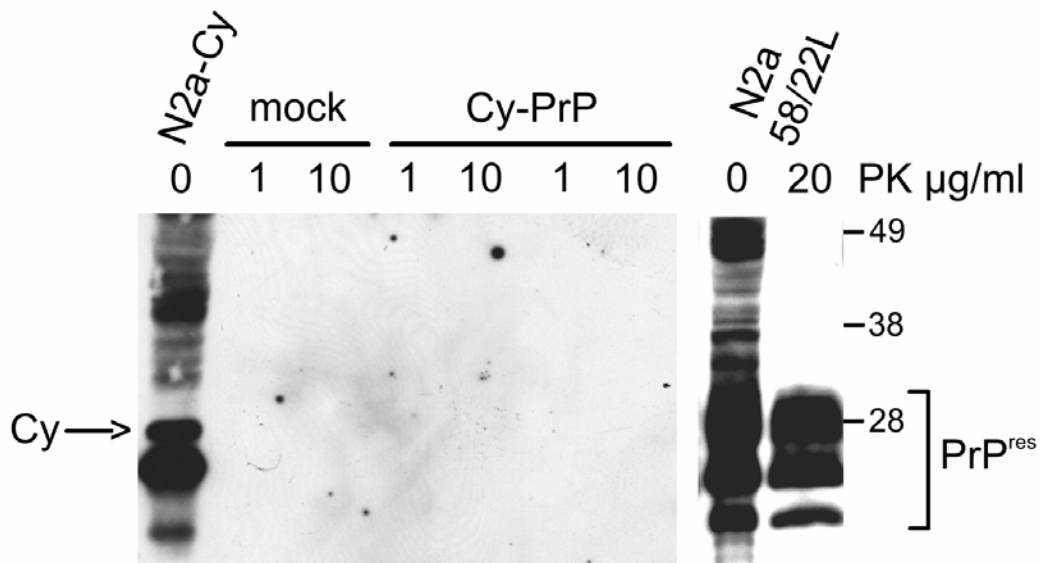


**Fig. 12** PK-digestion of Cy-PrP expressed in N2a cells. Cells were transiently transfected with Cy-PrP and their expression was induced overnight with 0.5  $\mu$ M PonA. Detection of PK-resistant Cy-PrP analysed by immunoblot using 3F4 antibody following proteinase K digestion. Mock transfected cells served as negative and scrapie-infected N2a58/22L as positive control. PrP<sup>res</sup> presents the PK-resistant part of PrP<sup>Sc</sup> after PK digestion including the N-terminal truncation of 90 aa.

No PK-resistant Cy-PrP was detected after digestion with 1 or 10  $\mu$ g/ml PK. In PrP<sup>Sc</sup>-containing N2a-58/22L cells significant amounts of PK-resistant PrP (PrP<sup>res</sup>) were detected (Fig. 12, last lane) following digestion with double concentrated PK (20  $\mu$ g/ml). Cy-PrP was completely degraded by PK and does not accumulate in PK-resistant aggregates. PK is a fungal protease with broad substrate spectrum. To analyse the stability of Cy-PrP as compared to PM-PrP in N2a cells containing mammalian proteases, the kinetics of Cy-PrP and PM-PrP degradation were determined by detection of Cy-PrP and PM-PrP at different time points by immunoblotting (Fig. 13). The stability of Cy-PrP in comparison to PM-PrP was reflected by the calculated half life of both PrPs in N2a cells. Amounts of PM-PrP and Cy-PrP decreased within 6-12 h after PonA withdrawal. Detection of  $\beta$ -actin demonstrated equal protein loading. The densitometric quantification showed that the half life for both PM-PrP and Cy-PrP was between 7 and 8 h (Fig. 13B). While PrP<sup>C</sup> is synthesised and degraded relatively rapidly ( $t_{0.5} \sim 5$  h), PrP<sup>Sc</sup> is synthesised slowly and appears to accumulate ( $t_{0.5} \sim 15$  h) (Borchelt *et al.*, 1990).

Cy-PrP degradation was not prolonged as compared to PM-PrP indicating absence of PrP<sup>Sc</sup>-like stability and protease resistance.

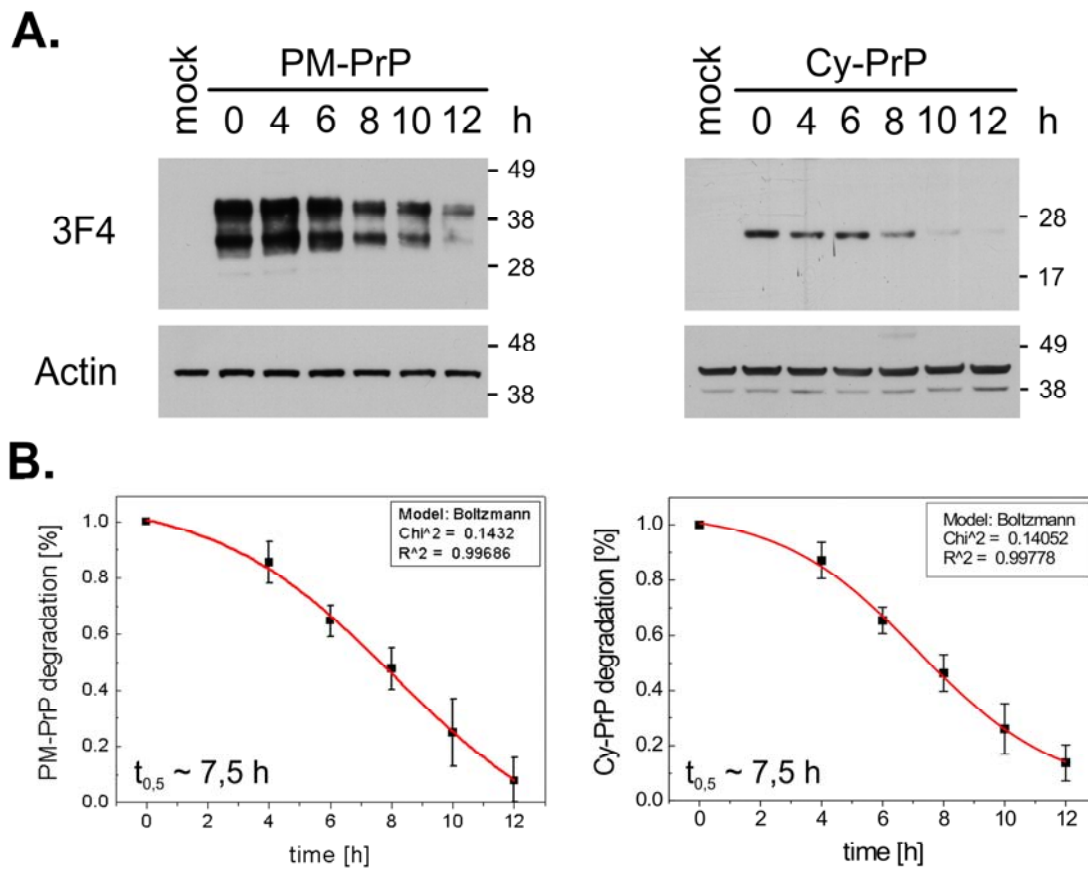


**Fig. 13 Degradation of Cy-PrP and PM-PrP in N2a cells.** Cells were transiently transfected with Cy-PrP or PM-PrP and their expression was induced overnight with 0.5  $\mu$ M PonA. PonA-containing medium was replaced with normal DMEM for indicated time points. (A) Time-dependent decrease of PM-PrP (left) and Cy-PrP (right) analysed by immunoblot using 3F4 antibody. Immunoblot against actin served as positive control. (B) Degradation curve for PM-PrP and Cy-PrP determined by densitometric evaluation of four different immunoblot experiments. The values are normalised as percentage to the PrP signal at time point 0h (mean  $\pm$  SEM). Curve fitting was achieved by interpolation using the Boltzmann model with indicated chi-square values. Fitting function was used to calculate half life ( $t_{0.5}$ ) of Cy-PrP and PM-PrP.

### 4.3.2 Role of proteasome in Cy-PrP and PM-PrP proteolysis

#### 4.3.2.1 Proteolysis under proteasome inhibition

Since mutant PrP or retro-translocated wt-PrP accumulates in cells with impaired proteasome activity (Fioriti *et al.*, 2005; Ma *et al.*, 2001; Ma *et al.*, 2002a; Wang *et al.*, 2005), it was assumed that Cy-PrP might be degraded by the proteasome. Thus, degradation of PM-PrP and Cy-PrP was monitored in N2a cells between 0 and 12 h upon removal of PonA treatment in absence or presence of the specific proteasome inhibitor epoxomicin (Fig. 14).

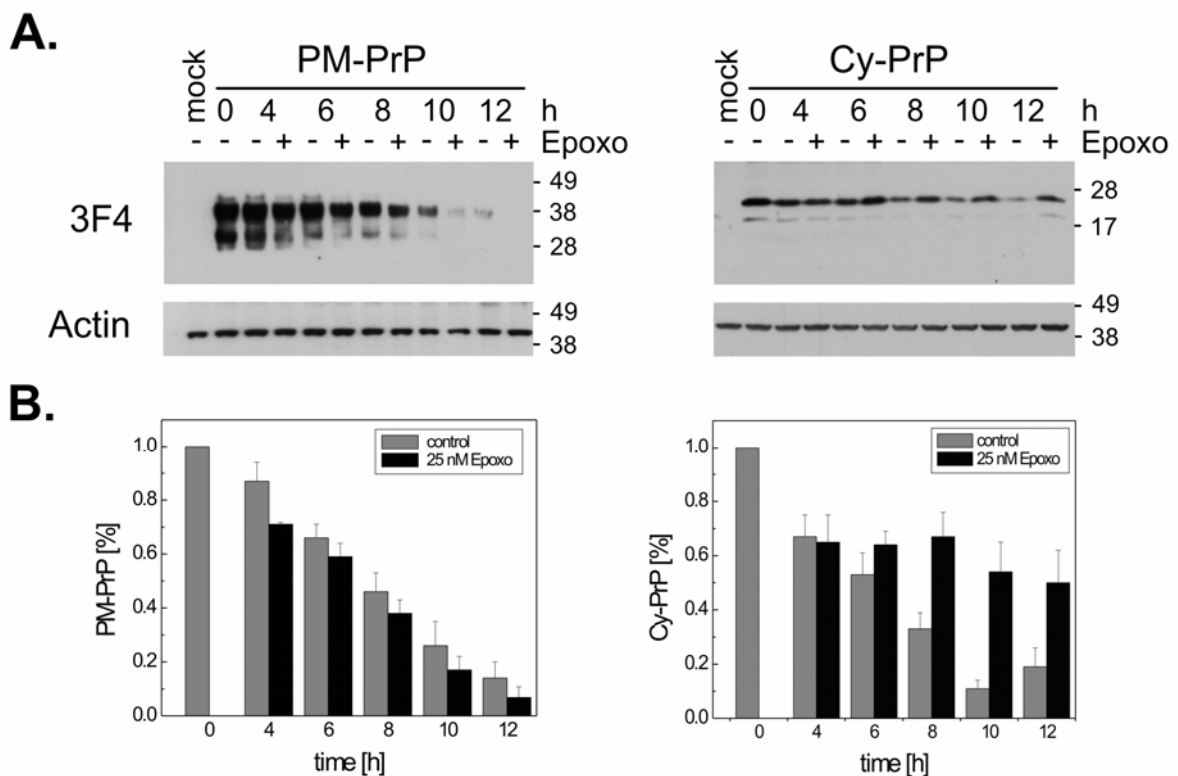


**Fig. 14 PM-PrP and Cy-PrP proteolysis under proteasome inhibition.** Cells were transiently transfected with PM-PrP or Cy-PrP and their expression was induced overnight with 0.5  $\mu$ M PonA. PonA-containing medium was replaced with either DMEM or supplemented with the proteasome inhibitor epoxomicin (Epoxo) for indicated time points. (A) PM-PrP and Cy-PrP degradation analysed by immunoblot using 3F4 antibody. Immunoblot against actin served as positive control. (B) Densitometric evaluation of the PM-PrP and Cy-PrP signal for four different immunoblot experiments normalised to the PrP signal at time point 0 h.



The amount of PM-PrP or Cy-PrP was analysed by immunoblots at indicated time points. The PM-PrP showed independently from the proteasome inhibition decreasing signal intensities (Fig. 14A, left panel). Densitometric quantification revealed that mature PM-PrP was proteasome-independently degraded with no altered half life (Fig. 14B, left panel). This was expected, since PM-PrP is located on the cell surface or in cellular compartments such as recycling vesicles and the Golgi apparatus where the proteasome is not located. However, long term exposure of immunoblot seen in Fig. 13 showed accumulation of the non-glycosylated PrP form after epoxomicin treatment (Fig. 15, + Epoxo 4-12 h) as compared to untreated cells (Fig. 15, - Epoxo 4-12 h) indicating retro-translocation of PrP from the ER into the cytosol for further degradation by the proteasome (Fioriti *et al.*, 2005; Wang *et al.*, 2005).

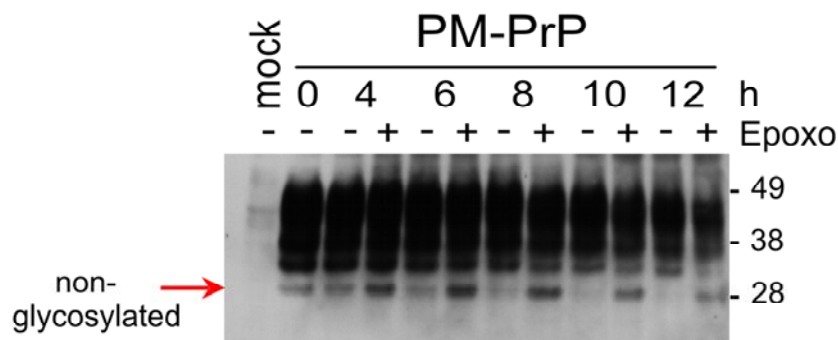


**Fig. 15 Accumulation of non-glycosylated band of PM-PrP after proteasome inhibition.** Cells were transiently transfected with PM-PrP or Cy-PrP and their expression was induced overnight with 0.5  $\mu$ M PonA. PonA-containing medium was replaced with either DMEM or supplemented with the proteasome inhibitor epoxomicin (Epoxo) for indicated time points. Panel shows PM-PrP signals analysed by immunoblot using 3F4 antibody following over exposure. Arrow indicates the non-glycosylated band of PM-PrP.

In the case of Cy-PrP a constant immunoblot signal was detected between 8 and 12 h in presence of epoxomicin (Fig. 14A, right panel), whereas untreated cells showed a continuous decrease of the Cy-PrP signal. These data demonstrate a strong inhibition of Cy-PrP proteolysis in presence of epoxomicin. Densitometric quantification of four independent experiments clearly confirmed that Cy-PrP proteolysis was dramatically decelerated by proteasome inhibition (Fig. 14B, right

panel). The half life of Cy-PrP was increased to more than 12 h (see black column) by proteasome inhibition.

Additionally, the Cy-PrP content was examined after 16 h PonA treatment in the presence of different proteasome inhibitor concentrations to support the data that Cy-PrP is a proteasomal substrate (Fig. 16). Immunoblot analysis demonstrated that Cy-PrP clearly accumulated with increasing epoxomicin concentration (Fig. 16A). Densitometric quantification confirmed that increasing proteasomal inhibition resulted in an approximately 4-fold increase of Cy-PrP content in N2a cells (Fig. 16B).

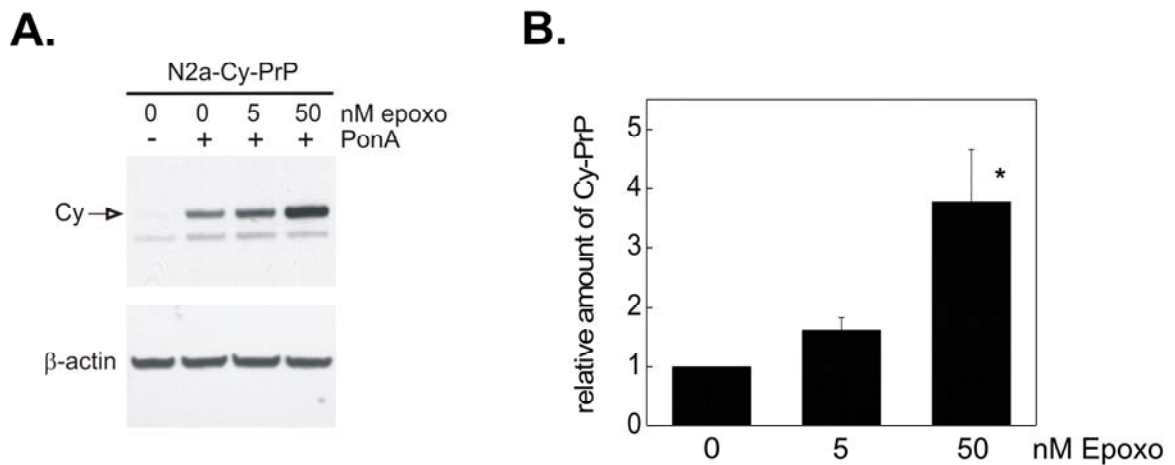


**Fig. 16 Cy-PrP accumulation after proteasome inhibition in N2a cells.** Cells were transiently transfected with Cy-PrP and expression was induced with 2  $\mu$ M PonA for 24 h. 16 h prior to cell lysis 50 nM epoxomicin (Epoxo) was added. (A) Cy-PrP accumulation analysed by immunoblot using 3F4 antibody. Immunoblot against actin served as positive control. (B) Densitometric evaluation of Cy-PrP signals from four different immunoblot experiments normalised to the Cy-PrP signals without Epoxo treatment (mean  $\pm$  SEM). Value of 50 nM Epoxo treated cells was significantly different to untreated Cy-PrP cells ( $P^* < 0.05$ ).

The correlation of Cy-PrP accumulation with increasing proteasome inhibitor concentration confirmed the results observed in Cy-PrP proteolysis experiments indicating that Cy-PrP is a substrate of the proteasome and must be therefore present in the cytosol.

#### 4.3.2.2 Proteasome activity after Cy-PrP expression

Since Cy-PrP is degraded by the proteasome, overexpression of Cy-PrP as well as PM-PrP could influence basic proteasomal activity in transiently transfected N2a cells. Thus, the activity of the 26S ATP-dependent proteasome complex was determined for Cy-PrP and PM-PrP expressing N2a cells using a native enzymatic activity gel (Fig. 17A). The cleavage of the proteasomal substrate LLVY-AMC by native 26S proteasome molecules in the gel was visible through fluorescence.

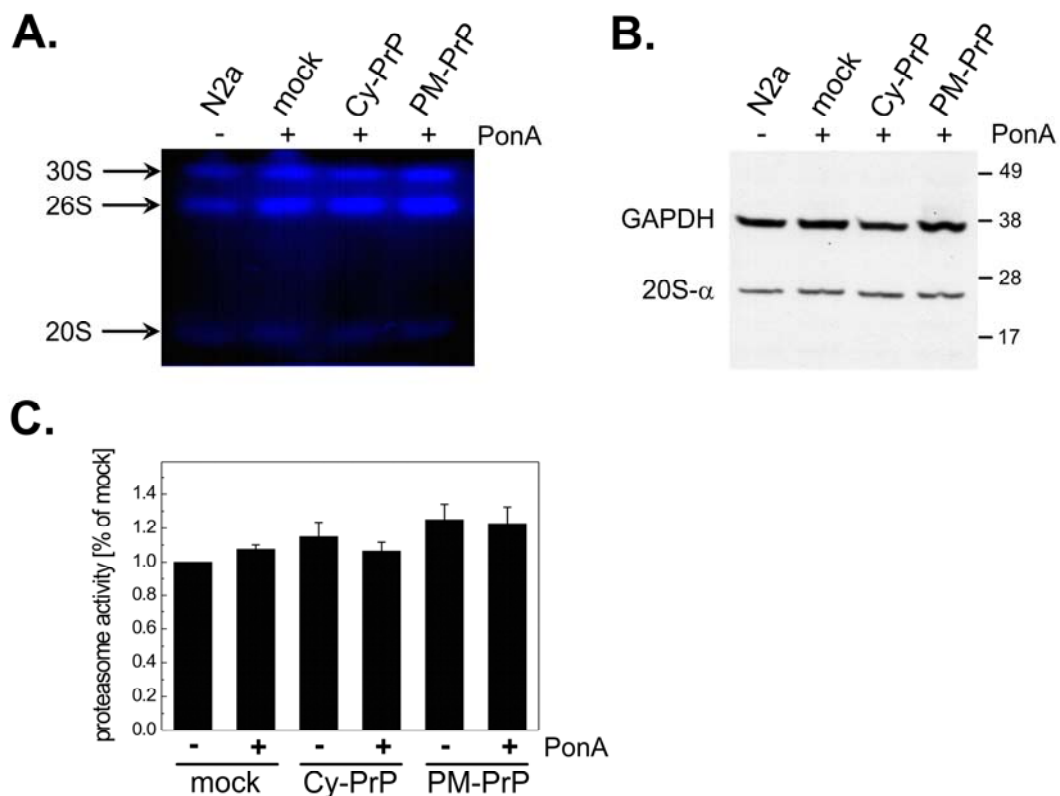


**Fig. 17 Proteasome activity and content in N2a cells expressing Cy-PrP or PM-PrP.** Cy-PrP or PM-PrP expression was induced in transiently transfected N2a cells by adding 0.5  $\mu$ M PonA for 16 h. Proteasomal cleavage of suc-LLVY-AMC was measured as fluorescence at 380 nm excitation and at 460 nm emission (A and C). (A) ATP-dependent proteasome activity observed as blue fluorescent bands in a native gel. (B) Immunoblot of 20S proteasome using anti-20S  $\alpha$ -subunit antibody. Anti-GAPDH served as loading control. (C) Plate reader assay of 26S proteasome activity. Proteasome activity is normalised to mock cells (mean  $\pm$  SEM). The value represents three independent experiments.

Strong substrate turnover was observed for cells expressing Cy-PrP and PM-PrP (Fig. 17A, lane Cy- and PM-PrP, + PonA). However, mock-transfected N2a cells showed also increased cleavage of the proteasome substrate (lane mock +) indicating that the transfection procedure alone elevates proteasome activity.

To exclude altered 26S proteasome activity in transfected cells due to increased proteasome expression, the samples were examined for their proteasome content by immunoblotting using a specific anti-20S  $\alpha$ -subunit antibody (Fig. 17B). Proteasomal  $\alpha$ -subunit protein levels were equal in non-transfected (N2a, -PonA) and transfected cells (mock, Cy- and PM-PrP, + PonA) independent of transgene expression demonstrating that increased proteasome activity was not the result of increased proteasome levels *per se*. Native proteasome activity gels allow qualitative analysis of the cellular proteasome activity. Since all of the transfected cells answered with a clear increase of the 26S proteasome activity, a second more quantitative plate reader fluorescence assay was applied to support the qualitative native gel results. In the plate reader assay the cleavage of the proteasomal substrate LLVY was detected by digital measurement of the emitted fluorescence units. Calculated proteasome activity values were normalised to the PonA-treated mock cells (Fig. 17C). Neither Cy-PrP (column Cy-PrP, + PonA) nor PM-PrP overexpression (column PM-PrP, + PonA) in N2a cells affected the proteolytical activity of the proteasome system as compared to the mock transfected N2a cells (column mock, + PonA). PonA itself exhibited no influence on 26S proteasome activity as demonstrated by columns - and + PonA of mock cells. Proteasome activity assays revealed transfection-mediated proteasome activation. The potential Cy-PrP-mediated cytotoxicity could have been counterbalanced through unspecific increased proteasome-mediated proteolysis of Cy-PrP.

#### **4.3.3 Viability in Cy-PrP expressing N2a cells after proteasome inhibition**

One reason for the lack of Cy-PrP cytotoxicity in transiently transfected N2a cells might be the increased proteasome activity caused by the transfection procedure, because Cy-PrP might be faster degraded by the proteasome. However, it was

proposed that neuronal death could be triggered by accumulation of cytosolic PrP due to impairment of the proteasomal degradation system. Thus, reduction of the proteasome activity by specific inhibitors might reveal cytotoxicity caused by Cy-PrP overexpression in N2a cells. To test this hypothesis, Cy-PrP and PM-PrP expression was induced in N2a cells in presence of the proteasome inhibitor epoxomicin followed by MTT viability assays 24 h post-induction (Fig. 18A).

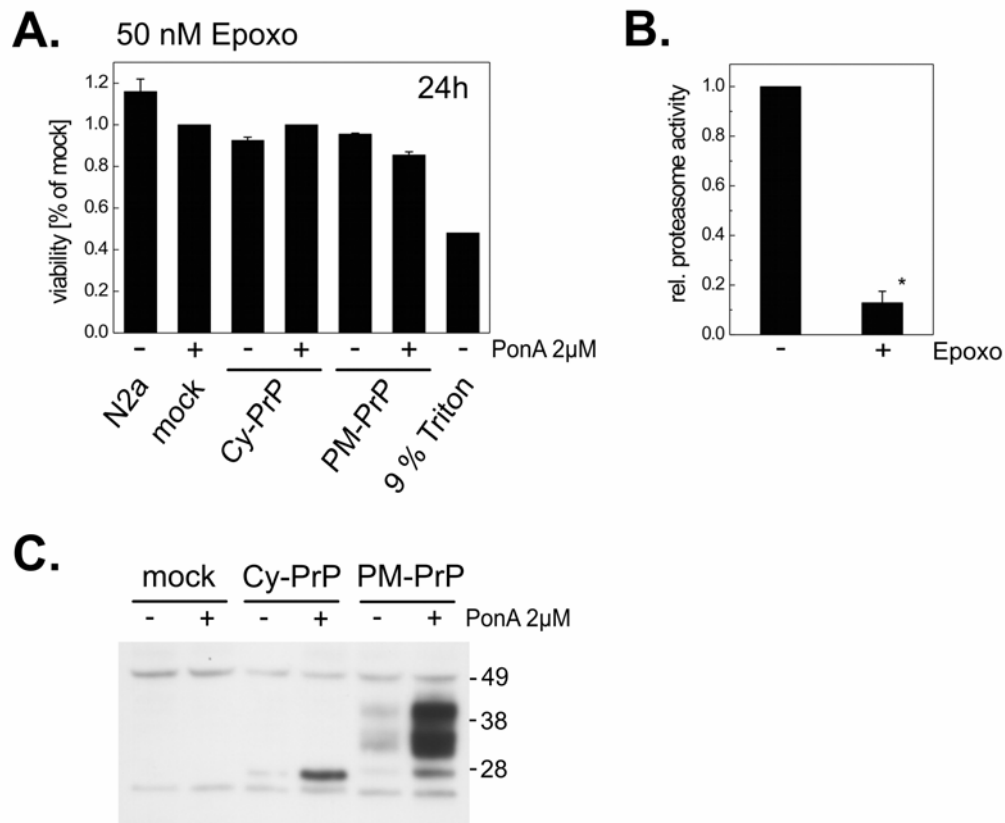


**Fig. 18 Proteasome inhibition does not reveal Cy-PrP-mediated cytotoxicity in N2a cells.**

Cells were transiently transfected with PM-PrP or Cy-PrP and their expression was induced with 2  $\mu$ M PonA for 24 h. 16 h prior to viability measurement 50 nM epoxomicin (Epoxo) was added. (A) Cell viability was measured by MTT assay 24 h post-induction. The values are shown as % of mock control (mean  $\pm$  SEM). Cells treated with 9 % triton served as positive control, which was significantly different from mock control ( $P \leq 0.05$ ). (B) Proteasome inhibition in N2a cells treated with 50 nM epoxo detected by measuring 26S-proteasome-mediated LLVY-AMC cleavage in plate reader. Proteasome activity was normalised to untreated N2a cells (mean  $\pm$  SEM). The value represents three independent experiments and was significantly different to untreated N2a cells (\* $P < 0.05$ ). (C) One representative immunoblot of Cy-PrP and PM-PrP expression in the samples used for MTT and LDH assay at 24 h post-induction.

Neither Cy-PrP (column Cy-PrP, + PonA) nor PM-PrP (column PM-PrP, + PonA) overexpressed in N2a cells during impaired proteasome activity influenced the cellular survival as compared to the non-induced (column Cy- and PM-PrP, - PonA) and mock-transfected N2a cells (column mock, + PonA). In contrast, treatment with 9% Triton-X-100 showed significantly ( $P^* < 0.05$ ) decreased survival of N2a cells (around 50 % to mock, last column). No toxic potential induced by PM-PrP was detected. To confirm the effective inhibition of the proteasome, 26S proteasome activity was analysed in fluorescence substrate-cleavage assays (Fig. 18B). Treatment with 50 nM of epoxomicin was sufficient to inactivate the proteasomal 26S activity in N2a cells. Immunoblot using 3F4 antibody ensured Cy-PrP and PM-PrP expression (Fig. 18C) in the samples used for MTT assays shown in Fig. 18A.

These results suggest that N2a cells tolerate high Cy-PrP levels and cytotoxicity of Cy-PrP is controlled by other cellular mechanisms than degradation through the proteasome complex.

## **4.4 Cellular localisation of Cy-PrP and PM-PrP in N2a cells**

### **4.4.1 Intracellular localisation of Cy-PrP**

The lack of Cy-PrP glycosylation and the proteasome-mediated proteolysis of Cy-PrP indicate cytosolic localisation of Cy-PrP. To confirm this cellular localisation, subcellular fractions were tested for the presence of Cy-PrP expression by immunoblotting (Fig. 19). Following PonA induction, N2a cells expressing Cy-PrP or PM-PrP were subjected to hypoosmotic lysis followed by centrifugation to separate the low density fraction containing cytosolic proteins and small vesicles from the high density fraction containing plasma membrane and large cellular compartments. Both fractions were analysed by immunoblot. As expected, almost no PM-PrP was detectable in the cytosolic fraction (Fig. 19, left panel, lane Pm-PrP + PonA) whereas a strong PM-PrP signal was found in the membrane fraction (Fig. 19, right panel, lane PM-PrP, + PonA). In contrast, Cy-PrP was localised in

both the cytosolic fraction (Fig. 19, left panel, lane Cy-PrP, + PonA) and the membrane fraction (Fig. 19, right panel, lane Cy-PrP, + PonA). In the latter only a low Cy-PrP concentration was detected, the majority of Cy-PrP was located in the cytosol. Counterstaining of  $\beta$ -actin, known as cytosolic marker, and calnexin, known as ER-membrane marker, underscored separation of both fractions, although weak signals of each marker was found in unrelated fractions indicating minor contaminations.

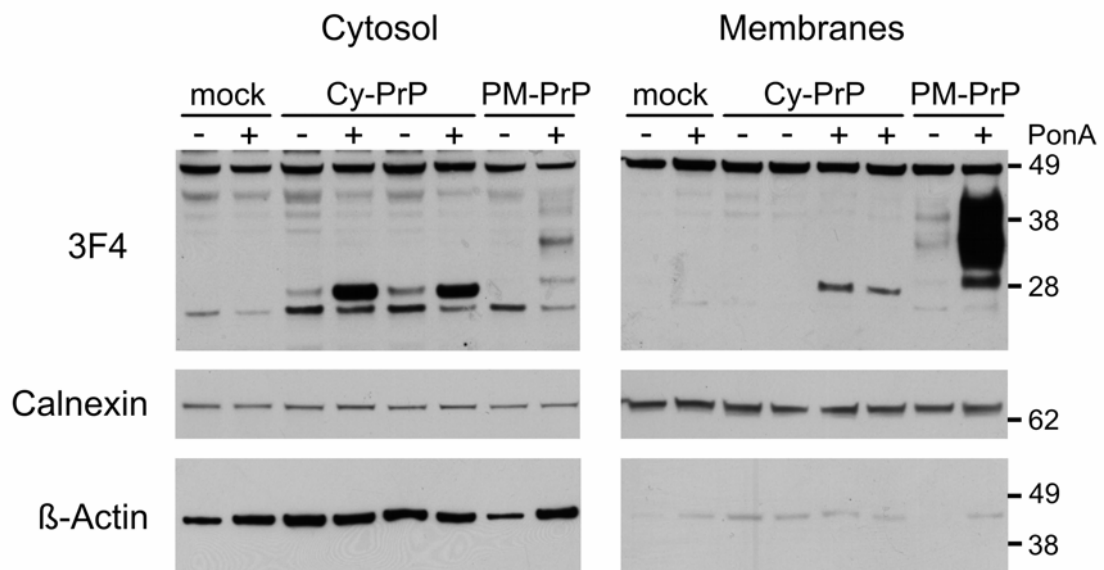


**Fig. 19 Cy-PrP mainly localises in the low density-cytosol fraction of N2a cells.** Cy-PrP or PM-PrP expression was induced in transiently transfected N2a cells by adding 0.5  $\mu$ M PonA for 16 h. Cells were lysed and subcellular fractions of low density (cytosol) and high density (membranes) were analysed for Cy-PrP and PM-PrP expression by immunoblotting using 3F4 antibody. Anti- $\beta$ -actin and anti-calnexin served as controls for both fractions.

However, these data confirmed the assumption that Cy-PrP is mainly localised in the cytosolic compartment whereas PM-PrP was localised in membranes, which was in line with the results showing that overexpressed full length PrP is found at the cell surface and in the Golgi apparatus (Haraguchi *et al.*, 1989; Stahl *et al.*, 1987; Taraboulos *et al.*, 1992).

To strengthen these observations, extracellular and intracellular immunofluorescence analyses were performed to visualise microscopically the localisation of overexpressed Cy-PrP and PM-PrP in N2a cells (Fig. 20). In

extracellular staining, a strong membrane staining was observed for PM-PrP (red) on the cell surface (Fig. 20A bottom panel). Extreme slight signals were also found for Cy-PrP (Fig. 20A middle panel), which showed a dot-like pattern (speckles) differently to PM-PrP.

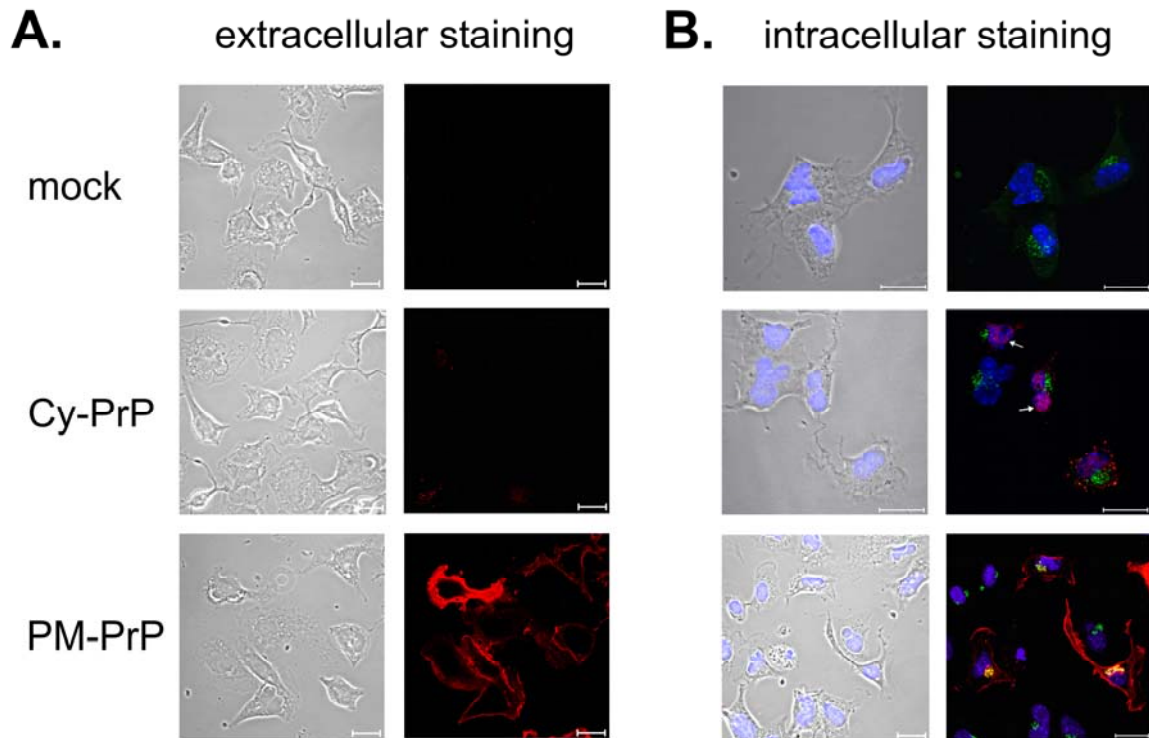


**Fig. 20 Cy-PrP accumulates in fine foci throughout N2a cells and is partially nucleus-associated.** Cy-PrP or PM-PrP expression was induced in transiently transfected N2a cells by adding 0.5  $\mu$ M PonA overnight. Immunofluorescence staining was performed using the anti-PrP 3F4 antibody (A and B) and anti-giantin antibody (B) followed by fluorescent dye conjugated secondary antibodies. (A) Extracellular staining with 3F4 anti-PrP without cell permeabilisation to detect PM-PrP and Cy-PrP (both red) (B) Extra- and intracellular PrP staining of permeabilised cells. Yellow colour in the merged images provides co-localisation of PM-PrP with giantin (green). Nucleus staining was performed with bis-benzimid (Hoechst 33342) solution (blue). scale bar: 20  $\mu$ m

Intracellular staining uncovered that Cy-PrPs (red) formed indeed those intracellular speckles unusual for cytosolic proteins (Fig. 20B, middle panel) and suggested that some cells in the extracellular staining were slightly permeable after fixation. In contrast, intracellular staining of PM-PrP confirmed its membrane-



distribution but showed also a structured pattern close to the nuclei (Fig. 20B, bottom panel). To discriminate intracellular localisation of Cy-PrP and PM-PrP, cells were counterstained for giantin, which is a known marker for the Golgi apparatus (Fig. 20B). Indeed, intracellular PM-PrP co-localised with giantin (Fig. 20B, bottom panel, merged) suggesting that PM-PrP was associated with the Golgi apparatus. In contrast, Cy-PrP did not co-localise with giantin and the dot-like structures of intracellular Cy-PrP were distinct from the PM-PrP pattern. Thus, Cy-PrP was not associated with the Golgi apparatus (Fig. 20B, middle panel, merged). However, a minority of intracellular Cy-PrP exhibited more diffuse staining pattern (Fig. 20B, middle panel, arrows). Counterstaining of intranuclear chromatin by bis-benzimid (Hoechst 33342) revealed that those Cy-PrP molecules localised with the nuclei. To analyse more detailed the intranuclear localisation of Cy-PrP, N2a cells were co-stained with bis-benzimid (Hoechst 33342) and Cy-PrP-antibody, and multilayer images were recorded. Focusing through several z-layers of different cells revealed that Cy-PrP was not located in the nucleus and the diffuse distribution rather surrounded the nucleus (Fig. 21). Thus, Cy-PrP might have been associated with other subcellular structures or compartments.

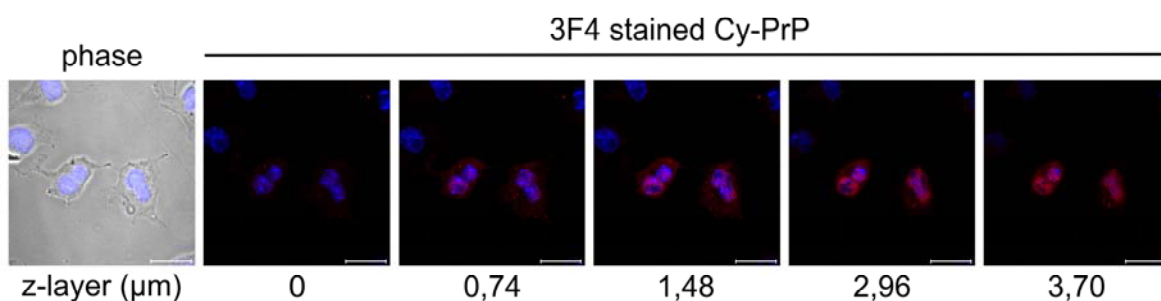


**Fig. 21 Immunofluorescence of nucleus-associated Cy-PrP in N2a cells.** Cy-PrP expression was induced in transiently transfected N2a cells by adding 0.5  $\mu\text{M}$  PonA overnight. Intracellular immunofluorescence staining was performed in Triton-permeabilised cells using the anti-PrP 3F4 antibody for Cy-PrP detection and bis-benzimid (Hoechst 33342) solution for nucleus staining (blue). Images were obtained by stack recording using Zeiss LSM 510 scanning confocal microscope. Images of different z-layers ( $\mu\text{m}$ ) are shown. Scale bar: 20  $\mu\text{m}$

#### 4.4.2 Cy-PrP co-localisation with Hsc70 in EEA1 positive vesicles

The above presented results demonstrated that overexpressed Cy-PrP formed fine foci throughout the N2a cells, different to a diffuse and homogenous distribution often observed for cytosolic proteins, and Cy-PrP might be associated with other compartments such as ER or endosomes and lysosomes. Thus, intracellular staining of Cy-PrPs was repeated along with different known markers characteristic for those compartments. Co-staining of Cy-PrP with disulfide isomerase (PDI), a marker for the ER, did not show co-localisation in merged images (Fig. 22, first panel) indicating Cy-PrP was not translocated into the ER lumen. In contrast, co-staining of Cy-PrP along with early endosome antigen 1 (EEA1), a marker for the presented endosomal compartment revealed intense overlap of both patterns in merged pictures (Fig. 22, middle panel) strongly suggesting that overexpressed Cy-PrP is recruited to endocytic vesicles. Recruitment of overexpressed cytosolic proteins to endosomal/lysosomal vesicles has been described and chaperones, especially Hsc70/Hsp70 and their co-chaperones, are involved in this process (Agarraberes and Dice, 2001; Chiang *et al.*, 1989; Cuervo *et al.*, 1997). Thus, Cy-PrP overexpressed in N2a cells was stained together with Hsc70 (Fig. 22, bottom panel). Indeed, the specific Hsc70 staining provided an inhomogeneous intracellular localisation similar to the speckles observed for Cy-PrP. Merging the pictures revealed intense overlap of both, Cy-PrP and Hsc70 staining, indicating that Cy-PrP and Hsc70 co-localise in N2a cells (Fig. 22, bottom panel, merged).

To demonstrate that Hsc70 co-localised specifically with Cy-PrP, a second immunofluorescence experiment was performed including PM-PrP- and mock-transfected N2a cells (Fig. 23). Neither in mock nor in PM-PrP-expressing cells Hsc70 clustered in dot-like structures (Fig. 23, top and bottom panel). In contrast, Cy-PrP expression has a striking effect on Hsc70 distribution showing homogenous Hsc70 was concentrated in fine foci (Fig. 23, middle panel), which co-localised with Cy-PrP speckles (Fig. 23, middle panel, merged).

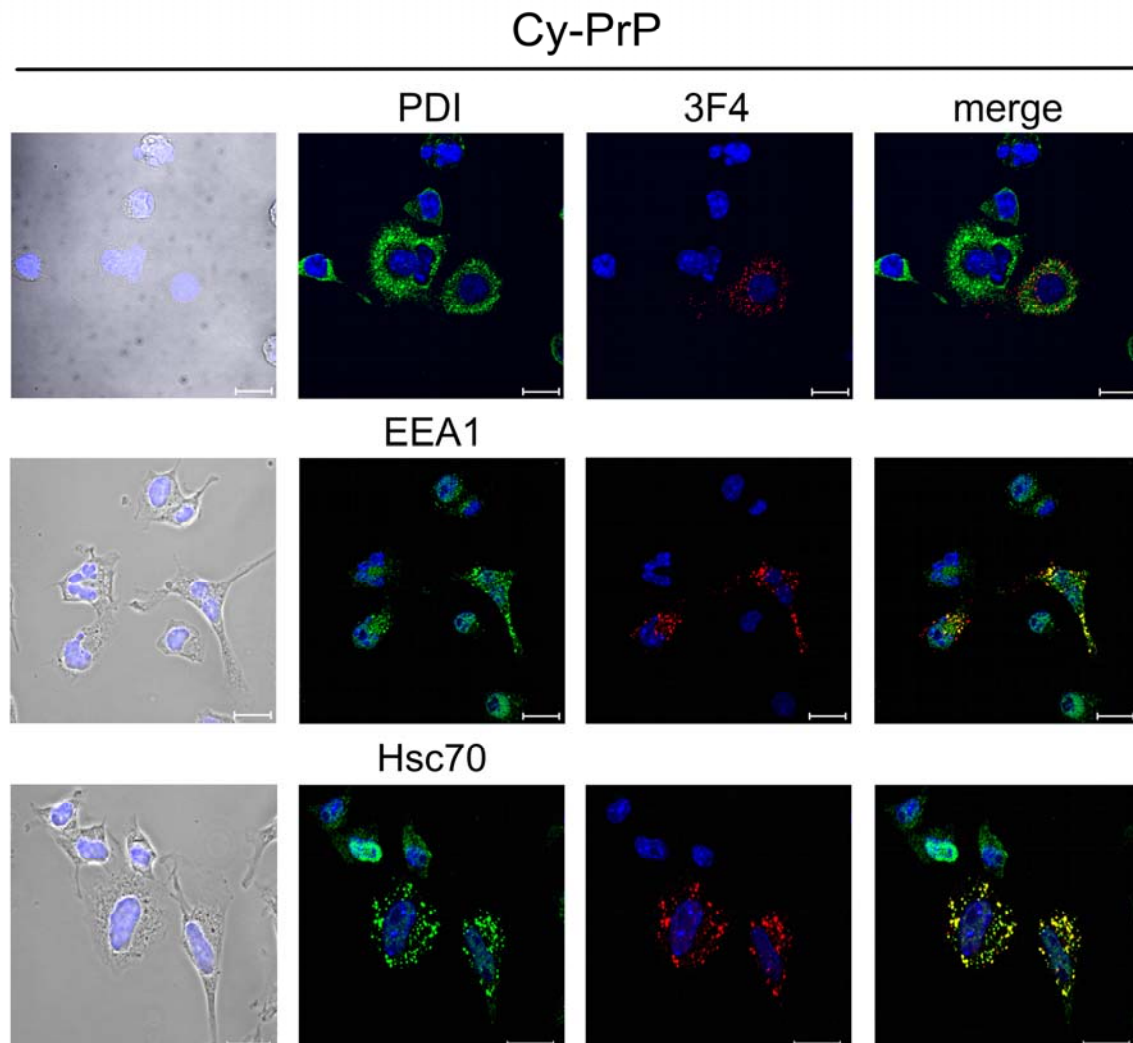


**Fig. 22 Cy-PrP co-localises with Hsc70 in EEA1-positive endocytic vesicles.** Cy-PrP expression was induced in transiently transfected N2a cells by adding 0.5  $\mu$ M PonA overnight. Cells were fixed, permeabilised with Triton-X-100, and stained with 3F4 anti-PrP antibody and anti-PDI, anti-giantin, anti-EEA1 or anti-Hsc70 antibody followed by Alexa488 (green)-conjugated and Alexa594 (red)-conjugated secondary antibody. Nucleus staining was performed with bis-benzimid (Hoechst) solution (blue). Co-staining of Cy-PrP (red) with PDI, giantin, EEA1 or Hsc70 (green). In the merged images Cy-PrP co-localises with EEA1 or Hsc70, producing a yellow colour, which was not observed with compartment markers PDI and giantin. Scale bar: 20  $\mu$ m

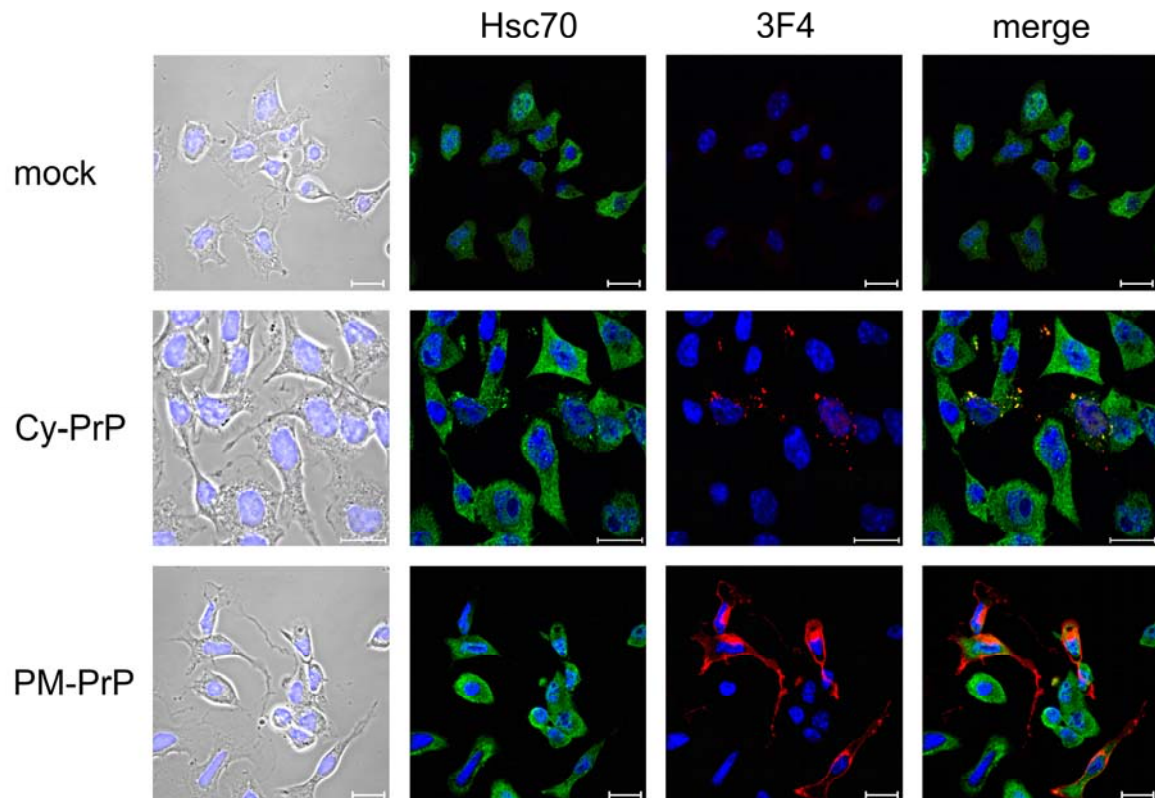


**Fig. 23 Redistribution of cytosolic Hsc70 by Cy-PrP expression in N2a cells.** Cy-PrP or PM-PrP expression was induced in transiently transfected N2a cells by adding 0.5  $\mu$ M PonA overnight. Cells were fixed, permeabilised with Triton-X-100, and stained with mouse anti-PrP antibody 3F4 and rat anti-Hsc70 antibody followed by Alexa488 (green)-conjugated anti-rat and Alexa594 (red)-conjugated anti-mouse secondary antibody. Nucleus staining was performed with bis-benzimid (Hoechst) solution (blue). Yellow colour in merged images provides co-localisation of Cy-PrP and Hsc70. Scale bar: 20  $\mu$ m

To test whether the intense dot-like Hsc70 staining in Cy-PrP expressing N2a cells was due to an increased Hsc70 protein level, cell extracts derived from mock, Cy-PrP and PM-PrP expressing cells were analysed by immunoblot using a specific anti-Hsc70 antibody (Fig. 24). In addition, transgene expression was confirmed using 3F4 antibody. In all cell extracts Hsc70 was detectable in similar quantities (band around 70 kDa), which excluded that Hsc70 redistribution or accumulation in fine foci was caused by an increased Hsc70 protein level in the cytosol of Cy-PrP expressing N2a cells.

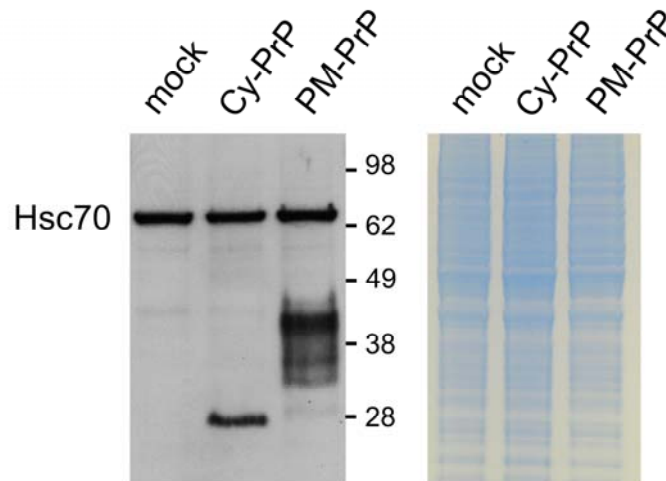


**Fig. 24 Hsc70 level is not altered by Cy-PrP expression in N2a cells.** Cy-PrP or PM-PrP expression was induced in transiently transfected N2a cells by adding 0.5  $\mu$ M PonA for 16 h. Cells were harvested and lysates were analysed for Hsc70 expression by immunoblotting using anti-Hsc70 antibody. Cy-PrP and PM-PrP expression was ensured using the 3F4 antibody. Right panel shows the coomassie stained gel as protein loading control.

Summary, these results suggest that homogenous distributed Hsc70 directed accumulated Cy-PrP to fine foci structures by binding and trafficking of Cy-PrP to endosomal vesicles. This would explain why transiently overexpressed Cy-PrP was not toxic during inhibition of the proteasome system in N2a cells.

#### 4.4.3 Binding of Cy-PrP by Hsc70

Immunofluorescence analyses provided the interesting result that Cy-PrP and Hsc70 co-localise in N2a cells, but did not proof direct binding of Cy-PrP by Hsc70. Therefore, specific Cy-PrP immunoprecipitation using the 3F4 antibody followed by immunoblot analysis with anti-Hsc70 may provide more detailed information on Cy-PrP/Hsc70 interaction. Unfortunately, the 3F4 antibody was not able to precipitate sufficient amounts of Cy-PrP from cell extracts as already observed by Wang *et al.* (2005). However, Cy-PrP was successfully immunoprecipitated using the anti-PrP antibodies 6H4, SAF32 and R340, which bind to different regions in the PrP sequence (Fig. 25A, lanes IP). Cy-PrP expression in the cell extracts of Cy-PrP transfected and induced N2a cells was also proven (Fig. 25A, lane L). Analysis of the supernatants of immunoprecipitation

experiments exhibited no signal for retained soluble Cy-PrP (Fig. 25A, lane S). Disadvantage of the used antibodies is their recognition of both transgene PrPs and endogenous murine PrP (PrP<sup>C</sup>) in transfected N2a cells resulting in co-precipitation of PrP<sup>C</sup> and MH2M PrPs (data not shown). Testing of Hsc70 co-precipitation with Cy-PrP specific 3F4 antibody revealed a significant Hsc70 signal in all analysed samples as well as in the mock and in PM-PrP expressing N2a cells (Fig. 25B). However, the amount of co-precipitated Hsc70 was increased by about 40 % in the Cy-PrP expressing N2a cells (Fig. 25B, lane 2). Detection of Cy-PrP and PM-PrP using 3F4 antibody ensured that immunoprecipitation experiments worked.

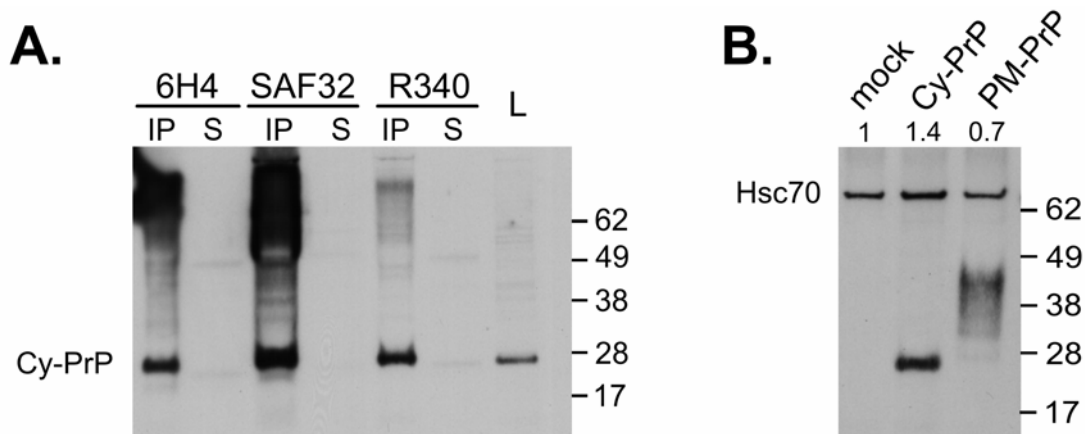


**Fig. 25 Cy-PrP immunoprecipitation and co-precipitation of Hsc70.** Lysates (200 µg) of PonA (0.5 µM) induced Cy-PrP-transfected N2a cells were immunoprecipitated with different PrP antibodies followed by immunoblot analysis using 3F4 antibody for Cy-PrP and PM-PrP detection and additionally anti-Hsc70 in B. (A) Cy-PrP in immunoprecipitates (IP) and supernatants (S) of anti-PrP immunoprecipitations using either antibody 6H4 and R340 with dilution 1:500 or SAF32 with 1:100 dilution. As positive control served 20 µg of pure lysate (L) of transiently Cy-PrP expressing N2A cells (B) Immunoblot analysis of Cy-PrP and PM-PrP immunoprecipitations (R340 anti-PrP) with co-immunoprecipitated Hsc70. Densitometric evaluation of Hsc70 signals from two independent experiments are shown as normalised values to mock control (= 1).

These data suggest that endogenous PrP<sup>C</sup> might be a natural substrate for Hsc70 and additional expression of Cy-PrP increases the amount of co-immunoprecipitated Hsc70 - a first hint for the regulator function of Hsc70 during appearance of cytosolic PrP.

## 4.5 Stable Cy-PrP expressing neuronal cell lines

### 4.5.1 Cy-PrP and PM-PrP expressing N2a cells

The experimental data obtained with transiently Cy-PrP expressing N2a cells showed that Cy-PrP is not intrinsically toxic to neuronal cells. However, the generation of a stable and constitutive Cy-PrP expressing cell lines failed yet, a finding, which was taken as support for the thesis that Cy-PrP mediates cytotoxicity (Ma *et al.* 2002). Since no acute Cy-PrP-mediated cytotoxicity was observed in the cellular model *in vitro*, establishment of stable Cy-PrP expressing N2a cell lines could argue against a long term effect on cell survival by Cy-PrP. The first attempt to generate stable cellular N2a-clones was done using the inducible ecdysone expression system, which was used in transient experiments. After transfection or transduction and selection of antibiotic-resistant cellular clones, no transactivator VgRXR was expressed on protein level, which hampered the expression of Cy-PrP. In the second attempt, the generation of stable clones was repeated using the non-inducible CMV-driven Cy-PrP expression plasmid. In total, 63 antibiotic-resistant cellular clones were selected and screened by immunoblotting using the 3F4 antibody. 43 N2a cell clones positive for Cy-PrP expression at different levels were identified (Table 5).

**Table 5** Stable Cy-PrP or PM-PrP expressing N2a cell clones

Transgene	tg-PrP expression level	count of clones
Cy-PrP	+	31
	++	7
	+++	5
	-	20
PM-PrP	+	6
	++	2
	+++	2
	-	2

One representative immunoblot presenting the clones 6, 18 and 25 with highest Cy-PrP expressing levels is shown in Fig. 26A. The specific band of around 27

kDa for Cy-PrP was detected in all three clones, but not in the parental N2a cells. Additional unspecific protein bands were observed at higher molecular weight (around 38 kDa) in some of the stable N2a-Cy-PrP cell lines.

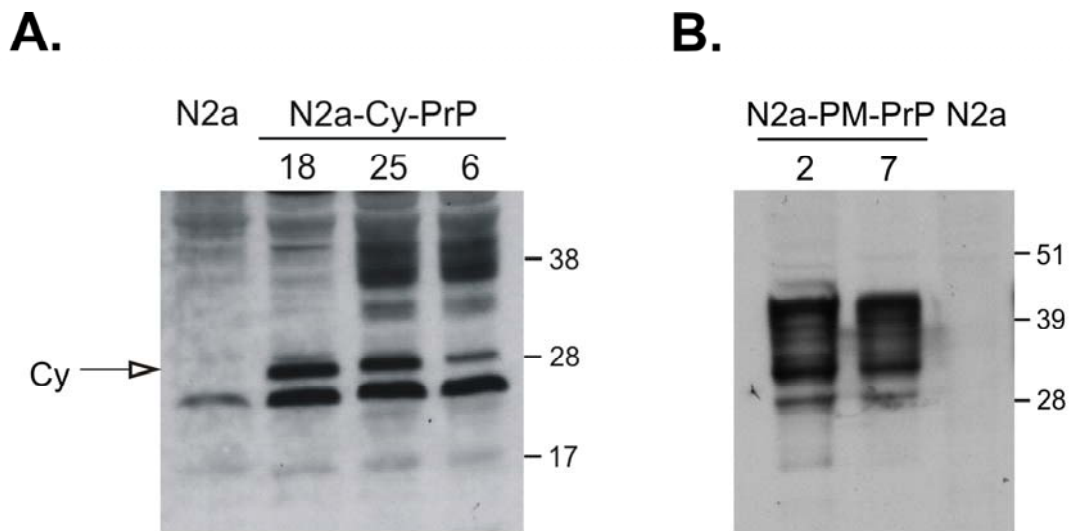


**Fig. 26 Stable N2a-Cy-PrP and N2a-PM-PrP cell lines.** N2a cells were stably transfected with Cy-PrP and PM-PrP followed by puromycin selection. Resistant cell clones were tested on transgene PrP expression by immunoblot using 3F4 antibody. Parental N2a cells served as negative control. (A) Immunoblot of N2a-Cy-PrP clone 6, 18 and 25. Arrow indicates specific Cy-PrP band. (B) Immunoblot of N2a-PM-PrP clone 2 and 7.

In a third step, the control cell lines stably expressing PM-PrP were generated as described using CMV-driven PM-PrP construct. Already 10 out of the first 12 selected antibiotic-resistant clones showed stable expression of PM-PrP (Table 5). Immunoblot of the highest PM-PrP expressing N2a clones, 2 and 7, is shown in Fig. 26B. The typical three-band pattern of PM-PrP was observed. In contrast, PM-PrP was not detected in the parental cell line N2a. The efficacy rate to generate Cy-PrP and PM-PrP expressing cell lines was 80 % for N2a-PM-PrP cells and 60 % for N2a-Cy-PrP cells. The successful generation of stable Cy-PrP expressing N2a cells might further argue against Cy-PrP-mediated cytotoxicity.



#### 4.5.2 Phenotype of N2a-Cy-PrP cell lines

To test whether Cy-PrP expression might have toxic effects in the stable cell lines, several clones were cultivated and examined for their morphology and proliferation. Most of the N2a-Cy-PrP clones (> 90 %) showed altered morphology in contrast to the parental N2a cells characterised by visual less cytosolic content, more ramified and prolonged cell shape and dramatically enhanced cell-cell interactions. The latter was already observed in very thin cell culture populations and complicated the subcloning procedure (Fig. 27).

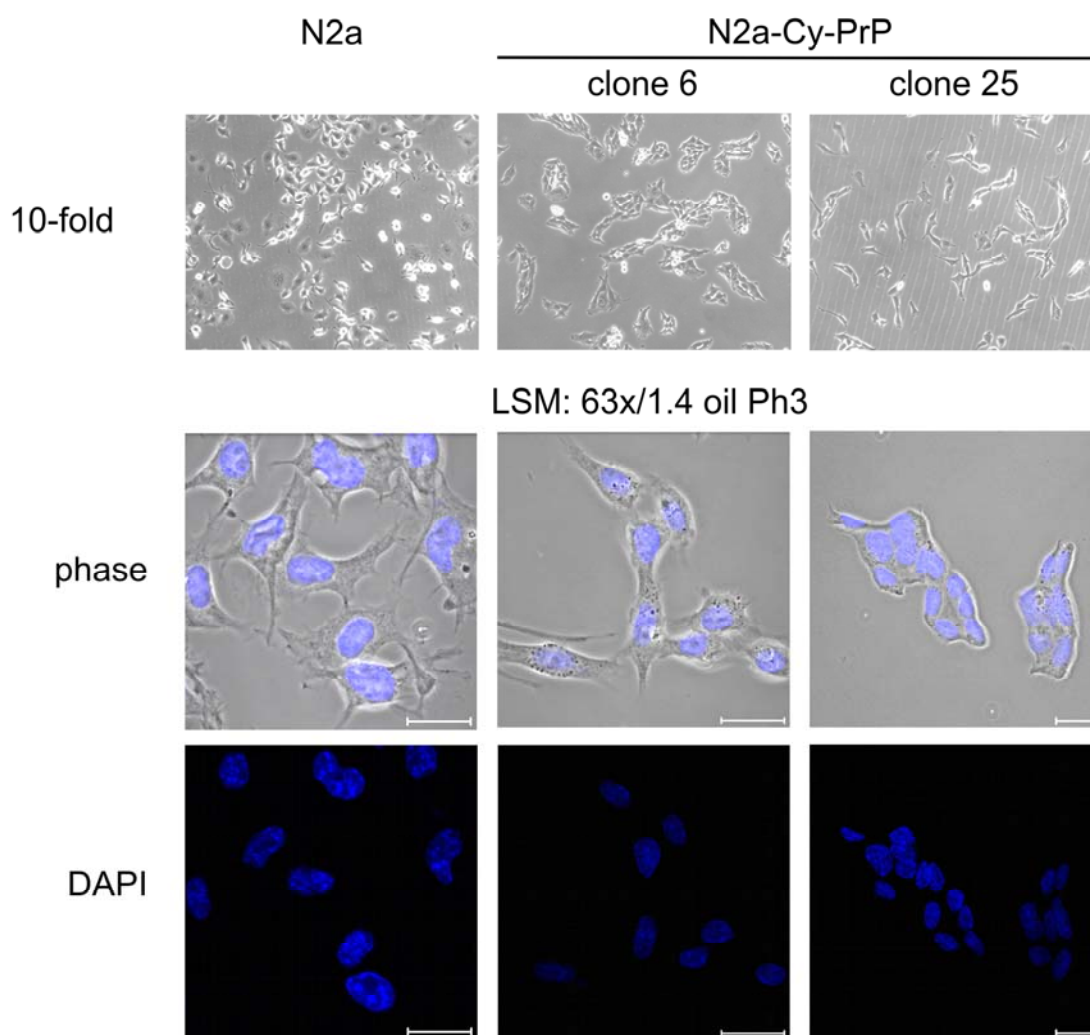


**Fig. 27 Altered morphology of N2a-Cy-PrP cell clones and nuclear chromatin staining.** Upper lane displays morphology of N2a-Cy-PrP clone 6 and 25 as compared to parental N2a cells. Below Hoechst-stained nuclei (blue) of N2a cells and N2a-Cy-PrP cell clones are shown recorded with 63xPh3 objective of a confocal laser scanning microscope (LSM). Scale bar: 20  $\mu$ m

In contrast, no N2a-PM-PrP clone showed such an altered morphological phenotype. N2a-Cy-PrP cell lines did not show reduced proliferation or apoptotic morphology such as apoptotic bodies or highly condensed chromatin-structure in the nuclei. The latter was examined in Hoechst-stained cells by immunofluorescence as shown in Fig. 27. Rather proliferation rate of N2a-Cy-PrP cell lines was dramatically accelerated as compared to N2a cells when the threshold of critical cell number was exceeded (Fig. 28).

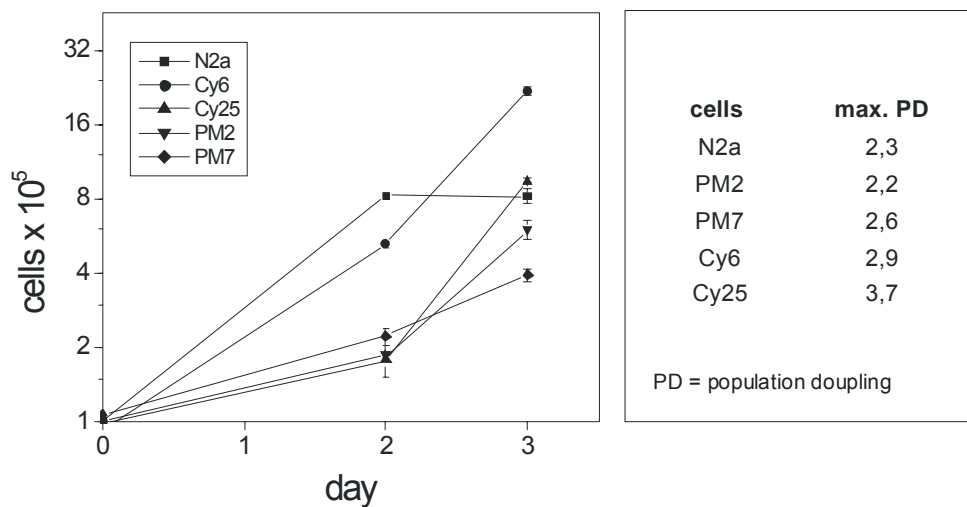


**Fig. 28** Growth curves and maximal population doubling per day (PD) of stable N2a-Cy and N2a-PM cell lines and N2a cells. Plot shows cell counts as function of the growing time. Values were used for calculation of the maximal PD (right).

The maximal population doubling rate (PD) of N2a cells and N2a-PM-PrP cell lines was around 2.2-2.6 per day (Fig. 28, right). The maximal PD of N2a-Cy25, which was the cell clone with the highest Cy-PrP expression, attained 3.7 per day.

#### 4.5.3 Localisation of Cy-PrP in N2a-Cy-PrP cell lines

To analyse cellular distribution of Cy-PrP, immunofluorescence experiments were performed with different stable N2a-Cy-PrP cell lines. Immunofluorescence experiments provided 3F4-specific Cy-PrP staining as red speckles throughout the cells as observed in transient transfection experiments and in proximity to plasma membrane strongly associated with regions of cell-cell contacts (Fig. 29). To

visualise the entire cellular Cy-PrP localisation, projection analyses were performed, where all z-layer images were summarised to one image with maximal transparency. Partially, the projection image of clone 6 displayed the localisation of Cy-PrP in fine foci through the entire cell. In contrast, the highest Cy-PrP expressing clone 25 showed a additional strong plasma membrane-like staining.

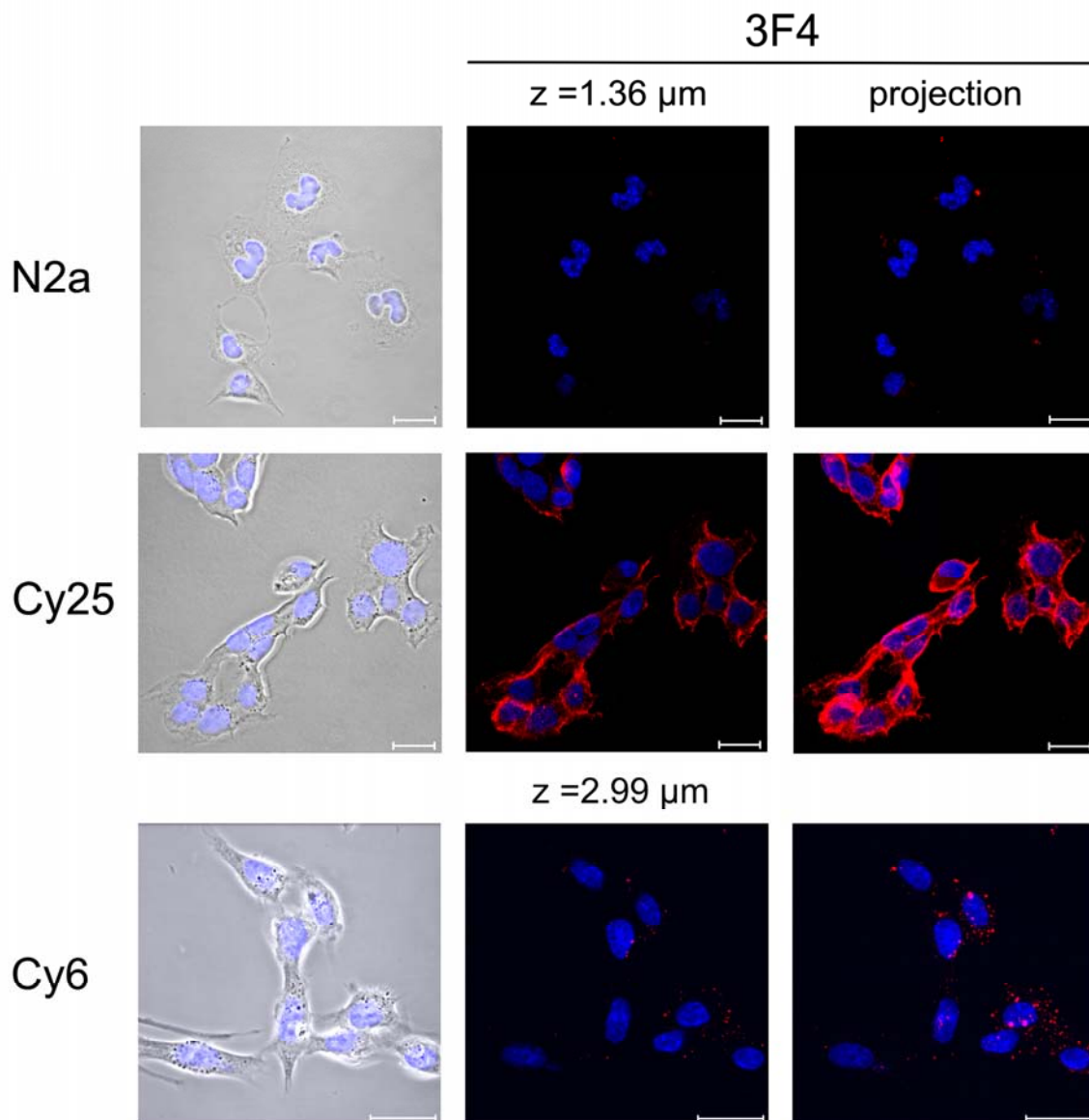


**Fig. 29 Immunofluorescence of Cy-PrP expression in stable N2a-Cy-PrP cell lines.** Cells were fixed, permeabilised with Triton-X-100, and stained with mouse anti-PrP antibody 3F4 antibody followed by Alexa594 (red)-conjugated anti-mouse secondary antibody. Nucleus staining was performed with bis-benzimid (Hoechst) solution (blue). Scale bar: 20 μm

For the first time, stable N2a-Cy-PrP cell lines were successfully established and their characteristics such as accelerated proliferation rate and the lack of apoptotic morphology supported the data of viability assays done with transient Cy-PrP expressing N2a cells. Therefore, Cy-PrP expression was not toxic *per se* to neuronal N2a cells. Nevertheless, Cy-PrP might affect the cell-cell interactions by altered cell adhesion molecule expression.

#### 4.5.4 Cy-PrP and PM-PrP expressing PrP<sup>0/0</sup> neuronal precursors

As described above, N2a-Cy-PrP cell lines exhibited an altered morphology accompanied by enhanced cell-cell interaction, which might be due to endogenous PrP<sup>C</sup>/Cy-PrP interaction. To discriminate between Cy-PrP-mediated effects and such possibly caused by Cy-PrP/endogenous PrP<sup>C</sup> interaction, PrP<sup>0/0</sup> neuronal precursor cells were stably transfected with Cy-PrP. So far, one positive Cy-PrP expressing cell clone was selected (Fig. 30A), whose morphology was not affected by Cy-PrP expression as compared to the control PrP<sup>0/0</sup> neuronal cells. Whether PrP<sup>C</sup> might have an influence on Cy-PrP function remains to be detailed investigated.

To determine the subcellular localisation of Cy-PrP in these PrP<sup>0/0</sup> neuronal cells, immunofluorescence experiments with co-staining of Cy-PrP and EEA1, Hsc70 or giantin (Fig. 30B) were performed. Interestingly, Cy-PrP was highly expressed in some cells and showed the same staining pattern as in transiently transfected N2a cells characterised by nucleus-associated localisation and intense speckles throughout the cell (Fig. 30B, 3F4). Furthermore, the immunofluorescence images also demonstrated that Cy-PrP co-localises with the endosomal marker EEA1 (Fig. 30B, upper panel) as well as with Hsc70 (Fig. 30B, middle panel), clearly seen as yellow colour in the merged images. As expected, no co-localisation was observed of Cy-PrP and giantin (Fig. 30B, lower panel merged image) indicating that Cy-PrP is not located in the Golgi apparatus in the PrP<sup>0/0</sup> neuronal precursor cells.

These data, observed in stable PrP<sup>0/0</sup>-Cy-PrP neuronal precursor cells, were in accord with the results from transient experiments in N2a cells suggesting that Hsc70/Hsp70 might prevent Cy-PrP-mediated cytotoxicity.

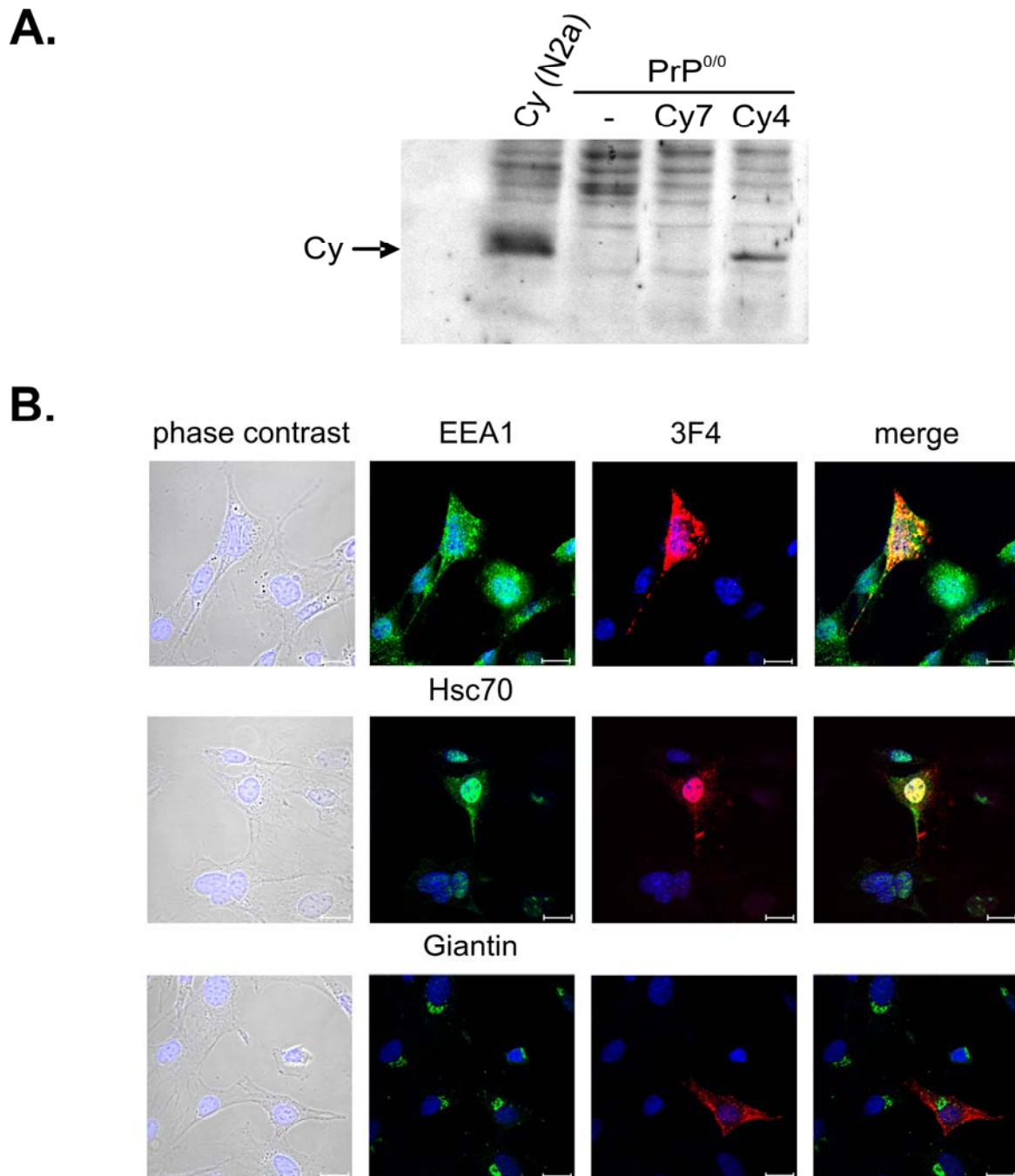


**Fig. 30 Cy-PrP expression in neuronal precursor cells.** Stably expressed Cy-PrP in neuronal cerebellar precursor PrP<sup>0/0</sup> cells. (A) Immunoblot of Cy-PrP clones Cy7 and Cy4 using 3F4 antibody. As positive control served transiently transfected N2a cells (lane Cy(N2a)). (B) Immunofluorescence analysis of co-stained Cy-PrP (red) with EEA1, Hsc70 or giantin (green). Cells were fixed, permeabilised with Triton-X-100, and stained with 3F4 anti-PrP antibody and anti-EEA1, anti-Hsc70 or anti-giantin antibody followed by Alexa488 (green)-conjugated and Alexa594 (red)-conjugated secondary antibody. Nucleus staining was performed with bis-benzimid (Hoechst) solution (blue) Co-localisation is displayed as yellow colour in the merged images. Scale bar: 20  $\mu$ m.

## 5 Discussion

### 5.1 Cy-PrP toxicity and proteasome in cell culture

#### 5.1.1 Cy-PrP is *per se* not toxic to neuronal cells

Retro-translocation of proteins from ER to the cytosol is the natural route for misfolded and malfunctioning proteins to undergo proteasomal degradation, a mechanism also known as ERAD. Recent studies have shown that membrane-associated PrP and mutant PrP underlie this pathway in neuronal cells (Yedidia *et al.* 2001; Rane *et al.* 2003; Wang *et al.* 2005). Ma and colleagues have shown that such cytosolic accumulated PrP is toxic to neuronal cells *in vitro* (2002a) and Cy-PrP expressed in transgenic mice induces loss of the granular layer of the cerebellar neurons *in vivo* (2002b). However, the postulated cytotoxicity of a cytosolic form of PrP is controversial discussed and the mechanisms of appearance and action are still not clearly characterised (Fioriti *et al.*, 2005; Heller *et al.*, 2003; Rambold *et al.*, 2006; Roucou *et al.*, 2003; Stewart and Harris, 2003). This study investigated the cytotoxic effects of cytosolic PrP in neuronal cells by inducible overexpression of a mutant form of PrP (Cy-PrP) lacking the N- and C-terminal trafficking signals. It was published that this Cy-PrP expression is toxic to neuronal N2a cells within 24 h (Ma *et al.*, 2002b; Roucou *et al.*, 2003). To confirm this, Cy-PrP was inducible expressed in neuronal N2a cells followed by cell viability analyses using the MTT and LDH assay after 24 h and 48 h (Fig. 8). Surprisingly, no Cy-PrP-mediated cytotoxicity was measurable. Furthermore, cell viability assays performed in 293T cells after 24 h of induced Cy-PrP expression (Fig. 10) confirmed the unidentified toxicity in N2a cells. Hence, Cy-PrP was also not toxic in non-neuronal cells. It has been shown that Cy-PrP expression in N2a cells correlates with increased apoptosis demonstrated by TUNEL assay (Ma *et al.*, 2002b) and detection of condensed chromatin with Hoechst 33342 staining (Roucou *et al.*, 2003). Since in this study the TUNEL assay was not clearly reproducible, Cy-PrP expressing cells were examined for caspase-3 activity. Caspase-3 is the central apoptosis enzyme activated by different apoptosis

pathways including ER stress response. Thus, its activity is a reliable marker for induced apoptosis in neuronal cells. However, Cy-PrP expression did not induce increased caspase-3 activity in N2a cells after 24 h (Fig. 11). It might be possible that 24 h Cy-PrP expression was not sufficient to induce apoptosis. But this data are contrary to Ma and colleagues who have shown 6 to 14% increase of apoptotic N2a cells after 24 h using the same inducible expression system (Ma *et al.*, 2002b). Others observed only around 25 % Cy-PrP-mediated increased cell death 24 h post-transfection in N2a cells determined by Hoechst stained condensed chromatin in the nuclei (Roucou *et al.*, 2003). However, in this study chromatin-staining in the nuclei after Cy-PrP expression showed no increased chromatin condensation in N2a cells 24 h post-transfection (Fig. 20, Fig. 22, Fig. 23). One might argue that the expression levels of Cy-PrP in several used N2a subpopulations were not comparable due to different susceptibility to Cy-PrP-mediated toxicity. But other neuronal cells were also not susceptible to Cy-PrP-mediated toxicity (Roucou *et al.*, 2003). Microinjection of Cy-PrP cDNA in human neuroblastoma cell lines as well as primary human neurons did not induce cell death including 72 h after injection (Roucou *et al.*, 2003). This is further in accordance with data obtained for N2a cells overexpressing a mutant PrP, which accumulates in the cytosol after proteasome inhibition without showing a cytotoxic effect in the MTT viability assay (Fioriti *et al.*, 2005). Furthermore, in this study stable Cy-PrP-expressing N2a cell lines were successfully generated, while attempts by others failed (Ma *et al.*, 2002b; Roucou *et al.*, 2003). These Cy-PrP cell lines with normal or increased proliferation rate and absence of apoptotic morphology (Fig. 27-29) are an additional indication that Cy-PrP is not extremely toxic. Moreover, neuronal cerebellar precursor cells from Zurich I PrP<sup>0/0</sup> mice were used to generate the stable Cy-PrP-expressing cell line Cy4. Even in these cells, morphological observations and nuclei visualisation using Hoechst dye were not able to detect Cy-PrP-mediated toxicity (Fig. 30). Thus, this study showed several lines of evidence that Cy-PrP overexpression is not toxic *per se* in short-term to neuronal cells and the cells might be protected either through recognition and degradation of Cy-PrP or binding of Cy-PrP to protective proteins.

Considering that neurodegeneration often appears with aging including inherited prion diseases and displays a long-term process, analysis of Cy-PrP involved in this process by transient transfection experiments may not be suitable. The

generated stably expressing Cy-PrP cell lines are an ideal starting point to investigate whether long-term Cy-PrP expression is detrimental to the cells by, for instance, analysis of Cy-PrP expression levels, Cy-PrP aggregation, and effects on cell growth and cell viability.

### 5.1.2 Stability and proteolysis of Cy-PrP

In most prion diseases, it has been shown that neuropathology is accompanied with widespread deposits of amyloid aggregates containing the structural converted PrP<sup>Sc</sup> (Collinge, 2001; Hope, 2000; Jackson and Clarke, 2000). Since then, the ability of derivatives of PrP<sup>C</sup>, such as PrP<sup>Sc</sup>, to form aggregates has been often used as parameter for neuronal toxicity. A characteristic of these detergent insoluble aggregates is their resistance to proteinase K digestion (Bolton *et al.*, 1982, McKinley *et al.*, 1983). However, no proteinase K resistant Cy-PrP was found after 16 h PonA induction in the used cellular model (Fig. 12). A second indicator for PrP<sup>Sc</sup>-like aggregation is the increased stability and prolonged half life as compared to PrP<sup>C</sup> (Borchelt *et al.*, 1990). However, it was demonstrated that overexpressed Cy-PrP is degraded like a short living protein similar to PrP<sup>C</sup> (Borchelt *et al.*, 1990). The proteolysis rate of Cy-PrP with the half life around 7.5 h was comparable to that of overexpressed full length PrP (PM-PrP) (Fig. 13). These findings support the lack of intrinsic Cy-PrP toxicity to N2a cells due to missing increased proteolysis and stabilisation as aggregates. Similar observations were obtained from experiments done with recombinant mPrP(23-231) (Hornemann *et al.*, 1997). Recombinant mPrP(23-231) is soluble, sensitive towards proteolytical digestion and does not aggregate irreversible in aqueous solution *in vitro*. However, Wang and colleagues failed to precipitate Cy-PrP using the 3F4 antibody, which was also found in this study (see 4.4.3), and assumed that Cy-PrP is aggregated due to the removal of such aggregates during the pre-clear centrifugation step within the procedure of immunoprecipitation (Wang *et al.*, 2005). In contrast, the precipitation of Cy-PrP worked well using antibodies recognising epitopes up- and down-stream of the 3F4-epitope (Fig. 25). This result does not further support this postulated aggregation theory. However, the 3F4-epitope might cover a binding site with higher affinity to other proteins such as already postulated for PrP<sup>Sc</sup> (Brown, 2000; Norstrom and Mastrianni, 2005; Satoh



*et al.*, 2005; Zanata *et al.*, 2002) and might explain the failed precipitation using the 3F4 antibody. Finally, Cy-PrP aggregates might exist and their formation depends on the cytosolic concentration, the intracellular localisation, and the kinetics between synthesis and degradation of Cy-PrP as well as the interaction with other cellular proteins.

In different neurodegenerative diseases and during aging proteasome activity is reduced, which causes accumulation of misfolded and malfunctioning proteins (Grune *et al.*, 2005; Keller *et al.*, 2000; Keller *et al.*, 2005; Korolainen *et al.*, 2002). Accumulation of misfolded proteins is suggested to be the common pathogenic mechanism in some neurodegenerative disorders including prion disease. Thus, the Cy-PrP proteolysis was further detailed analysed for the responsible protease with the proteasomal system as primary target for investigations. Indeed, Cy-PrP proteolysis after proteasome inhibition was dramatically decelerated indicated by prolonged half life of around 12 h (Fig. 14), which is comparable with that of PrP<sup>Sc</sup> (half life 15 h). Additionally, strong Cy-PrP accumulation was observed after proteasome inhibition (Fig. 16). Both results indicate that Cy-PrP is recognised and degraded by the proteasome. Strikingly, no influence on cell viability was detected during inhibition of proteasomal activity (Fig. 18). The Cy-PrP expression neither increased the proteasome activity nor altered the entire proteasome level in N2a cells (Fig. 17). The presented data together with the PK-digestion experiment do not confirm previous suggestions, that cytosolic accumulated PrP will aggregate, and aggregated PrP molecules are resistant to further degradation and might trigger cytotoxicity (Ma *et al.*, 1999; Ma *et al.*, 2002a). However, long-term Cy-PrP expression might cause Cy-PrP aggregation by a yet unknown mechanism. In further studies using the generated N2a-Cy-PrP cells, Cy-PrP aggregation might be detectable through higher molecular weight of Cy-PrP signals with increasing number of cell passages. Moreover, the fibrillar character of Cy-PrP aggregates could be analysed via the specific amyloid fibril staining with Thioflavin S or (trans, trans)-1-bromo-2,5-bis-(3-hydroxycarbonyl-4-hydroxy) styrylbenzene (BSB) in a time-dependent manner (Ando *et al.*, 2003; Hoefert *et al.*, 2004; Konarkowska *et al.*, 2006; Santa-Maria *et al.*, 2006).

Finally, it has to be mentioned that continuous Cy-PrP expression appears to increase the ATP-dependent proteasome activity in the N2a-Cy-PrP cell lines 6 and 25 (data not shown) as compared to parental N2a cells. This changed

proteolytical activity could signalise a continuous stress situation, which has only consequences during prolonged cultivation.

### 5.1.3 Retro-translocated Cy-PrP

PrP accumulation in the cytosol has been shown clearly, however the nature of such cytosolic PrP is controversially discussed. Different studies using stable cells expressing wt-PrP or mutant PrP demonstrate accumulation of a non-glycosylated, N-terminal signal peptide-bearing form of PrP (NSP-PrP) in the cytosol during proteasome inhibition (Driscaldi *et al.*, 2003; Fioriti *et al.*, 2005). This small fraction of NSP-PrP appears not to be translocated into the ER. The authors claimed that PrP is not subjected to ERAD and the natural occurrence of Cy-PrP is therefore unlikely. In fact, they discussed that observed cytosolic NSP-PrP is a result of elevated transgenic PrP expression due to proteasome inhibitor-mediated increased CMV-promotor activity followed by overloaded ER translocation. In contrast, detailed analysis of endogenous wt-PrP in several cell lines and primary neurons revealed that a portion of PrP is retro-translocated to the cytosol for degradation by the proteasome (Wang *et al.*, 2005). Consistent with these data, the accumulation of a non-glycosylated PM-PrP isoform was found during proteasome inhibition in PM-PrP overexpressing N2a cells (Fig. 15), although PM-PrP expression was already stopped. The occurrence of this form of PrP cannot be the result of increased PM-PrP synthesis by epoxomicin-mediated elevated CMV-promoter activity. The molecular weight of this form of non-glycosylated PrP was slightly higher as compared to overexpressed transgenic Cy-PrP (e.g. Fig. 7Fig. 9Fig. 19). The NSP contains 23 aa, which would result in an additional molecular weight of approximately 2.5 kDa. This supports the theory of retro-translocated PrP carrying the NSP, which becomes visible. To confirm this, PM-PrP expressing N2a cells have to be analysed by immunoblotting using a specific anti-NSP antibody (Stewart and Harris, 2003). On the other hand, PM-PrP like PrP<sup>C</sup> undergoes a variety of proteolytic processing events and another proteolytic form of PM-PrP might be detected, which is not related to retro-translocation into the cytosol. For instance, PrP<sup>C</sup> can be cleaved at aa 110 and 111 by ADAM family proteases such as ADAM 10 and ADAM 17 to produce a 17-kDa C-terminal fragment C1 (Jimenez-Huete *et al.*, 1998; Pan *et al.*, 1992; Shyng *et al.*, 1993).

PrP<sup>C</sup> can also be cleaved by ROS within or adjacent to the octarepeats to generate a 21-kDa C-terminal fragment C2 (Jimenez-Huete *et al.*, 1998; Pan *et al.*, 1992; Taraboulos *et al.*, 1992). However, both proteolytical cleavage products of PM-PrP would provide lower molecular weight signals as compared to transgenic Cy-PrP of around 27 kDa. Thus, the appearance of NSP-PrP derived from PM-PrP becomes more evident.

In addition, if PrP is mainly post-translational imported into ER, the putative transmembrane domain of PrP will induce misfolding in the cytosol interfering the import into the ER (Heller *et al.*, 2003). Such non-glycosylated and misfolded NSP-PrP associates with the ER membranes and decreases cell viability (Heller *et al.*, 2003). In contrast, Heller *et al.* showed that expressed Cy-PrP also adopts a misfolded conformation; however, this has no adverse effect on cell growth. In this study, accumulated non-glycosylated PM-PrP (Fig. 15) was not significant toxic after 24 h PM-PrP expression in presence of proteasome inhibition in N2a cells (Fig. 18). Continuous PM-PrP overexpression might cause saturation of ER-translocation and could result in the accumulation of NSP-PrP and cell death, which needs further investigation. On the other hand, retro-translocation of misfolded or malfunctioned proteins involves Ca-dependent ER chaperones like Bip and calnexin. By this way a continuous traffic jam of misfolded or malfunctioned PrPs in the ER might cause alterations in the Ca-homeostasis (Bushmarina *et al.*, 2006; Verkhatsky, 2002; Zhang and Kaufman, 2006) followed by ER-stress response and apoptosis (Ferreiro *et al.* 2006; Hetz *et al.*, 2003; Kristensson *et al.*, 1993; Sandberg *et al.*, 2004; Wong *et al.*, 1996; Yadavalli *et al.* 2004).

Taken together the presented data support that cytosolic PrP is a result of ER retro-translocation, but cytotoxicity might be triggered by not retro-translocated NSP-PrP generated by impaired ER import during or after translation. These findings further let conclude that high levels of Cy-PrP escaped from proteolysis and an impaired proteasome system are not sufficient to induce Cy-PrP-mediated neuronal cell death. Furthermore, cell type and cell line, respectively, might determine the tolerance against the Cy-PrP and NSP-PrP in the *in vitro* experiments.

#### 5.1.4 Cy-PrP/membrane interaction as toxic event

One recent publication showed that Cy-PrP-mediated cytotoxicity is due to association of Cy-PrP with membranes (Wang *et al.*, 2006), since Cy-PrP expressed in N2a cells migrates with endogenous PrP and calnexin in the membrane fraction of sucrose gradients. Previous studies indicated that PrP interacts with lipids (Baron and Caughey, 2003; Kazlauskaitė *et al.*, 2003; Morillas *et al.*, 1999; Sanghera and Pinheiro, 2002) and that recombinant PrP can bind and disrupt liposomes composed of negatively charged phospholipids (Kazlauskaitė *et al.*, 2003). One might speculate that Cy-PrP disrupts the phospholipid bilayer via interaction with the hydrophobic core of membranes, causing increasing calcium concentration and increasing levels of calcium-responsive phospholipase (cPLA2), as observed in degenerating cerebellum of transgenic mice expressing Cy-PrP (Wang *et al.* 2006). However in this study Cy-PrP was mainly separated with the soluble cytosolic fraction (Fig. 19). Only a small part of Cy-PrP was associated with the plasma membrane/ER membrane fraction as observed for the full length PM-PrP and no Cy-PrP-mediated toxicity was found (Fig. 8, Fig. 10 and Fig. 11). Thus, the postulated mechanism of the Cy-PrP-mediated impairment of calcium homeostasis via membrane disruption and cPLA2 activation as toxic signal cascade is inconsistent with these data. Furthermore, neurons in the forebrain tolerate higher amounts of Cy-PrP and do not show neuronal death *in vivo* (Wang *et al.* 2006). It is rather likely that Cy-PrP degradation (see 4.3.1) and interaction with protective cytosolic proteins prevents neuronal N2a cells from this mechanism.

#### 5.2 Cy-PrP localisation in early endosomal vesicles

This study showed cytosolic localisation of Cy-PrP by immunoblot analyses of cytosolic and membrane fractions (Fig. 19). Immunofluorescence microscopy revealed a strong co-localisation of Cy-PrP with EEA1, a marker for early endosomes (Lawe *et al.*, 2000; Mu *et al.*, 1995, Wilson *et al.*, 2000)(Fig. 22). Early endosomes are low density vesicles more present in the cytosol than in the high density membrane fractions (Bergeron *et al.*, 1986; Kjekens *et al.*, 1995; Shah *et*

*et al.*, 2006). EEA1 is a hydrophilic peripheral membrane protein partitioning in the aqueous phase after triton-detergent solubilisation as used here (Mu *et al.*, 1995). Thus, both data were convergent to exclude that Cy-PrP is mainly plasma membrane-located. It was rather that high amount of Cy-PrP localised intracellular in EEA1-positive endosomal vesicles in transient Cy-PrP expressing N2a cells (Fig. 22). Further experiments to separate early and late endosomes as well as lysosomes using OptiPrep iodixanol density gradient (Axis Shield) would support the observed data. Lysosomal markers like “lysotracker green” and LAMP1 have been failed in immunofluorescence experiments (data not shown) and analyses using NH<sub>4</sub>Cl, as inhibitor of lysosomal proteases provided no hint for lysosomal degradation of Cy-PrP (data not shown).

Firstly, EEA1 functions as tethering/docking molecule that provides directionality to the vesicular transport from the plasma membrane to the early endosomes (Rubino *et al.*, 2000; Wilson *et al.*, 2000). EEA1 is exclusively localised to early endosomes and not present in clathrin-coated vesicles (CCV) (Rubino *et al.*, 2000; Wilson *et al.*, 2000). These data let conclude that co-localisation of Cy-PrP with EEA1 represents a Cy-PrP transport to the early endosomal compartment. This process might be triggered by the N-terminal domain of Cy-PrP, containing the basic motive NH<sub>2</sub>-KKRPK, which is also sufficient for direct internalisation of PrP<sup>C</sup> (Sunyach *et al.*, 2003; Taylor *et al.*, 2005). This can be tested using a truncated Cy-PrP (aa27-231) or via alanine-scanning mutagenesis.

Secondly, other authors postulated a direct interaction of Cy-PrP with the plasma membrane, which could trigger EEA1-mediated docking at this locations followed by uptake of Cy-PrP into early endosomes to prevent disruption of cell membrane associated cell signalling or transport function. These vesicular inclusions could reduce levels of diffuse Cy-PrP in the cytosol and the risk of neuronal death as observed for huntingtin in primary neurons (Arrasate *et al.*, 2004). EEA1 uptake within the endosomal membrane and its function are dependent on PI(3)P, Rab5-GTP and calmodulin binding (Lawe *et al.*, 2000; Lawe *et al.*, 2003; Rubino *et al.*, 2000; Simonsen *et al.*, 1998). Reduction of EEA1 or Rab5-GTP through RNA interference as well the inhibition of calmodulin binding by the specific inhibitor W7, which showed already re-localisation of EEA1 to the cytosol (Lawe *et al.*, 2003), might increase Cy-PrP-mediated cytotoxicity in N2a or other cellular

models. This would demonstrate both, Cy-PrP is toxic to cells and the endosomal compartment plays a pivotal protective function.

Thirdly, internalisation of mature PrP<sup>C</sup> is mediated by clathrin coated pits into recycling endosomes from which it is rapidly retrieved to the cell membrane (Shyng *et al.*, 1994; Sunyach *et al.*, 2003; Taylor *et al.*, 2005). During this process PrP<sup>C</sup> passes Rab5-containing early endosomes (Magalhaes *et al.*, 2002; Sunyach *et al.*, 2003). Cy-PrP located in early endosomes could interact with mature PrP<sup>C</sup>. If Cy-PrP has conformational similarities to PrP<sup>Sc</sup> as postulated by Ma and colleagues (Ma *et al.*, 1999; Ma *et al.*, 2002a) and the known fact that early endosomes are identified as potential sites for the generation of PrP<sup>Sc</sup> by PrP<sup>Sc</sup>/PrP<sup>C</sup> interaction (Biswas *et al.*, 2006; Brown, 2000; Feughelman and Willis, 2002; Norstrom *et al.*, 2005; Warwicker, 2000), it might be possible that Cy-PrP mediates conversion of PrP<sup>C</sup> to a PrP<sup>Sc</sup>-like isoform and contributes to neuronal death in a time dependent manner. In fact, this study demonstrated that Cy-PrP is not PK-resistant and forms no proteolysis-resistant aggregates like PrP<sup>Sc</sup>, since Cy-PrP was completely degraded by the proteasome.

Fourthly, Cy-PrP could interact with PrP<sup>C</sup> in a toxic manner by inhibition of the signalling function of PrP<sup>C</sup> *in vivo*, e.g. within the Fyn-kinase pathway, on neuronal differentiation and survival (Chen *et al.*, 2003; Kanaani *et al.*, 2005; Santuccione *et al.*, 2005; Steele *et al.*, 2006) as well as during neuronal activation via synaptic vesicles. Furthermore, interaction of Cy-PrP with other membrane associated proteins than PrP<sup>C</sup> might be also a toxic event *in vivo*, especially when it occurs closely to synaptic membranes (Wang *et al.*, 2006). In support to this hypothesis, Cy-PrP was observed in close proximity to the plasma membrane, mainly in regions of cell-cell contacts, in the highest stable Cy-PrP expressing N2a cell line (Cy25)(Fig. 29, middle panel). Cy-PrP-mediated effects on neuronal cell-cell communication, synaptic neurotransmitter release and neuronal differentiation could be examined using primary neurons followed by *in vivo* studies with mice expressing Cy-PrP in neuronal subtypes. However, toxic accumulation of Cy-PrP/PrP<sup>C</sup> complexes might be rather a long-term effect. It has to be therefore analysed, whether continuous Cy-PrP expression has an effect on the PrP<sup>C</sup> level on the plasma membrane or endosomal aggregation as well as on the Fyn kinase signalling. Thus, further investigations using the generated stable N2a-Cy-PrP cell lines would be helpful to answer these questions.

### 5.3 Hsc70/Hsp70 - prevention against Cy-PrP toxicity

The lack of Cy-PrP cytotoxicity in the used N2a cell model could also be due to the existence of a secondary defence system against the toxic accumulation of Cy-PrP in neuronal cells. The major difference between the normal and disease-associated isoforms of PrP is a conformational change, leading to the hypothesis that chaperones may be involved in the folding of PrP and hence in the progression of the disease (Kenward *et al.*, 1996; Telling *et al.*, 1995). Hsp70 family appears to play a particular role in prion disease, since it has been shown that Hsp70 co-localises with ubiquitin-protein conjugates in vesicle structures of the endosome/lysosome system of scrapie-infected mouse brain (Arnold *et al.*, 1995; Laszlo *et al.*, 1992). Regarding cytosolic PrP, ER retro-translocated PrP co-localises with Hsc70 in aggresomes after proteasome inhibition (Ma *et al.*, 2001). In this study Cy-PrP co-localisation with Hsc70 in EEA1-positive vesicle structures was observed at higher expression levels. The expression level of Hsc70 was not affected by Cy-PrP expression in N2a cells (Fig. 24). However, Cy-PrP seems to have a redistributing effect on Hsc70 (Fig. 23), since in mock and PM-PrP-expressing N2a cells Hsc70 staining was diffuse and showed homogenous cellular Hsc70 distribution, which was lost in favour of Hsc70 focal aggregation in Cy-PrP-expressing N2a cells. This is consistent with data obtained with the inducible Hsc70-counterpart Hsp70 and the co-chaperone Hsp40, which co-localise after proteasome inhibition with cytosolic PrP in immunofluorescence experiments and sucrose gradient fractions (Rambold *et al.*, 2006). Moreover, Cy-PrP co-immunoprecipitates with Hsp70 indicating that the cytosolic chaperone Hsp70 interacts with Cy-PrP. It has been shown that *in vitro* Hsp70 and Hsc70 interact with lipids and promote the liposome aggregation in a time and protein concentration dependent manner (Arispe *et al.*, 2002; Ma *et al.*, 2001). Furthermore, accumulated inducible Hsp72 protects Purkinje cells against cell death in Creutzfeldt-Jacob disease (CJD) (Kovacs *et al.*, 2001) and Hsp70/Hsc70 reduces huntingtin toxicity and aggregation in neurons (Novoselova *et al.*, 2005; Warrick *et al.*, 1999). In SH-SY5Y human neuroblastoma cells, Hsc70 and Hsp40 overexpression prevents cytosolic PrP-induced apoptosis (Rambold *et al.*, 2006). The cytoprotective activity of Hsp70/Hsc70 is thought to be related to its

chaperone activity (Nollen *et al.*, 2002). Taken together, these data support the findings in this study indicating that Cy-PrP cytotoxicity in neuronal cells could be prevented by the protective function of high levels of Hsc70. What might be the molecular mechanism of Hsc70/Cy-PrP interaction (Fig. 31)?

Cy-PrP produced by retro-translocation (Jin *et al.*, 2000; Ma *et al.*, 2001; Roucou *et al.*, 2003; Wang *et al.*, 2005; Zanusso *et al.*, 1999) or impaired import into the ER (Heller *et al.*, 2003; Rane *et al.*, 2004) is degraded by the proteasome (Fig. 14). Thereby, hydrophobic residues of translated Cy-PrP are recognised by Hsc70, which promotes the folding process through cycles of substrate binding and release regulated by their ATP activity (Hartl and Hayer-Hartl, 2002; Rudiger *et al.*, 1997). Function of such Hsc70/Cy-PrP complexes is dependent on co-chaperone binding (Hohfeld *et al.*, 1995; Hohfeld and Jentsch, 1997; Minami *et al.*, 1996). ER-associated degradation (ERAD) of Cy-PrP by the proteasome might be mediated by binding of co-chaperone BAG-1 to the Hsc70/Cy-PrP complex. BAG-1 binds the proteasome and interacts with the ubiquitin-ligase CHIP followed by Cy-PrP release from Hsc70, Cy-PrP ubiquitination and proteasomal degradation (Alberti *et al.*, 2002; Luders *et al.*, 2000). It has to be mentioned that the cellular level of BAG-1 is approximately 1 % of Hsp70 (Nollen *et al.*, 2000; Nollen *et al.*, 2002; Takayama *et al.*, 1997) indicating that BAG-1 can bind only a fraction of Hsp/Hsc70 molecules. Otherwise, when Cy-PrP formation overcomes its proteolytical removal, excess Cy-PrP molecules interact with Hsc70, whose chaperone activity controls Cy-PrP folding in order to prevent cytotoxic aggregation. Although Hsc70 co-immunoprecipitation with PrP was increased in the Cy-PrP expressing cells, the binding of Cy-PrP by Hsc70 was not clearly demonstrated in this study. Therefore, *in vitro* binding assays such as plasmonresonance spectroscopy with purified Cy-PrP and Hsc70 could provide information about Cy-PrP/Hsc70 interaction. Furthermore, usage of distinct PrP peptides, e.g. PrP106-126, or truncated PrP isoforms could help to identify the Cy-PrP/Hsc70 binding site in PrP.



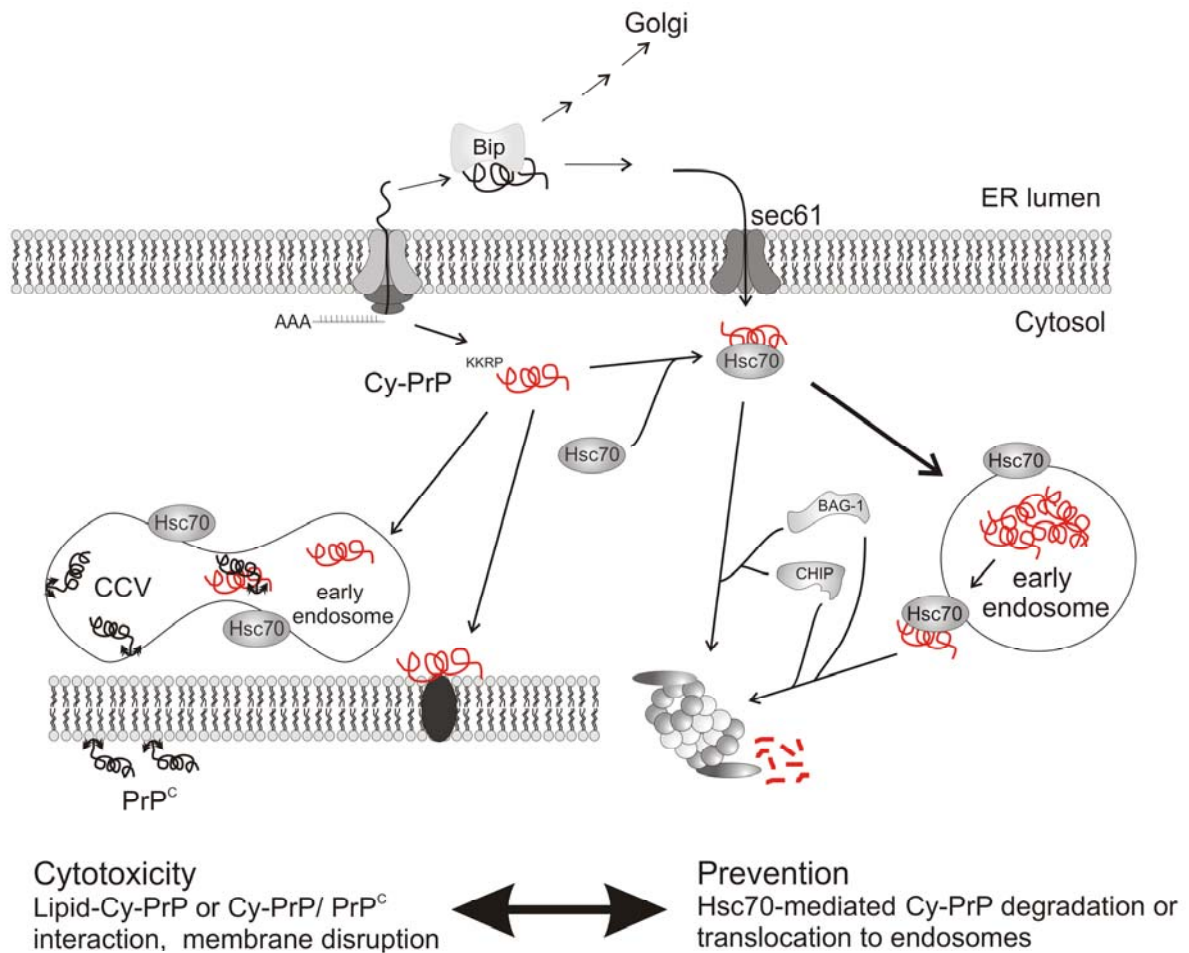


**Fig. 31 Model of Cy-PrP metabolism – cytotoxicity versus prevention by Hsc70.** ER imported nascent PrP binds luminal chaperone Bip; transport to Golgi compartment following correct chaperone-mediated folding (e.g. calnexin); misfolded or incorrect modified (N-glycosylation) PrP is retro-translocated via sec61 to the cytosol, named Cy-PrP. Cy-PrP can be toxic by (Wang et al. 2006) disruption of the intracellular membranes and the plasma membrane or by endosomal interaction with clathrin-endocytosed PrP<sup>C</sup> in fused clathrin coated vesicles (CCV) and early endosomes, also mediated by Hsc70 (clathrin uncoating). The latter likely might be an *in vivo* effect resulting in an impaired synaptic vesicle recycling or neurotransmitter release or PrP<sup>C</sup> signalling. Thereby, direct Cy-PrP traffic to CCVs/early endosomes might be triggered its N-terminal basic tetra peptide KKR. However, Hsc70 also appears to have protective potential against Cy-PrP induced toxicity, maybe dependent on the Hsc70 level and the energy stage (ATP). Theoretically, Cy-PrP could bind Hsc70 via its hydrophobic core (aa) followed by BAG1- and CHIP-mediated proteasomal degradation. Excess Cy-PrP remains bound to Hsc70 to avoid uncontrolled aggregation, and it is translocated to early endosomes to remove Cy-PrP from the cytosol. Later on, Hsc70-mediated re-traffic of Cy-PrP to the cytosol is assumed for further proteasomal degradation. Therefore, the steady state level of Cy-PrP and chaperones, particularly Hsc70, as well as the availability of ATP and synaptic activity determine Cy-PrP-mediated cytotoxicity *in vivo*.

To remove the potential toxic Cy-PrP from cytosol, Hsc70 might mediate Cy-PrP translocation across intracellular membranes into endosomal vesicles (Agarraberes *et al.*, 2001; Arispe *et al.*, 2002; Cuervo *et al.*, 1997; Terlecky *et al.*, 1992) explaining the observed co-localisation of Cy-PrP and the endosomal marker EEA1 (Fig. 22 and 30). It is known that cytosolic proteins are internalised and degraded in lysosomes in a Hsc73-mediated fashion (Chiang *et al.*, 1989; Terlecky *et al.*, 1992) However, further Cy-PrP degradation by lysosomes after delivery to the endosome/lysosome system by Hsc70-mediated transport is not assumed (see 5.2, first section).

Nevertheless, *in vivo* Cy-PrP expression level varies in different brain regions and is extremely toxic to granular cerebellar neurons in transgenic mice (Ma *et al.*, 2002b; Wang *et al.*, 2006). Such observed neuronal cell type-dependent cytotoxicity might be due to differences in the synaptic excitation or anti-stress systems, as chaperone response as well as ubiquitin-proteasome system. Indeed, the basal expression level of Hsc70 and the stress induced expression of Hsp70 vary in several neuronal cell types (Belay *et al.*, 2006; Foster *et al.*, 1995; Guzhova *et al.*, 2001; Manzerra *et al.*, 1996; Tanaka *et al.*, 2002; Voisin *et al.*, 1996). Neuronal cell types that exhibit high levels of Hsc70, such as specific hippocampal neurons and cerebellar Purkinje cells, are not triggered to undergo stress-induced cell death as compared to other neuronal populations such as granular cerebellar neurons lacking Hsc70 (Belay *et al.*, 2006; Tanaka *et al.*, 2002). Furthermore, high level of constitutively expressed Hsc70 appears to have a damping effect on stress-induced Hsp70 expression (Foster *et al.*, 1995; Manzerra *et al.*, 1996). Moreover, a 10-fold reduction in Hsp70 basal expression was observed upon differentiation in neuroblastoma cells (Guzhova *et al.*, 2001). Thus, the differentiation state and pool of chaperones expressed in different neuronal cell types may contribute to Cy-PrP mediated cytotoxicity *in vivo*. All these findings support our data obtained in the N2a neuroblastoma cell model and demonstrate that distinct chaperone expression is connected to neuroprotection. Concerning Cy-PrP-mediated cytotoxicity and the postulated hypothesis of Cy-PrP triggered membrane disruption (Wang *et al.*, 2006), a participation of Hsp70/Hsc70 has to be considered, since these chaperones are present in lipid raft in cells of forebrain and cerebellum (Chen *et al.*, 2005). Interestingly, in CJD patients it has been shown that neuropathological changes are mainly restricted to cell populations or

brain regions in which Hsp70/Hsc70 was expressed at lower levels. Indeed, apoptosis induction was higher in the Hsp70-negative granular cell layer as compared to Purkinje cells, which express high Hsp70 levels. Moreover, brain regions showing severe spongiform changes and gliosis exhibit fewer Hsp70-immunoreactive neurons (Kovacs *et al.*, 2001).

In addition, it should be investigated whether neuronal differentiation has an influence on the Hsc70/Hsp70 pool and can reveal Cy-PrP-mediated toxicity in stable N2a-Cy-PrP cell lines and PrP<sup>0/0</sup>-Cy4. In order to prove the hypothesis that Hsc70 prevents Cy-PrP-mediated toxicity in N2a-Cy-PrP cells, siRNA approaches could be performed to knock down Hsc70 expression followed by viability and apoptosis assays in these cells.

## 5.4 Cy-PrP and N2a cell morphology

During the generation of stable Cy-PrP expressing N2a cells most of the selected cell clones exhibited a new morphology characterised by visual less cytosolic content, more ramified and prolonged cell shape and dramatically enhanced cell-cell interactions (Fig. 29). Surprisingly, this phenotype was not found in any of the N2a-PM-PrP cell lines. These observations might indicate a Cy-PrP-mediated alteration of cell adhesion. To ensure that this phenomenon is due to the expression of Cy-PrP, the protein could be knocked down by a siRNA approach to return the morphology to the parental cells. This would be a novel unpublished Cy-PrP-mediated effect in neuronal cells. Nevertheless, analyses of several adhesion molecules such as E/N-cadherine, p120,  $\alpha$ - and  $\beta$ -catenin or NCAM as well as members of signalling cascades like Akt1/2 and SRC phosphorylation would be suggestive to examine, how Cy-PrP might influence this complex cell adhesion system. Interestingly, the selected Cy4 clone derived from PrP<sup>0/0</sup> cells showed no altered phenotype as compared to the parental cells. Hence, N2a-Cy-PrP phenotype might be a result of Cy-PrP and endogenous PrP<sup>C</sup> interaction, e.g. in the endosomal compartment (see 2.2.2 and 5.2). Therefore, generated N2a-Cy-PrP cell lines are potent cellular models to analyse Cy-PrP effects on cell adhesion in presence of endogenous level of PrP<sup>C</sup>.

## 5.5 Putative consequences for Cy-PrP expression *in vivo*

Co-localisation of Cy-PrP with EEA1 (Fig. 22Fig. 30) and Hsc70 (Fig. 22Fig. 23Fig. 30) arise the question of its consequences for the neuronal interaction *in vivo*. It is known that early endosomes and Hsc70 are important for the synaptic function and the recycling of synaptic vesicles as well as different neurotransmitter receptors (Bronk *et al.*, 2001; Buchner and Gundersen, 1997; Holroyd *et al.*, 1999; Selak *et al.*, 2004; Selak and Fritzler, 2004; Shimizu *et al.*, 2003; Stahl *et al.*, 1999; Tobaben *et al.*, 2001; Washbourne *et al.*, 2004; Zinsmaier and Bronk, 2001). Hence, the speculated Hsc70-mediated transport of Cy-PrP to early endosomes within synaptic areas might influence the normal synaptic vesicles maturation and the neurotransmitter release. Such Cy-PrP induced synapsis dysfunction *in vivo* could explain the contradicting results concerning the Cy-PrP toxicity observed in different cell models *in vitro*. Furthermore, PrP<sup>C</sup> plays a role in the fine-tuning of synaptic activity and plasticity examined in PrP knock out mice (see also 2.2.3). These results are supported by the fact that recombinant PrP induces rapid polarisation and development of synapses in embryonic rat hippocampal neurons (Kanaani *et al.*, 2005). Assumed Cy-PrP/PrP<sup>C</sup> interactions in the endosomes might result in similar neuropathological effects as detected in prion-diseased brains, maybe due to loss of normal PrP<sup>C</sup> function. In the cerebellum of CJD patients PrP deposits accumulated in the synapses correlating with abnormal synaptic protein expression (Ferrer, 2002). Scrapie-infected mice showed also synapses loss associated with abnormal PrP precedes (Jeffrey *et al.*, 2000), intrinsic dysfunction of cortical and hippocampal neurons (Jefferys *et al.*, 1994) and altered properties of the membrane and synapses (Johnston *et al.*, 1997). Moreover, it has been speculated that PrP<sup>C</sup> may be a constituent of the synaptic vesicle membrane (Fournier *et al.*, 1995) and affects the neurotransmitter release via synaptic vesicles as shown for acetylcholine in neuromuscular junction (Re *et al.*, 2006). Thus, Cy-PrP localisation in endosomes followed by its presence in synaptic vesicles could have disastrous consequences for the neuron-neuron signalling and synaptic plasticity in the brain, when Cy-PrP impairs the PrP<sup>C</sup> and Hsc70 function during synaptic vesicle maturation, release and their recycling process.

## 6 References

- Agarraberes FA and Dice JF (2001) A molecular chaperone complex at the lysosomal membrane is required for protein translocation. *J Cell Sci*, **114**, 2491-2499.
- Alberti S, Demand J, Esser C, Emmerich N, Schild H, and Hohfeld J (2002) Ubiquitylation of BAG-1 suggests a novel regulatory mechanism during the sorting of chaperone substrates to the proteasome. *J Biol Chem*, **277**, 45920-45927.
- Ando Y, Haraoka K, Terazaki H, Tanoue Y, Ishikawa K, Katsuragi S, Nakamura M, Sun X, Nakagawa K, Sasamoto K, Takesako K, Ishizaki T, Sasaki Y, and Doh-ura K (2003) A novel tool for detecting amyloid deposits in systemic amyloidosis in vitro and in vivo. *Lab Invest*, **83**, 1751-1759.
- Arispe N, Doh M, and De Maio A (2002) Lipid interaction differentiates the constitutive and stress-induced heat shock proteins Hsc70 and Hsp70. *Cell Stress Chaperones*, **7**, 330-338.
- Arnold JE, Tipler C, Laszlo L, Hope J, Landon M, and Mayer RJ (1995) The abnormal isoform of the prion protein accumulates in late-endosome-like organelles in scrapie-infected mouse brain. *J Pathol*, **176**, 403-411.
- Arrasate M, Mitra S, Schweitzer ES, Segal MR, and Finkbeiner S (2004) Inclusion body formation reduces levels of mutant huntingtin and the risk of neuronal death. *Nature*, **431**, 805-810.
- Bahadi R, Farrelly PV, Kenna BL, Kourie JI, Tagliavini F, Forloni G, and Salmona M (2003) Channels formed with a mutant prion protein PrP(82-146) homologous to a 7-kDa fragment in diseased brain of GSS patients. *Am J Physiol Cell Physiol*, **285**, C862-C872.
- Baron GS and Caughey B (2003) Effect of glycosylphosphatidylinositol anchor-dependent and -independent prion protein association with model raft membranes on conversion to the protease-resistant isoform. *J Biol Chem*, **278**, 14883-14892.
- Baron U, Gossen M, and Bujard H (1997) Tetracycline-controlled transcription in eukaryotes: novel transactivators with graded transactivation potential. *Nucleic Acids Res*, **25**, 2723-2729.
- Belay HT and Brown IR (2006) Cell death and expression of heat-shock protein Hsc70 in the hyperthermic rat brain. *J Neurochem*.
- Bergeron JJ, Searle N, Khan MN, and Posner BI (1986) Differential and analytical subfractionation of rat liver components internalizing insulin and prolactin. *Biochemistry*, **25**, 1756-1764.

- Bergstrom AL, Cordes H, Zsuzger N, Heegaard PM, Laursen H, and Chabry J (2005) Amidation and structure relaxation abolish the neurotoxicity of the prion peptide PrP106-126 in vivo and in vitro. *J Biol Chem*, **280**, 23114-23121.
- Bian J, Nazor KE, Angers R, Jernigan M, Seward T, Centers A, Green M, and Telling GC (2006) GFP-tagged PrP supports compromised prion replication in transgenic mice. *Biochem Biophys Res Commun*, **340**, 894-900.
- Biasini E, Fioriti L, Ceglia I, Invernizzi R, Bertoli A, Chiesa R, and Forloni G (2004) Proteasome inhibition and aggregation in Parkinson's disease: a comparative study in untransfected and transfected cells. *J Neurochem*, **88**, 545-553.
- Biswas S, Langeveld JP, Tipper D, and Lu S (2006) Intracellular accumulation of a 46kDa species of mouse prion protein as a result of loss of glycosylation in cultured mammalian cells. *Biochem Biophys Res Commun*.
- Bolten DC, McKinley MP, and Prusiner SB (1982) Identification of a protein that purifies with the scrapie prion. *Science*, **218**, 1309-1311.
- Bolton DC, Meyer RK, and Prusiner SB (1985) Scrapie PrP 27-30 is a sialoglycoprotein. *J Virol*, **53**, 596-606.
- Bonifacino JS and Weissman AM (1998) Ubiquitin and the control of protein fate in the secretory and endocytic pathways. *Annu Rev Cell Dev Biol*, **14**, 19-57.
- Borchelt DR, Scott M, Taraboulos A, Stahl N, and Prusiner SB (1990) Scrapie and cellular prion proteins differ in their kinetics of synthesis and topology in cultured cells. *J Cell Biol*, **110**, 743-752.
- Borchelt DR, Taraboulos A, and Prusiner SB (1992) Evidence for synthesis of scrapie prion proteins in the endocytic pathway. *J Biol Chem*, **267**, 16188-16199.
- Brandner S, Isenmann S, Raeber A, Fischer M, Sailer A, Kobayashi Y, Marino S, Weissmann C, and Aguzzi A (1996a) Normal host prion protein necessary for scrapie-induced neurotoxicity. *Nature*, **379**, 339-343.
- Brandner S, Raeber A, Sailer A, Blattler T, Fischer M, Weissmann C, and Aguzzi A (1996b) Normal host prion protein (PrP<sup>C</sup>) is required for scrapie spread within the central nervous system. *Proc Natl Acad Sci U S A*, **93**, 13148-13151.
- Bronk P, Wenniger JJ, Dawson-Scully K, Guo X, Hong S, Atwood HL, and Zinsmaier KE (2001) Drosophila Hsc70-4 is critical for neurotransmitter exocytosis in vivo. *Neuron*, **30**, 475-488.
- Brown DR (2000) PrP<sup>Sc</sup>-like prion protein peptide inhibits the function of cellular prion protein. *Biochem J*, **352 Pt 2**, 511-518.
- Brown DR (2001) Prion and prejudice: normal protein and the synapse. *Trends Neurosci*, **24**, 85-90.
- Brown DR and Besinger A (1998) Prion protein expression and superoxide dismutase activity. *Biochem J*, **334 ( Pt 2)**, 423-429.

- Brown DR, Qin K, Herms JW, Madlung A, Manson J, Strome R, Fraser PE, Kruck T, von Bohlen A, Schulz-Schaeffer W, Giese A, Westaway D, and Kretzschmar H (1997a) The cellular prion protein binds copper in vivo. *Nature*, **390**, 684-687.
- Brown DR, Schulz-Schaeffer WJ, Schmidt B, and Kretzschmar HA (1997b) Prion protein-deficient cells show altered response to oxidative stress due to decreased SOD-1 activity. *Exp Neurol*, **146**, 104-112.
- Brown DR, Schulz-Schaeffer WJ, Schmidt B, and Kretzschmar HA (1997c) Prion protein-deficient cells show altered response to oxidative stress due to decreased SOD-1 activity. *Exp Neurol*, **146**, 104-112.
- Brown DR, Wong BS, Hafiz F, Clive C, Haswell SJ, and Jones IM (1999) Normal prion protein has an activity like that of superoxide dismutase. *Biochem J*, **344 Pt 1**, 1-5.
- Buchner E and Gundersen CB (1997) The DnaJ-like cysteine string protein and exocytotic neurotransmitter release. *Trends Neurosci*, **20**, 223-227.
- Bueler H, Aguzzi A, Sailer A, Greiner RA, Autenried P, Aguet M, and Weissmann C (1993) Mice devoid of PrP are resistant to scrapie. *Cell*, **73**, 1339-1347.
- Bueler H, Fischer M, Lang Y, Bluethmann H, Lipp HP, DeArmond SJ, Prusiner SB, Aguet M, and Weissmann C (1992) Normal development and behaviour of mice lacking the neuronal cell-surface PrP protein. *Nature*, **356**, 577-582.
- Bushmarina NA, Blanchet CE, Vernier G, and Forge V (2006) Cofactor effects on the protein folding reaction: acceleration of alpha-lactalbumin refolding by metal ions. *Protein Sci*, **15**, 659-671.
- Campana V, Sarnataro D, Fasano C, Casanova P, Paladino S, and Zurzolo C (2006) Detergent-resistant membrane domains but not the proteasome are involved in the misfolding of a PrP mutant retained in the endoplasmic reticulum. *J Cell Sci*, **119**, 433-442.
- Capellari S, Parchi P, Russo CM, Sanford J, Sy MS, Gambetti P, and Petersen RB (2000) Effect of the E200K mutation on prion protein metabolism. Comparative study of a cell model and human brain. *Am J Pathol*, **157**, 613-622.
- Carimalo J, Cronier S, Petit G, Peyrin JM, Boukhtouche F, Arbez N, Lemaigre-Dubreuil Y, Brugg B, and Miquel MC (2005) Activation of the JNK-c-Jun pathway during the early phase of neuronal apoptosis induced by PrP106-126 and prion infection. *Eur J Neurosci*, **21**, 2311-2319.
- Caughey B and Raymond GJ (1991) The scrapie-associated form of PrP is made from a cell surface precursor that is both protease- and phospholipase-sensitive. *J Biol Chem*, **266**, 18217-18223.
- Chen S, Bawa D, Besshoh S, Gurd JW, and Brown IR (2005) Association of heat shock proteins and neuronal membrane components with lipid rafts from the rat brain. *J Neurosci Res*, **81**, 522-529.

- Chen S, Mange A, Dong L, Lehmann S, and Schachner M (2003) Prion protein as trans-interacting partner for neurons is involved in neurite outgrowth and neuronal survival. *Mol Cell Neurosci*, **22**, 227-233.
- Chesebro B (2003) Introduction to the transmissible spongiform encephalopathies or prion diseases. *Br Med Bull*, **66**, 1-20.
- Chesebro B, Trifilo M, Race R, Meade-White K, Teng C, LaCasse R, Raymond L, Favara C, Baron G, Priola S, Caughey B, Masliah E, and Oldstone M (2005) Anchorless prion protein results in infectious amyloid disease without clinical scrapie. *Science*, **308**, 1435-1439.
- Chiang HL, Terlecky SR, Plant CP, and Dice JF (1989) A role for a 70-kilodalton heat shock protein in lysosomal degradation of intracellular proteins. *Science*, **246**, 382-385.
- Chiesa R, Drisaldi B, Quaglio E, Migheli A, Piccardo P, Ghetti B, and Harris DA (2000) Accumulation of protease-resistant prion protein (PrP) and apoptosis of cerebellar granule cells in transgenic mice expressing a PrP insertional mutation. *Proc Natl Acad Sci U S A*, **97**, 5574-5579.
- Chiesa R and Harris DA (2001) Prion diseases: what is the neurotoxic molecule? *Neurobiol Dis*, **8**, 743-763.
- Cisse MA, Sunyach C, Lefranc-Jullien S, Postina R, Vincent B, and Checler F (2005) The disintegrin ADAM9 indirectly contributes to the physiological processing of cellular prion by modulating ADAM10 activity. *J Biol Chem*, **280**, 40624-40631.
- Collinge J (2001) Prion diseases of humans and animals: their causes and molecular basis. *Annu Rev Neurosci*, **24**, 519-550
- Collinge J, Whittington MA, Sidle KC, Smith CJ, Palmer MS, Clarke AR, and Jefferys JG (1994) Prion protein is necessary for normal synaptic function. *Nature*, **370**, 295-297.
- Criado JR, Sanchez-Alavez M, Conti B, Giacchino JL, Wills DN, Henriksen SJ, Race R, Manson JC, Chesebro B, and Oldstone MB (2005) Mice devoid of prion protein have cognitive deficits that are rescued by reconstitution of PrP in neurons. *Neurobiol Dis*, **19**, 255-265.
- Cuervo AM, Dice JF, and Knecht E (1997) A population of rat liver lysosomes responsible for the selective uptake and degradation of cytosolic proteins. *J Biol Chem*, **272**, 5606-5615.
- Dorandeu A, Wingertsman L, Chretien F, Delisle MB, Vital C, Parchi P, Montagna P, Lugaresi E, Ironside JW, Budka H, Gambetti P, and Gray F (1998) Neuronal apoptosis in fatal familial insomnia. *Brain Pathol*, **8**, 531-537.
- Drisaldi B, Stewart RS, Adles C, Stewart LR, Quaglio E, Biasini E, Fioriti L, Chiesa R, and Harris DA (2003) Mutant PrP is delayed in its exit from the endoplasmic



- reticulum, but neither wild-type nor mutant PrP undergoes retrotranslocation prior to proteasomal degradation. *J Biol Chem*, **278**, 21732-21743.
- Ersdal C, Ulvund MJ, Espenes A, Benestad SL, Sarradin P, and Landsverk T (2005) Mapping PrP<sup>Sc</sup> propagation in experimental and natural scrapie in sheep with different PrP genotypes. *Vet Pathol*, **42**, 258-274.
- Ferreiro E, Resende R, Costa R, Oliveira CR, and Pereira CM (2006) An endoplasmic-reticulum-specific apoptotic pathway is involved in prion and amyloid-beta peptides neurotoxicity. *Neurobiol Dis*.
- Ferrer I (1999) Nuclear DNA fragmentation in Creutzfeldt-Jakob disease: does a mere positive in situ nuclear end-labeling indicate apoptosis? *Acta Neuropathol (Berl)*, **97**, 5-12.
- Ferrer I (2002) Synaptic pathology and cell death in the cerebellum in Creutzfeldt-Jakob disease. *Cerebellum*, **1**, 213-222.
- Feughelman M and Willis BK (2002) Potential involvement of copper and thiol-disulphide interchange in prion proteins' conformational conversion. *Med Hypotheses*, **59**, 321-324.
- Fioriti L, Dossena S, Stewart LR, Stewart RS, Harris DA, Forloni G, and Chiesa R (2005) Cytosolic prion protein (PrP) is not toxic in N2a cells and primary neurons expressing pathogenic PrP mutations. *J Biol Chem*, **280**, 11320-11328.
- Forloni G, Angeretti N, Chiesa R, Monzani E, Salmona M, Bugiani O, and Tagliavini F (1993) Neurotoxicity of a prion protein fragment. *Nature*, **362**, 543-546.
- Forloni G, Iussich S, Awan T, Colombo L, Angeretti N, Girola L, Bertani I, Poli G, Caramelli M, Grazia BM, Farina L, Limido L, Rossi G, Giaccone G, Ironside JW, Bugiani O, Salmona M, and Tagliavini F (2002) Tetracyclines affect prion infectivity. *Proc Natl Acad Sci U S A*, **99**, 10849-10854.
- Foster JA, Rush SJ, and Brown IR (1995) Localization of constitutive and hyperthermia-inducible heat shock mRNAs (hsc70 and hsp70) in the rabbit cerebellum and brainstem by non-radioactive in situ hybridization. *J Neurosci Res*, **41**, 603-612.
- Fournier JG, Escaig-Haye F, Billette d, V, and Robain O (1995) Ultrastructural localization of cellular prion protein (PrP<sup>c</sup>) in synaptic boutons of normal hamster hippocampus. *C R Acad Sci III*, **318**, 339-344.
- Fournier JG, Escaig-Haye F, and Grigoriev V (2000) Ultrastructural localization of prion proteins: physiological and pathological implications. *Microsc Res Tech*, **50**, 76-88.
- Galimi F, Saez E, Gall J, Hoong N, Cho G, Evans RM, and Verma IM (2005) Development of ecdysone-regulated lentiviral vectors. *Mol Ther*, **11**, 142-148.

- Giese A, Groschup MH, Hess B, and Kretzschmar HA (1995) Neuronal cell death in scrapie-infected mice is due to apoptosis. *Brain Pathol*, **5**, 213-221.
- Gorodinsky A and Harris DA (1995) Glycolipid-anchored proteins in neuroblastoma cells form detergent-resistant complexes without caveolin. *J Cell Biol*, **129**, 619-627.
- Gossen M and Bujard H (1992) Tight control of gene expression in mammalian cells by tetracycline-responsive promoters. *Proc Natl Acad Sci U S A*, **89**, 5547-5551.
- Grant SG, O'Dell TJ, Karl KA, Stein PL, Soriano P, and Kandel ER (1992) Impaired long-term potentiation, spatial learning, and hippocampal development in fyn mutant mice. *Science*, **258**, 1903-1910.
- Gray F, Chretien F, Adle-Biassette H, Dorandeu A, Ereau T, Delisle MB, Kopp N, Ironside JW, and Vital C (1999) Neuronal apoptosis in Creutzfeldt-Jakob disease. *J Neuropathol Exp Neurol*, **58**, 321-328.
- Grune T, Merker K, Jung T, Sitte N, and Davies KJ (2005) Protein oxidation and degradation during postmitotic senescence. *Free Radic Biol Med*, **39**, 1208-1215.
- Gu Y, Verghese S, Mishra RS, Xu X, Shi Y, and Singh N (2003) Mutant prion protein-mediated aggregation of normal prion protein in the endoplasmic reticulum: implications for prion propagation and neurotoxicity. *J Neurochem*, **84**, 10-22.
- Guzhova I, Kislyakova K, Moskaliova O, Fridlanskaya I, Tytell M, Cheetham M, and Margulis B (2001) In vitro studies show that Hsp70 can be released by glia and that exogenous Hsp70 can enhance neuronal stress tolerance. *Brain Res*, **914**, 66-73.
- Haeberle AM, Ribaut-Barassin C, Bombarde G, Mariani J, Hunsmann G, Grassi J, and Bailly Y (2000) Synaptic prion protein immuno-reactivity in the rodent cerebellum. *Microsc Res Tech*, **50**, 66-75.
- Hanahan D, Jessee J, and Bloom FR (1991) Plasmid transformation of *Escherichia coli* and other bacteria. *Methods Enzymol*, **204**, 63-113.
- Haraguchi T, Fisher S, Olofsson S, Endo T, Groth D, Tarentino A, Borchelt DR, Teplow D, Hood L, Burlingame A, and . (1989) Asparagine-linked glycosylation of the scrapie and cellular prion proteins. *Arch Biochem Biophys*, **274**, 1-13.
- Harris DA (2003) Trafficking, turnover and membrane topology of PrP. *Br Med Bull*, **66**, 71-85.
- Harris DA, Huber MT, van Dijken P, Shyng SL, Chait BT, and Wang R (1993) Processing of a cellular prion protein: identification of N- and C-terminal cleavage sites. *Biochemistry*, **32**, 1009-1016.
- Hartl FU and Hayer-Hartl M (2002) Molecular chaperones in the cytosol: from nascent chain to folded protein. *Science*, **295**, 1852-1858.

- Heller U, Winklhofer KF, Heske J, Reintjes A, and Tatzelt J (2003) Post-translational import of the prion protein into the endoplasmic reticulum interferes with cell viability: a critical role for the putative transmembrane domain. *J Biol Chem*, **278**, 36139-36147.
- Herms J, Tings T, Gall S, Madlung A, Giese A, Siebert H, Schurmann P, Windl O, Brose N, and Kretzschmar H (1999) Evidence of presynaptic location and function of the prion protein. *J Neurosci*, **19**, 8866-8875.
- Hetz C, Russelakis-Carneiro M, Maundrell K, Castilla J, and Soto C (2003) Caspase-12 and endoplasmic reticulum stress mediate neurotoxicity of pathological prion protein. *EMBO J*, **22**, 5435-5445.
- Hetz C, Russelakis-Carneiro M, Walchli S, Carboni S, Vial-Knecht E, Maundrell K, Castilla J, and Soto C (2005) The disulfide isomerase Grp58 is a protective factor against prion neurotoxicity. *J Neurosci*, **25**, 2793-2802.
- Hill AF and Collinge J (2003) Subclinical prion infection in humans and animals. *Br Med Bull*, **66**, 161-170.
- Hoefert VB, Aiken JM, McKenzie D, and Johnson CJ (2004) Labeling of the scrapie-associated prion protein in vitro and in vivo. *Neurosci Lett*, **371**, 176-180.
- Hohfeld J and Jentsch S (1997) GrpE-like regulation of the hsc70 chaperone by the anti-apoptotic protein BAG-1. *EMBO J*, **16**, 6209-6216.
- Hohfeld J, Minami Y, and Hartl FU (1995) Hip, a novel cochaperone involved in the eukaryotic Hsc70/Hsp40 reaction cycle. *Cell*, **83**, 589-598.
- Holroyd C, Kistner U, Annaert W, and Jahn R (1999) Fusion of endosomes involved in synaptic vesicle recycling. *Mol Biol Cell*, **10**, 3035-3044.
- Hooper NM (2005) Roles of proteolysis and lipid rafts in the processing of the amyloid precursor protein and prion protein. *Biochem Soc Trans*, **33**, 335-338.
- Hope J. (2000) Prions and neurodegenerative diseases. *Curr Opin Genet Dev*, **10**, 568-574
- Hornemann S, Korth C, Oesch B, Riek R, Wider G, Wuthrich K, and Glockshuber R (1997) Recombinant full-length murine prion protein, mPrP(23-231): purification and spectroscopic characterization. *FEBS Lett*, **413**, 277-281.
- Jackson GS and Clarke AR (2000) Mammalian prion proteins. *Curr Opin Struct Biol*, **10**, 69-74
- Jefferys JG, Empson RM, Whittington MA, and Prusiner SB (1994) Scrapie infection of transgenic mice leads to network and intrinsic dysfunction of cortical and hippocampal neurones. *Neurobiol Dis*, **1**, 25-30.
- Jeffrey M, Halliday WG, Bell J, Johnston AR, MacLeod NK, Ingham C, Sayers AR, Brown DA, and Fraser JR (2000) Synapse loss associated with abnormal PrP

precedes neuronal degeneration in the scrapie-infected murine hippocampus. *Neuropathol Appl Neurobiol*, **26**, 41-54.

Jimenez-Huete A, Lievens PM, Vidal R, Piccardo P, Ghetti B, Tagliavini F, Frangione B, and Prelli F (1998) Endogenous proteolytic cleavage of normal and disease-associated isoforms of the human prion protein in neural and non-neural tissues. *Am J Pathol*, **153**, 1561-1572.

Jin T, Gu Y, Zanusso G, Sy M, Kumar A, Cohen M, Gambetti P, and Singh N (2000) The chaperone protein BiP binds to a mutant prion protein and mediates its degradation by the proteasome. *J Biol Chem*, **275**, 38699-38704.

Johnston AR, Black C, Fraser J, and MacLeod N (1997) Scrapie infection alters the membrane and synaptic properties of mouse hippocampal CA1 pyramidal neurones. *J Physiol*, **500 ( Pt 1)**, 1-15.

Kanaani J, Prusiner SB, Diacovo J, Baekkeskov S, and Legname G (2005) Recombinant prion protein induces rapid polarization and development of synapses in embryonic rat hippocampal neurons in vitro. *J Neurochem*, **95**, 1373-1386.

Katayama T, Imaizumi K, Manabe T, Hitomi J, Kudo T, and Tohyama M (2004) Induction of neuronal death by ER stress in Alzheimer's disease. *J Chem Neuroanat*, **28**, 67-78.

Kazlauskaitė J, Sanghera N, Sylvester I, Venien-Bryan C, and Pinheiro TJ (2003) Structural changes of the prion protein in lipid membranes leading to aggregation and fibrillization. *Biochemistry*, **42**, 3295-3304.

Keller JN, Hanni KB, and Markesbery WR (2000) Possible involvement of proteasome inhibition in aging: implications for oxidative stress. *Mech Ageing Dev*, **113**, 61-70.

Keller JN, Schmitt FA, Scheff SW, Ding Q, Chen Q, Butterfield DA, and Markesbery WR (2005) Evidence of increased oxidative damage in subjects with mild cognitive impairment. *Neurology*, **64**, 1152-1156.

Kenward N, Landon M, Laszlo L, and Mayer RJ (1996) Heat shock proteins, molecular chaperones and the prion encephalopathies. *Cell Stress Chaperones*, **1**, 18-22.

Kjeken R, Brech A, Lovdal T, Roos N, and Berg T (1995) Involvement of early and late lysosomes in the degradation of mannosylated ligands by rat liver endothelial cells. *Exp Cell Res*, **216**, 290-298.

Kocisko DA, Come JH, Priola SA, Chesebro B, Raymond GJ, Lansbury PT, and Caughey B (1994) Cell-free formation of protease-resistant prion protein. *Nature*, **370**, 471-474.

Konarkowska B, Aitken JF, Kistler J, Zhang S, and Cooper GJ (2006) The aggregation potential of human amylin determines its cytotoxicity towards islet beta-cells. *FEBS J*, **273**, 3614-3624.

- Korolainen MA, Goldsteins G, Alafuzoff I, Koistinaho J, and Pirttila T (2002) Proteomic analysis of protein oxidation in Alzheimer's disease brain. *Electrophoresis*, **23**, 3428-3433.
- Korte S, Vassallo N, Kramer ML, Kretzschmar HA, and Herms J (2003) Modulation of L-type voltage-gated calcium channels by recombinant prion protein. *J Neurochem*, **87**, 1037-1042.
- Kovacs GG, Kurucz I, Budka H, Adori C, Muller F, Acs P, Kloppel S, Schatzl HM, Mayer RJ, and Laszlo L (2001) Prominent stress response of Purkinje cells in Creutzfeldt-Jakob disease. *Neurobiol Dis*, **8**, 881-889.
- Kretzschmar HA, Tings T, Madlung A, Giese A, and Herms J (2000) Function of PrP(C) as a copper-binding protein at the synapse. *Arch Virol Suppl*, 239-249.
- Kristensson K, Feuerstein B, Taraboulos A, Hyun WC, Prusiner SB, and DeArmond SJ (1993) Scrapie prions alter receptor-mediated calcium responses in cultured cells. *Neurology*, **43**, 2335-2341.
- Laemmli UK (1970) Cleavage of structural proteins during the assembly of the head of bacteriophage T4. *Nature*, **227**, 680-685.
- Laszlo L, Lowe J, Self T, Kenward N, Landon M, McBride T, Farquhar C, McConnell I, Brown J, Hope J, and . (1992) Lysosomes as key organelles in the pathogenesis of prion encephalopathies. *J Pathol*, **166**, 333-341.
- Lawe DC, Patki V, Heller-Harrison R, Lambright D, and Corvera S (2000) The FYVE domain of early endosome antigen 1 is required for both phosphatidylinositol 3-phosphate and Rab5 binding. Critical role of this dual interaction for endosomal localization. *J Biol Chem*, **275**, 3699-3705.
- Lawe DC, Sitouah N, Hayes S, Chawla A, Virbasius JV, Tuft R, Fogarty K, Lifshitz L, Lambright D, and Corvera S (2003) Essential role of Ca<sup>2+</sup>/calmodulin in Early Endosome Antigen-1 localization. *Mol Biol Cell*, **14**, 2935-2945.
- LeBlanc P, Baas D, and Darlix JL (2004) Analysis of the interactions between HIV-1 and the cellular prion protein in a human cell line. *J Mol Biol*, **337**, 1035-1051.
- Ledent P, Duez C, Vanhove M, Lejeune A, Fonce E, Charlier P, Rhazi-Filali F, Thamm I, Guillaume G, Samyn B, Devreese B, Van Beeumen J, Lamotte-Brasseur J, and Frere JM (1997) Unexpected influence of a C-terminal-fused His-tag on the processing of an enzyme and on the kinetic and folding parameters. *FEBS Lett*, **413**, 194-196.
- Legname G, Baskakov IV, Nguyen HO, Riesner D, Cohen FE, DeArmond SJ, and Prusiner SB (2004) Synthetic mammalian prions. *Science*, **305**, 673-676.
- Lindholm D, Wootz H, and Korhonen L (2006) ER stress and neurodegenerative diseases. *Cell Death Differ*, **13**, 385-392.
- Lucassen PJ, Williams A, Chung WC, and Fraser H (1995) Detection of apoptosis in murine scrapie. *Neurosci Lett*, **198**, 185-188.

- Luders J, Demand J, and Hohfeld J (2000) The ubiquitin-related BAG-1 provides a link between the molecular chaperones Hsc70/Hsp70 and the proteasome. *J Biol Chem*, **275**, 4613-4617.
- Ma J and Lindquist S (1999) De novo generation of a PrPSc-like conformation in living cells. *Nat Cell Biol*, **1**, 358-361.
- Ma J and Lindquist S (2001) Wild-type PrP and a mutant associated with prion disease are subject to retrograde transport and proteasome degradation. *Proc Natl Acad Sci U S A*, **98**, 14955-14960.
- Ma J and Lindquist S (2002a) Conversion of PrP to a self-perpetuating PrPSc-like conformation in the cytosol. *Science*, **298**, 1785-1788.
- Ma J, Wollmann R, and Lindquist S (2002b) Neurotoxicity and neurodegeneration when PrP accumulates in the cytosol. *Science*, **298**, 1781-1785.
- Magalhaes AC, Silva JA, Lee KS, Martins VR, Prado VF, Ferguson SS, Gomez MV, Brentani RR, and Prado MA (2002) Endocytic intermediates involved with the intracellular trafficking of a fluorescent cellular prion protein. *J Biol Chem*, **277**, 33311-33318.
- Maglio LE, Martins VR, Izquierdo I, and Ramirez OA (2006) Role of cellular prion protein on LTP expression in aged mice. *Brain Res*, **1097**, 11-18.
- Mallucci G, Dickinson A, Linehan J, Klohn PC, Brandner S, and Collinge J (2003) Depleting neuronal PrP in prion infection prevents disease and reverses spongiosis. *Science*, **302**, 871-874.
- Mallucci GR, Ratten S, Asante EA, Linehan J, Gowland I, Jefferys JG, and Collinge J (2002) Post-natal knockout of prion protein alters hippocampal CA1 properties, but does not result in neurodegeneration. *EMBO J*, **21**, 202-210.
- Manson JC, Clarke AR, McBride PA, McConnell I, and Hope J (1994) PrP gene dosage determines the timing but not the final intensity or distribution of lesions in scrapie pathology. *Neurodegeneration*, **3**, 331-340.
- Manzerra P and Brown IR (1996) The neuronal stress response: nuclear translocation of heat shock proteins as an indicator of hyperthermic stress. *Exp Cell Res*, **229**, 35-47.
- McKinley MP, Bolton DC, and Prusiner SB (1983) A protease-resistant protein is a structural component of the scrapie prion. *Cell*, **35**, 57-62.
- Mehlase J and Grune T (2002) Proteolytic response to oxidative stress in mammalian cells. *Biol Chem*, **383**, 559-567.
- Meyer-Ficca ML, Meyer RG, Kaiser H, Brack AR, Kandolf R, and Kupper JH (2004) Comparative analysis of inducible expression systems in transient transfection studies. *Anal Biochem*, **334**, 9-19.

- Minami Y, Hohfeld J, Ohtsuka K, and Hartl FU (1996) Regulation of the heat-shock protein 70 reaction cycle by the mammalian DnaJ homolog, Hsp40. *J Biol Chem*, **271**, 19617-19624.
- Morillas M, Swietnicki W, Gambetti P, and Surewicz WK (1999) Membrane environment alters the conformational structure of the recombinant human prion protein. *J Biol Chem*, **274**, 36859-36865.
- Morot-Gaudry-Talarmain Y, Rezaei H, Guernonprez L, Treguer E, and Grosclaude J (2003) Selective prion protein binding to synaptic components is modulated by oxidative and nitrosative changes induced by copper(II) and peroxynitrite in cholinergic synaptosomes, unveiling a role for calcineurin B and thioredoxin. *J Neurochem*, **87**, 1456-1470.
- Mouillet-Richard S, Ermonval M, Chebassier C, Laplanche JL, Lehmann S, Launay JM, and Kellermann O (2000) Signal transduction through prion protein. *Science*, **289**, 1925-1928.
- Mouillet-Richard S, Laurendeau I, Vidaud M, Kellermann O, and Laplanche JL (1999) Prion protein and neuronal differentiation: quantitative analysis of prnp gene expression in a murine inducible neuroectodermal progenitor. *Microbes Infect*, **1**, 969-976.
- Mu FT, Callaghan JM, Steele-Mortimer O, Stenmark H, Parton RG, Campbell PL, McCluskey J, Yeo JP, Tock EP, and Toh BH (1995) EEA1, an early endosome-associated protein. EEA1 is a conserved alpha-helical peripheral membrane protein flanked by cysteine "fingers" and contains a calmodulin-binding IQ motif. *J Biol Chem*, **270**, 13503-13511.
- Mullis KB and Faloona FA (1987) Specific synthesis of DNA in vitro via a polymerase-catalyzed chain reaction. *Methods Enzymol*, **155**, 335-350.
- Naslavsky N, Stein R, Yanai A, Friedlander G, and Taraboulos A (1997) Characterization of detergent-insoluble complexes containing the cellular prion protein and its scrapie isoform. *J Biol Chem*, **272**, 6324-6331.
- Negro A, Ballarin C, Bertoli A, Massimino ML, and Sorgato MC (2001) The metabolism and imaging in live cells of the bovine prion protein in its native form or carrying single amino acid substitutions. *Mol Cell Neurosci*, **17**, 521-538.
- No D, Yao TP, and Evans RM (1996) Ecdysone-inducible gene expression in mammalian cells and transgenic mice. *Proc Natl Acad Sci U S A*, **93**, 3346-3351.
- Nollen EA, Brunsting JF, Song J, Kampinga HH, and Morimoto RI (2000) Bag1 functions in vivo as a negative regulator of Hsp70 chaperone activity. *Mol Cell Biol*, **20**, 1083-1088.
- Nollen EA and Morimoto RI (2002) Chaperoning signaling pathways: molecular chaperones as stress-sensing 'heat shock' proteins. *J Cell Sci*, **115**, 2809-2816.

- Norstrom EM and Mastrianni JA (2005) The AGAAAAGA palindrome in PrP is required to generate a productive PrP<sup>Sc</sup>-PrP<sup>C</sup> complex that leads to prion propagation. *J Biol Chem*, **280**, 27236-27243.
- Novoselova TV, Margulis BA, Novoselov SS, Sapozhnikov AM, van der SJ, Cheetham ME, and Guzhova IV (2005) Treatment with extracellular HSP70/HSC70 protein can reduce polyglutamine toxicity and aggregation. *J Neurochem*, **94**, 597-606.
- Pan KM, Stahl N, and Prusiner SB (1992) Purification and properties of the cellular prion protein from Syrian hamster brain. *Protein Sci*, **1**, 1343-1352.
- Prusiner SB (1998) Prions. *Proc Natl Acad Sci U S A*, **95**, 13363-13383.
- Prusiner SB, Groth D, Serban A, Koehler R, Foster D, Torchia M, Burton D, Yang SL, and DeArmond SJ (1993) Ablation of the prion protein (PrP) gene in mice prevents scrapie and facilitates production of anti-PrP antibodies. *Proc Natl Acad Sci U S A*, **90**, 10608-10612.
- Rachidi W, Mange A, Senator A, Guiraud P, Riandel J, Benboubetra M, Favier A, and Lehmann S (2003) Prion infection impairs copper binding of cultured cells. *J Biol Chem*, **278**, 14595-14598.
- Rambold AS, Miesbauer M, Rapaport D, Bartke T, Baier M, Winklhofer KF, and Tatzelt J (2006) Association of Bcl-2 with misfolded prion protein is linked to the toxic potential of cytosolic PrP. *Mol Biol Cell*, **17**, 3356-3368.
- Rane NS, Yonkovich JL, and Hegde RS (2004) Protection from cytosolic prion protein toxicity by modulation of protein translocation. *EMBO J*, **23**, 4550-4559.
- Re L, Rossini F, Re F, Bordicchia M, Mercanti A, Fernandez OS, and Barocci S (2006) Prion protein potentiates acetylcholine release at the neuromuscular junction. *Pharmacol Res*, **53**, 62-68.
- Riek R, Hornemann S, Wider G, Billeter M, Glockshuber R, and Wuthrich K (1996b) NMR structure of the mouse prion protein domain PrP(121-321). *Nature*, **382**, 180-182.
- Riek R, Hornemann S, Wider G, Billeter M, Glockshuber R, and Wuthrich K (1996a) NMR structure of the mouse prion protein domain PrP(121-321). *Nature*, **382**, 180-182.
- Riek R, Hornemann S, Wider G, Glockshuber R, and Wuthrich K (1997) NMR characterization of the full-length recombinant murine prion protein, mPrP(23-231). *FEBS Lett*, **413**, 282-288.
- Roucou X, Guo Q, Zhang Y, Goodyer CG, and LeBlanc AC (2003) Cytosolic prion protein is not toxic and protects against Bax-mediated cell death in human primary neurons. *J Biol Chem*, **278**, 40877-40881.



- Rubino M, Miaczynska M, Lippe R, and Zerial M (2000) Selective membrane recruitment of EEA1 suggests a role in directional transport of clathrin-coated vesicles to early endosomes. *J Biol Chem*, **275**, 3745-3748.
- Rudiger S, Buchberger A, and Bukau B (1997) Interaction of Hsp70 chaperones with substrates. *Nat Struct Biol*, **4**, 342-349.
- Ryu EJ, Harding HP, Angelastro JM, Vitolo OV, Ron D, and Greene LA (2002) Endoplasmic reticulum stress and the unfolded protein response in cellular models of Parkinson's disease. *J Neurosci*, **22**, 10690-10698.
- Safar J, Wang W, Padgett MP, Ceroni M, Piccardo P, Zopf D, Gajdusek DC, and Gibbs CJ, Jr. (1990) Molecular mass, biochemical composition, and physicochemical behavior of the infectious form of the scrapie precursor protein monomer. *Proc Natl Acad Sci U S A*, **87**, 6373-6377.
- Saiki RK, Scharf S, Faloona F, Mullis KB, Horn GT, Erlich HA, and Arnheim N (1985) Enzymatic amplification of beta-globin genomic sequences and restriction site analysis for diagnosis of sickle cell anemia. *Science*, **230**, 1350-1354.
- Sakudo A, Lee DC, Li S, Nakamura T, Matsumoto Y, Saeki K, Itohara S, Ikuta K, and Onodera T (2005a) PrP cooperates with STI1 to regulate SOD activity in PrP-deficient neuronal cell line. *Biochem Biophys Res Commun*, **328**, 14-19.
- Sakudo A, Lee DC, Nishimura T, Li S, Tsuji S, Nakamura T, Matsumoto Y, Saeki K, Itohara S, Ikuta K, and Onodera T (2005b) Octapeptide repeat region and N-terminal half of hydrophobic region of prion protein (PrP) mediate PrP-dependent activation of superoxide dismutase. *Biochem Biophys Res Commun*, **326**, 600-606.
- Sales N, Hassig R, Rodolfo K, Di Giamberardino L, Traiffort E, Ruat M, Fretier P, and Moya KL (2002) Developmental expression of the cellular prion protein in elongating axons. *Eur J Neurosci*, **15**, 1163-1177.
- Sales N, Rodolfo K, Hassig R, Faucheux B, Di Giamberardino L, and Moya KL (1998) Cellular prion protein localization in rodent and primate brain. *Eur J Neurosci*, **10**, 2464-2471.
- Salmona M, Morbin M, Massignan T, Colombo L, Mazzoleni G, Capobianco R, Diomede L, Thaler F, Mollica L, Musco G, Kourie JJ, Bugiani O, Sharma D, Inouye H, Kirschner DA, Forloni G, and Tagliavini F (2003) Structural properties of Gerstmann-Strausler-Scheinker disease amyloid protein. *J Biol Chem*, **278**, 48146-48153.
- Sambrook J and Russel DW. Molecular cloning. 1-3. 2001. Cold Spring Harbour Laboratory Press, New York.
- Ref Type: Generic
- Sandberg MK, Wallen P, Wikstrom MA, and Kristensson K (2004) Scrapie-infected GT1-1 cells show impaired function of voltage-gated N-type calcium channels (Ca(v) 2.2) which is ameliorated by quinacrine treatment. *Neurobiol Dis*, **15**, 143-151.

- Sanghera N and Pinheiro TJ (2002) Binding of prion protein to lipid membranes and implications for prion conversion. *J Mol Biol*, **315**, 1241-1256.
- Santa-Maria I, Perez M, Hernandez F, Avila J, and Moreno FJ (2006) Characteristics of the binding of thioflavin S to tau paired helical filaments. *J Alzheimers Dis*, **9**, 279-285.
- Santuccione A, Sytnyk V, Leshchyns'ka I, and Schachner M (2005) Prion protein recruits its neuronal receptor NCAM to lipid rafts to activate p59fyn and to enhance neurite outgrowth. *J Cell Biol*, **169**, 341-354.
- Satoh J, Onoue H, Arima K, and Yamamura T (2005) The 14-3-3 protein forms a molecular complex with heat shock protein Hsp60 and cellular prion protein. *J Neuropathol Exp Neurol*, **64**, 858-868.
- Scott M, Groth D, Foster D, Torchia M, Yang SL, DeArmond SJ, and Prusiner SB (1993) Propagation of prions with artificial properties in transgenic mice expressing chimeric PrP genes. *Cell*, **73**, 979-988.
- Selak S, Braun JE, and Fritzler MJ (2004) Characterization of early endosome antigen 1 in neural tissues. *Biochem Biophys Res Commun*, **323**, 1334-1342.
- Selak S and Fritzler MJ (2004) Altered neurological function in mice immunized with early endosome antigen 1. *BMC Neurosci*, **5**, 2.
- Senator A, Rachidi W, Lehmann S, Favier A, and Benboubetra M (2004) Prion protein protects against DNA damage induced by paraquat in cultured cells. *Free Radic Biol Med*, **37**, 1224-1230.
- Senner V, Sotoodeh A, and Paulus W (2001) Regulated gene expression in glioma cells: a comparison of three inducible systems. *Neurochem Res*, **26**, 521-524.
- Shah M, Patel K, Mukhopadhyay S, Xu F, Guo G, and Sehgal PB (2006) Membrane-associated STAT3 and PY-STAT3 in the cytoplasm. *J Biol Chem*, **281**, 7302-7308.
- Sherman MY and Goldberg AL (2001) Cellular defenses against unfolded proteins: a cell biologist thinks about neurodegenerative diseases. *Neuron*, **29**, 15-32.
- Shimizu H, Kawamura S, and Ozaki K (2003) An essential role of Rab5 in uniformity of synaptic vesicle size. *J Cell Sci*, **116**, 3583-3590.
- Shyng SL, Heuser JE, and Harris DA (1994) A glycolipid-anchored prion protein is endocytosed via clathrin-coated pits. *J Cell Biol*, **125**, 1239-1250.
- Shyng SL, Huber MT, and Harris DA (1993) A prion protein cycles between the cell surface and an endocytic compartment in cultured neuroblastoma cells. *J Biol Chem*, **268**, 15922-15928.

- Simonsen A, Lippe R, Christoforidis S, Gaullier JM, Brech A, Callaghan J, Toh BH, Murphy C, Zerial M, and Stenmark H (1998) EEA1 links PI(3)K function to Rab5 regulation of endosome fusion. *Nature*, **394**, 494-498.
- Smith WW, Jiang H, Pei Z, Tanaka Y, Morita H, Sawa A, Dawson VL, Dawson TM, and Ross CA (2005) Endoplasmic reticulum stress and mitochondrial cell death pathways mediate A53T mutant alpha-synuclein-induced toxicity. *Hum Mol Genet*, **14**, 3801-3811.
- Spielhauer C and Schatzl HM (2001) PrPC directly interacts with proteins involved in signaling pathways. *J Biol Chem*, **276**, 44604-44612.
- Stahl B, Tobaben S, and Sudhof TC (1999) Two distinct domains in hsc70 are essential for the interaction with the synaptic vesicle cysteine string protein. *Eur J Cell Biol*, **78**, 375-381.
- Stahl N, Borchelt DR, Hsiao K, and Prusiner SB (1987) Scrapie prion protein contains a phosphatidylinositol glycolipid. *Cell*, **51**, 229-240.
- Steele AD, Emsley JG, Ozdinler PH, Lindquist S, and Macklis JD (2006) Prion protein (PrP<sup>c</sup>) positively regulates neural precursor proliferation during developmental and adult mammalian neurogenesis. *Proc Natl Acad Sci U S A*, **103**, 3416-3421.
- Stewart RS and Harris DA (2003) Mutational analysis of topological determinants in prion protein (PrP) and measurement of transmembrane and cytosolic PrP during prion infection. *J Biol Chem*, **278**, 45960-45968.
- Suggs SV, Wallace RB, Hirose T, Kawashima EH, and Itakura K (1981) Use of synthetic oligonucleotides as hybridization probes: isolation of cloned cDNA sequences for human beta 2-microglobulin. *Proc Natl Acad Sci U S A*, **78**, 6613-6617.
- Sunyach C, Jen A, Deng J, Fitzgerald KT, Frobert Y, Grassi J, McCaffrey MW, and Morris R (2003) The mechanism of internalization of glycosylphosphatidylinositol-anchored prion protein. *EMBO J*, **22**, 3591-3601.
- Supattapone S, Nguyen HO, Muramoto T, Cohen FE, DeArmond SJ, Prusiner SB, and Scott M (2000) Affinity-tagged miniprion derivatives spontaneously adopt protease-resistant conformations. *J Virol*, **74**, 11928-11934.
- Tagliavini F, Forloni G, Colombo L, Rossi G, Girola L, Canciani B, Angeretti N, Giampaolo L, Peressini E, Awan T, De Gioia L, Ragg E, Bugiani O, and Salmona M (2000) Tetracycline affects abnormal properties of synthetic PrP peptides and PrP(Sc) in vitro. *J Mol Biol*, **300**, 1309-1322.
- Takayama S, Bimston DN, Matsuzawa S, Freeman BC, Aime-Sempe C, Xie Z, Morimoto RI, and Reed JC (1997) BAG-1 modulates the chaperone activity of Hsp70/Hsc70. *EMBO J*, **16**, 4887-4896.
- Tanaka S, Kitagawa K, Ohtsuki T, Yagita Y, Takasawa K, Hori M, and Matsumoto M (2002) Synergistic induction of HSP40 and HSC70 in the mouse hippocampal

- neurons after cerebral ischemia and ischemic tolerance in gerbil hippocampus. *J Neurosci Res*, **67**, 37-47.
- Taraboulos A, Raeber AJ, Borchelt DR, Serban D, and Prusiner SB (1992) Synthesis and trafficking of prion proteins in cultured cells. *Mol Biol Cell*, **3**, 851-863.
- Tatzelt J, Zuo J, Voellmy R, Scott M, Hartl U, Prusiner SB, and Welch WJ (1995) Scrapie prions selectively modify the stress response in neuroblastoma cells. *Proc Natl Acad Sci U S A*, **92**, 2944-2948.
- Taylor DR, Watt NT, Perera WS, and Hooper NM (2005) Assigning functions to distinct regions of the N-terminus of the prion protein that are involved in its copper-stimulated, clathrin-dependent endocytosis. *J Cell Sci*, **118**, 5141-5153.
- Telling GC, Scott M, Mastrianni J, Gabizon R, Torchia M, Cohen FE, DeArmond SJ, and Prusiner SB (1995) Prion propagation in mice expressing human and chimeric PrP transgenes implicates the interaction of cellular PrP with another protein. *Cell*, **83**, 79-90.
- Terlecky SR, Chiang HL, Olson TS, and Dice JF (1992) Protein and peptide binding and stimulation of in vitro lysosomal proteolysis by the 73-kDa heat shock cognate protein. *J Biol Chem*, **267**, 9202-9209.
- Tidwell JL, Houenou LJ, and Tytell M (2004) Administration of Hsp70 in vivo inhibits motor and sensory neuron degeneration. *Cell Stress Chaperones*, **9**, 88-98.
- Tobaben S, Thakur P, Fernandez-Chacon R, Sudhof TC, Rettig J, and Stahl B (2001) A trimeric protein complex functions as a synaptic chaperone machine. *Neuron*, **31**, 987-999.
- Tsai B, Ye Y, and Rapoport TA (2002) Retro-translocation of proteins from the endoplasmic reticulum into the cytosol. *Nat Rev Mol Cell Biol*, **3**, 246-255.
- Turk E, Teplow DB, Hood LE, and Prusiner SB (1988) Purification and properties of the cellular and scrapie hamster prion proteins. *Eur J Biochem*, **176**, 21-30.
- Varela-Nallar L, Toledo EM, Chacon MA, and Inestrosa NC (2006) The functional links between prion protein and copper. *Biol Res*, **39**, 39-44.
- Vassallo N and Herms J (2003) Cellular prion protein function in copper homeostasis and redox signalling at the synapse. *J Neurochem*, **86**, 538-544.
- Verkhatsky A (2002) The endoplasmic reticulum and neuronal calcium signalling. *Cell Calcium*, **32**, 393-404.
- Vey M, Pilkuhn S, Wille H, Nixon R, DeArmond SJ, Smart EJ, Anderson RG, Taraboulos A, and Prusiner SB (1996) Subcellular colocalization of the cellular and scrapie prion proteins in caveolae-like membranous domains. *Proc Natl Acad Sci U S A*, **93**, 14945-14949.

- Vincent B, Paitel E, Saftig P, Frobert Y, Hartmann D, De Strooper B, Grassi J, Lopez-Perez E, and Checler F (2001) The disintegrins ADAM10 and TACE contribute to the constitutive and phorbol ester-regulated normal cleavage of the cellular prion protein. *J Biol Chem*, **276**, 37743-37746.
- Voisin PJ, Pardue S, Macouillard F, Yehia G, Labouesse J, and Morrison-Bogorad M (1996) Differential expression of heat shock 70 proteins in primary cultures from rat cerebellum. *Brain Res*, **739**, 215-234.
- Wang X, Wang F, Arterburn L, Wollmann R, and Ma J (2006) The interaction between cytoplasmic PrP and the hydrophobic lipid core of membrane correlates with neurotoxicity. *J Biol Chem*.
- Wang X, Wang F, Sy MS, and Ma J (2005) Calpain and other cytosolic proteases can contribute to the degradation of retro-translocated prion protein in the cytosol. *J Biol Chem*, **280**, 317-325.
- Warrick JM, Chan HY, Gray-Board, Chai Y, Paulson HL, and Bonini NM (1999) Suppression of polyglutamine-mediated neurodegeneration in *Drosophila* by the molecular chaperone HSP70. *Nat Genet*, **23**, 425-428.
- Warwicker J (2000) Modeling a prion protein dimer: predictions for fibril formation. *Biochem Biophys Res Commun*, **278**, 646-652.
- Washbourne P, Liu XB, Jones EG, and McAllister AK (2004) Cycling of NMDA receptors during trafficking in neurons before synapse formation. *J Neurosci*, **24**, 8253-8264.
- Weissmann C and Flechsig E (2003) PrP knock-out and PrP transgenic mice in prion research. *Br Med Bull*, **66**, 43-60.
- Whittington MA, Sidle KC, Gowland I, Meads J, Hill AF, Palmer MS, Jefferys JG, and Collinge J (1995) Rescue of neurophysiological phenotype seen in PrP null mice by transgene encoding human prion protein. *Nat Genet*, **9**, 197-201.
- Wilson JM, de Hoop M, Zorzi N, Toh BH, Dotti CG, and Parton RG (2000) EEA1, a tethering protein of the early sorting endosome, shows a polarized distribution in hippocampal neurons, epithelial cells, and fibroblasts. *Mol Biol Cell*, **11**, 2657-2671.
- Wong BS, Brown DR, Pan T, Whiteman M, Liu T, Bu X, Li R, Gambetti P, Olesik J, Rubenstein R, and Sy MS (2001) Oxidative impairment in scrapie-infected mice is associated with brain metals perturbations and altered antioxidant activities. *J Neurochem*, **79**, 689-698.
- Wong K, Qiu Y, Hyun W, Nixon R, VanCleave J, Sanchez-Salazar J, Prusiner SB, and DeArmond SJ (1996) Decreased receptor-mediated calcium response in prion-infected cells correlates with decreased membrane fluidity and IP3 release. *Neurology*, **47**, 741-750.

- Yadavalli R, Guttmann RP, Seward T, Centers AP, Williamson RA, and Telling GC (2004) Calpain-dependent endoproteolytic cleavage of PrPSc modulates scrapie prion propagation. *J Biol Chem*, **279**, 21948-21956.
- Yedidia Y, Horonchik L, Tzaban S, Yanai A, and Taraboulos A (2001) Proteasomes and ubiquitin are involved in the turnover of the wild-type prion protein. *EMBO J*, **20**, 5383-5391.
- Yoo BC, Krapfenbauer K, Cairns N, Belay G, Bajo M, and Lubec G (2002) Overexpressed protein disulfide isomerase in brains of patients with sporadic Creutzfeldt-Jakob disease. *Neurosci Lett*, **334**, 196-200.
- Zanata SM, Lopes MH, Mercadante AF, Hajj GN, Chiarini LB, Nomizo R, Freitas AR, Cabral AL, Lee KS, Juliano MA, de Oliveira E, Jachieri SG, Burlingame A, Huang L, Linden R, Brentani RR, and Martins VR (2002) Stress-inducible protein 1 is a cell surface ligand for cellular prion that triggers neuroprotection. *EMBO J*, **21**, 3307-3316.
- Zanusso G, Petersen RB, Jin T, Jing Y, Kanoush R, Ferrari S, Gambetti P, and Singh N (1999) Proteasomal degradation and N-terminal protease resistance of the codon 145 mutant prion protein. *J Biol Chem*, **274**, 23396-23404.
- Zhang K and Kaufman RJ (2006) Protein folding in the endoplasmic reticulum and the unfolded protein response. *Handb Exp Pharmacol*, 69-91.
- Zinsmaier KE and Bronk P (2001) Molecular chaperones and the regulation of neurotransmitter exocytosis. *Biochem Pharmacol*, **62**, 1-11.

## 7 Abbreviations

aa	amino acid
A	adenosine
AMC	7-amino-4-methylcoumarin
Asn	asparagines
ATP	adenosine tri-phosphate
BCA	bicinchoninic acid
BFGF	basic fibroblast growth factor
bp	base pair
BSA	bovine serum albumin
BSB	[(trans,trans),-1-bromo-2,5-bis-(3-hydroxycarbonyl-4-hydroxy) styrylbenzene
BSE	bovine spongiforme encephalopathy
CJD	Creutzfeldt-Jakob disease
CMV	cytomegalovirus
cPLA <sub>2</sub>	calcium-dependent cytosolic phospholipase A <sub>2</sub>
Cy-PrP	prion protein containing amino acids23-231
d	days
DMEM	“Dulbecco’s modified Eagle’s medium”
DMSO	dimethyl sulfoxide
DNA	deoxyribonucleic acid
DTT	dithiothreitol
EDTA	ethylene diamine tetra-acetate
EEA1	early endosomal antigen 1
EndoH	Endoglycosidase H
Epoxo	epoxomicin
ER	endoplasmatic reticulum
ERAD	endoplasmatic reticulum associated degradation
FACS	flow cytometry
FFI	fatal familial insomnia
Fig	Figure
FITC	fluorescence isothiocyanate

---

GFP	green fluorescence protein
GSS	Gerstmann-Sträussler-Scheinker disease
GPI	glycosylphosphatidylinositol
h	hours
Hsp	heat shock protein
Hsc	cognate form of heat shock protein
Ig	immunoglobulin
IB	immunoblotting
IP	immunoprecipitation
IF	immunofluorescence
kb	kilobasepairs
kDa	kilodalton
l	litre
LDH	lactate dehydrogenase
LB	Luria Bertani
µg	microgram
MH2M	chimeric mouse-hamster-mouse prion protein
min	minutes
ml	millilitre
MTT	3-(4,5-dimethylthiazol-2-yl)-2,5-diphenyltetrazolium bromide
N2a	murine neuroblastoma cell line
NSP	N-terminal signal peptide
NTPs	nucleoside triphosphates
OD	optical density
PBS	phosphate buffered saline
PCR	polymerase chain reaction
PDI	protein disulfide isomerase
PEI	Paul-Ehrlich-Institut
PFA	paraformaldehyde
PK	proteinase K
PM-PrP	plasma membrane located full length prion protein
PMSF	phenylmethylsulfonylfluoride
Prnp	mouse prion protein gene
PrP <sup>C</sup>	cellular prion protein



---

PrP <sup>0/0</sup>	PrP <sup>C</sup> knock out (Zurich I) cerebellar neuronal precursor cell line
PrP <sup>Sc</sup>	pathogenic isoform of the prion protein
R340	polyclonal anti-PrP antibody
RPE	R-phycoerythrin
RT	room temperature
SAF32	anti-PrP antibody binding the N-terminal region
SDS	sodium dodecyl sulfate
SDS-PAGE	sodium dodecyl sulfate polyacrylamid gel electrophoresis
sec	seconds
6H4	anti-PrP antibody binding epitope aa144-152
Tab	table
TAE	Tris-acetate-EDTA
TD	annealing temperature
Tris	Tris-(hydroxymethyl)-aminomethane
TSE	transmissible spongiform encephalopathies
TUNEL	terminal-dUTP nick end labelling
wt	wild-type
3F4	PrP-specific monoclonal antibody binding epitope aa109-112
293T	human embryonal kidney cell line expressing the large T antigen

## Curriculum vitae

### Personal information

Name: Jana Mehlhase  
Postal address: Lorscher Str. 5, 63225 Langen, Germany  
Birthday and –place: 03.06. 1974, Mittweida, Germany  
Nationality: German  
Family status: single

### Education

09/ 1981	08/ 1990	Allgemeine Oberschule, Berlin
09/ 1990	06/ 1994	Albert Einstein-Gymnasium, Berlin
06/ 1994		Degree: General qualification for university entrance (Allgemeine Hochschulreife)

### Study of Biology and Ph.D. Thesis

10/1994	05/2001	<b>Diploma study</b> of Biology at the Humboldt-University, Berlin <u>Degree:</u> Master (Diplom-Biologin) <u>Master thesis (Diplomarbeit):</u> „Oxidative stress and proteolysis in microglia and macrophages “
06/2001	09/2002	<b>Research assistant</b> , Chair of Dr. Tilman Grune, Medical Faculty at the Humboldt-University, Berlin Neuroscience Research Centre <u>Project:</u> „Role of the microglia in the iron-metabolism of the brain – damage of iron-binding proteins following free radical treatment“
10/2002	dato	<b>PhD student</b> at the Paul-Ehrlich-Institut, Langen <u>PhD Thesis:</u> „Characterisation of cytosolic prion protein-mediated putative cytotoxicity in neuronal cell lines“

## Publications

**Mehlhase, J.**, Gieche J., Ullrich O., Sitte N. and Grune, T. (2000) LPS-induced protein oxidation and proteolysis in BV-2 microglia. *IUBMB Life* 50, 331-335

Gieche J., **Mehlhase J.**, Licht A., Zacke T., Sitte N. and Grune, T. (2001) Protein oxidation and proteolysis in RAW264.7 macrophages: effects of PMA activation. *Biochim. Biophys. Acta* 1538, 321-328

**Mehlhase J.** and Grune T. (2002) Proteolytic response to oxidative stress in mammalian cells. *Biol. Chem.* 383, 559-567. Review.

Shringarpure R., Grune T., **Mehlhase J.** and Davies, KJ. (2003) Ubiquitin conjugation is not required for the degradation of oxidized proteins by proteasome. *J Biol Chem.* 278, 311-318

**Mehlhase J.**, Sandig G., Pantopoulos K. and Grune T. (2005) Oxidation-induced ferritin turnover in microglial cells: role of proteasome. *Free Radic Biol Med.* 38(2), 276-85.

**Mehlhase J.**, Gieche J., Widmer R. and Grune T. (2006) Ferritin levels in microglia depend upon activation: modulation by reactive oxygen species. *Biochim. Biophys. Acta - Molecular Cell Research* 1763(3), 854-859

**Mehlhase J.**, Hahmann J., Loewer J. and Montrasio F. (2006) Hsc70-mediated translocation of cytosolic PrP into EEA1-positive vesicles prevents cytosolic PrP-induced neurotoxicity. *in preparation*

## Acknowledgement

Prof. Dr. Johannes Löwer danke ich für die Möglichkeit, am Paul-Ehrlich-Institut unter optimalen Arbeitsbedingungen promovieren zu können.

Frau Prof. Dr. Anna Starzinski-Powitz danke ich für die freundliche Betreuung von Universitätsseite.

Herrn Dr. Fabio Montrasio danke ich für das Thema dieser Doktorarbeit, die Begeisterung für die Thematik der Prionen sowie für die Unterstützung bei der Durchführung der Arbeit in seiner Arbeitsgruppe am Paul-Ehrlich-Institut.

Ganz besonders bedanken möchte ich mich an dieser Stelle bei meinem Mentor PD Dr. Christian Buchholz für seine konstruktiven Vorschläge und seine organisatorische Unterstützung.

Joanna Hamann danke ich für ihre umfassende Hilfe im Laboralltag und die herausragende Zusammenarbeit auf der „Zielgeraden“ insbesondere was die geliebten IPs angeht. Frau Dr. Annette Reisinger danke ich für das Korrekturlesen und die wissenschaftliche Interaktion. Marco Pietrella sei gedankt für seine uneingeschränkte Freundschaft und seinen unerschütterlichen Humor, was die Qualität der Arbeitsatmosphäre deutlich erhöhte.

Ein großes Dankeschön geht an Dr. Klaus Boller, der mich in die konfokale Fluoreszenzmikroskopie und Elektronenmikroskopie einführte und bei den Experimenten immer mit Rat und Tat zur Seite stand.

Ich danke allen Kollegen aus Pr1, NG3, ZT, Abteilung 3 und Abteilung 6 für Ihre Hilfsbereitschaft und die freundliche Arbeitsatmosphäre. Dabei möchte ich besonders Matthias Hamdorf danken, der für mich nebenbei das pIND-GFP Konstrukt klonierte, zahlreiche Computerprobleme löste und methodische Tricks und Kniffe verriet. Silja Wessler und Christiane Weyding waren sehr gute Motivationskünstler und unterstützten mich tatkräftig bei der Nutzung von

Reference Manager und Corel Graphics Suite. Daphne Nikles danke ich für die fachlichen Diskussionen, die perfekte Zusammenarbeit als Doktorandenvertreter und die vielen schönen Unternehmungen.

Melanie Kraemer danke ich für unsere Freundschaft, das unschöne Korrekturlesen sowie für die vielen guten Gespräche und für Ihre moralische Unterstützung in allen Belangen.

Katrin Hafez sei mein ganz persönlicher Dank gewidmet für die zahlreichen fachlichen Diskussionen, die konstante Zielorientierung und ihre Vorbildfunktion betreffs selbständigen und strukturiertes Arbeitens trotz erfüllter Freizeitgestaltung und privater Weiterbildung.

Anschließend danke ich meiner Familie, die mich immer tatkräftig in allen Belangen unterstützt hat. Mein ganz besonderer Dank geht an Richard Schneider für zahlreiche konstruktive fachliche Diskussionen, das unermüdliche Korrekturlesen und die vielen sprachlichen Verbesserungen, von denen die Arbeit profitiert. In den letzten Jahren hast Du die meiste emotionale Last getragen und mich immer wieder motiviert. Danke!